People's Democratic Republic of Algeria
Ministry of Higher Education and Scientific Research
8 May 1945 Guelma University

Faculty : Sciences and Technology
Department : Electronic and Telecommunications
Domiciliation laboratory: Telecommunications (LT)

THESIS

IN VEW OF OBTAINING
THE DOCTORATE DEGREE IN 3rd CYCLE

Domain : **Sciences and Technology** Field : **Telecommunications**
Speciality : **Telecommunications**

Presented by

TABA Somia

Entitled

Contribution to the Development of Advanced Techniques for Massive MIMO Communication Systems

Defended : 05/10/2023 In front of the board of examiners composed of:

Mr ABED Djamel	**Professor**	Univ. of 8 Mai 1945, Guelma	Chairman
Mr REDADAA Salah	**Professor**	Univ. of 8 Mai 1945, Guelma	Supervisor
Mr IKNI Samir	**MCB**	Univ. of 8 Mai 1945, Guelma	Co-supervisor
Mr BENATIA Djamel	**Professor**	Univ. of Batna2	Examiner
Mm GRAINI Leila	**MCA**	Univ. of 8 Mai 1945, Guelma	Examiner

Academic year: 2022/2023

My beloved Parents, my caring Brother and my dear Sisters, Med, and my kind uncle Mohamed

This thesis is dedicated to you

Acknowledgements

First and foremost, I express my gratitude to Allah for guiding me, providing me the patience to complete this valuable undertaking, and blessing me with this achievement.

Sincere gratitude goes to my family for their constant love and support. The confidence and encouragement I have received from them has been beyond measure. Thanks for their patience throughout the lengthy hours devoted to research. I owe this achievement to their invaluable support.

I would like to express my appreciation to my advisor, Salah Redadaa, a professor at 8 mai 1945 University, as well as my co-adviser, Samir Ikni, a teacher at 8 mai 1945 University. I am grateful for their support, the trust they have shown in me, and their constructive feedback throughout this journey.

I warmly thank the members of the jury for their thorough examination of the thesis and their valuable feedback.

Finally, I'd like to sincerely thank all the people who have helped me and wished me well along the way.

Abstract

The relentless demand for faster data rates, extremely low latency and significant improvements in quality of service (QoS) has given rise to the emergence of the fifth generation (5G) of wireless transmission technologies. This latest generation of cellular networks has brought many advances over previous generations. 5G uses a powerful waveform known as orthogonal frequency division multiplexing (OFDM) due to its inherent advantages such as high capacity, immunity to multipath fading and the ease of implementation. However, the drawback of this technique is its high peak-to-average power ratio (PAPR), which degrades signal quality at the receiver and hampers the overall efficiency of the 5G system. Various methods have been proposed in the literature to mitigate PAPR in OFDM systems. In the second chapter of this thesis, we provided a comprehensive overview of the most effective PAPR reduction techniques and concluded that the partial transmission sequence (PTS) technique was the most promising among them. However, despite its efficiency and distortion-free nature, this scheme suffers from an exponentially increasing complexity. Therefore, the aim of this thesis is to reduce PAPR levels in OFDM systems by introducing a new PTS technique that creates a good compromise between PAPR mitigation and complexity. To achieve this goal, two contributions have been presented, in which the PTS technique has been combined with efficient meta-heuristic algorithms, resulting in new PTS alternatives that offer efficient PAPR reduction while maintaining competitive complexity. The results are compared with other techniques described in the existing literature, validating the effectiveness of the proposed approaches.

- **Keywords:** 5G, OFDM, PAPR, PTS, PSO, WOA

Résumé

La demande incessante de débits de données plus rapides, d'une latence extrêmement faible et d'améliorations significatives de la qualité de service (QoS) a donné lieu à l'émergence de la cinquième génération (5G) de technologies de transmission sans fil. Cette dernière génération de réseaux cellulaires a apporté de nombreuses avancées par rapport aux générations précédentes. Cette dernière utilise une forme d'onde puissante connue sous le nom de multiplexage par répartition orthogonale de la fréquence (OFDM) en raison de ses avantages inhérents tels qu'une capacité élevée, l'immunité aux évanouissements par trajets multiples et la facilité de mise en œuvre. Toutefois, l'inconvénient de cette technique est son rapport puissance de crête/puissance moyenne (PAPR) élevé, qui dégrade la qualité du signal au niveau du récepteur et entrave l'efficacité globale du système 5G. Diverses méthodes ont été proposées dans la littérature pour atténuer le PAPR dans les systèmes OFDM. Dans le deuxième chapitre de cette thèse, nous avons fourni un aperçu complet des techniques de réduction du PAPR les plus efficaces et conclu que la technique de la séquence de transmission partielle (PTS) était la plus prometteuse d'entre elles. Cependant, malgré son efficacité et sa nature sans distorsion, ce schéma souffre d'une complexité qui augmente de façon exponentielle. Par conséquent, l'objectif de cette thèse est de réduire les niveaux de PAPR dans les systèmes OFDM en introduisant une nouvelle technique PTS qui crée un bon compromis entre l'atténuation du PAPR et la complexité. Pour atteindre cet objectif, deux contributions ont été présentées, dans lesquelles la technique PTS a été combinée avec des algorithmes méta-heuristiques efficaces, résultant en de nouvelles alternatives PTS qui offrent une réduction efficace du PAPR tout en maintenant une complexité compétitive. Les résultats sont comparés à d'autres techniques décrites dans la littérature existante, ce qui valide l'efficacité des approches proposées.

- **Mots-clés:** 5G, OFDM, PAPR, PTS, PSO, WOA

ملخص

أدى الطلب المستمر على معدلات بيانات أسرع ، وزمن انتقال منخفض للغاية ، وتحسينات كبيرة في جودة الخدمة (QoS) إلى ظهور الجيل الخامس (5G) من تقنيات الإرسال اللاسلكي. أحدث هذا الجيل الأخير من الشبكات الخلوية العديد من التطورات مقارنة بالأجيال السابقة. يستخدم الأخير شكل موجة قوي يُعرف باسم تعدد الإرسال بتقسيم التردد المتعامد (OFDM) نظرًا لمزاياه المتأصلة مثل السعة العالية ، والمناعة من الخبو متعدد المسارات ، وسهولة الإعداد. ومع ذلك ، فإن الجانب السلبي لهذه التقنية هو نسبة الذروة إلى القدرة المتوسطة (PAPR) ، التي تقلل من جودة الإشارة في المستقبل وتعيق الكفاءة الكلية لنظام 5G . تم اقتراح طرق مختلفة في الأبحاث العلمية لتقليل ال PAPR في أنظمة OFDM. في الفصل الثاني من هذه الأطروحة ، قدمنا نظرة عامة شاملة عن أكثر تقنيات الحد من ال PAPR فاعلية وخلصنا إلى أن تقنية تسلسل الإرسال الجزئي (PTS) هي الأكثر واعدة. ومع ذلك ، على الرغم من كفاءتها وطبيعتها الخالية من التشويه ، فإن هذا المخطط يعاني من التعقيد المتزايد بشكل كبير. لذلك ، فإن الهدف من هذه الأطروحة هو تقليل مستويات ال PAPRفي أنظمة ال OFDM من خلال طرح تقنية تسلسل ارسال جزئي جديدة بحيث تخلق مفاضلة جيدة بين التخفيف ال PAPR والتعقيد .ولتحقيق هذا الهدف ، تم تقديم مساهمتين ، تم فيهما دمج تقنية الPTS مع الخوارزميات الميتاهوريستية الفعالة ، مما أدى إلى بدائل جديدة لل PTS توفر تقليلًا فعالًا لـل PAPR مع الحفاظ على التعقيد تنافسي. تتم مقارنة النتائج بالتقنيات الأخرى الموضحة في الأعمال السابقة، وبالتي نؤكد فعالية الأساليب المقترحة.

الكلمات المفتاحية: 5G, OFDM, PAPR, PTS, PSO, WOA.

General Introduction

Radio communications trace their origins to the late 19th century when Marconi made a groundbreaking achievement by transmitting the first electromagnetic wave across significant distances [1]. This invention served as a catalyst for the exponential growth of wireless technologies and provided the foundation for further advancements. It attracted a great deal of attention from military forces during the second world war. They employed radio waves in various military activities, such as tracking and object detection. In the 1970s, cellular networks took a major step forward in making mobile communication possible over vast areas, laying the foundations for future generations. The transition from 1G to 4G has enabled mobile users to benefit from considerable improvements in terms of capacity, data transmission speed and functionality. However, the rise of Internet of Things (IoT) applications, autonomous vehicles, smart cities, and virtual reality along with the necessity to overcome limitations faced by 4G LTE networks, has paved the way for the development of fifth-generation (5G) systems [2].

5G has brought about a revolutionary transformation in network designs and interfaces, encompassing a wide array of applications, which have been specifically designed to cater to the ever-increasing demands of an interconnected world. Their objective is to deliver considerably accelerated data transfer speeds, diminished latency, increased capacity, and greater reliability than preceding releases. As a result, several techniques have been developed to fulfill the requirements of 5G, including massive multiple-input multiple-output (MIMO), millimeter-wave (mmWave) frequency utilization, and beamforming. By providing ultra-low latency in the range of milliseconds, 5G technology enables real-time applications like remote surgery and autonomous cars, allowing for instant communication and rapid response times. In addition, the problem of network congestion is effectively resolved through the use of higher frequency bands, enhanced spectrum efficiency and sophisticated network control features, resulting in a substantial rise in network capacity.

The 3rd Generation Partnership Project (3GPP) release 15 incorporates essential components of both 5G and LTE, collectively known as 5G New Radio (NR). The 5G NR specifications encompass various aspects, including synchronization, numerology, and waveform. These aspects have been specifically defined and further improved to cater to a wide range of use cases and applications. The adaptable architecture of 5G NR is carefully designed to provide high-speed data rates, minimal latency, smooth mobility, and improved reliability.

The 5G NR system utilizes the orthogonal frequency division multiplexing (OFDM) waveform, which incorporates distinctive numerology and spectrum that were not employed in LTE. OFDM is a multi-carrier modulation technique extensively utilized in diverse wireless communication technologies. It offers numerous benefits, including high spectral efficiency and the capability to achieve high data rates even in channels affected by frequency-selective fading. Within the architecture design of NR, OFDM is employed for both the uplink and downlink transmissions. OFDM was selected as the primary waveform for the 5G NR system due to its notable advantages, which include:

- Spectral efficiency

By dividing the available spectrum into closely spaced subcarriers, OFDM enhances spectral efficiency by effectively utilizing the frequency resources. Each of these subcarriers can be allocated to different users or services. This allocation ensures the maximum utilization of the system's spectral efficiency, enabling the optimal use of the available frequency resources.

- Scalability and flexibility

This benefit is attained due to the flexibility of the OFDM waveform, allowing it to adapt to different bandwidth limitations and cater to diverse channel conditions. OFDM has the capability to seamlessly adjust and support various frequency bands while effectively handling a wide range of data. Consequently, it is highly suitable for deployment in a variety of scenarios, offering the adaptability needed to meet the ever-changing demands and requirements of different networks.

- Resistance to interference

OFDM withstands both narrowband interference and multipath fading well. By using multiple subcarriers with orthogonal frequency spacing, it enables robust communication in environments characterized by changing the conditions of a channel, including city zones and domestic settings.

- Interoperability with current systems

Building on prior wireless transmission systems and leveraging accumulated expertise, researchers were able to capitalize on existing technologies and advance them for the 5G NR system.

- Optimal Resource Allocation

Data transmission will be optimized according to the user's needs and channel requirements using coding and modulation techniques and dynamic resource assignment support.

However, the main drawback of the OFDM technique is the high peak-to-average power ratio (PAPR) [3]. The latter occurs when a significant number of subcarrier components are coherently summed via IFFT operation. Besides that, the power amplifier's nonlinearity degrades the systems' efficiency. Thus, applying a high-cost amplifier with sufficient dynamic range is essential. Consequently, PAPR reduction is crucial in OFDM transmitters [4].

In earlier studies, many PAPR reduction techniques have been investigated. Among which, partial transmit sequence (PTS) is known for its inherent robustness in lowering PAPR levels in OFDM systems while neither distorting the signal nor restricting the number of subcarriers [5]. This approach combines the scrambled signals from the partial transmit sequence groups. Scrambling is performed by multiplying each PTS subblock by an appropriate phase factor, chosen to reduce the PAPR of the transmitted signal. The search for the ideal set of phase factors is performed by an exhaustive search. However, the complexity resulting from testing all possible combinations is enormous, especially as the number of sub-blocks (V) increases, as W^{V-1} searches must be performed to find an optimal solution (W represents the number of allowed phase factors). This renders the technique impractical due to its excessively high computational burden.

Extensive research in this field has led to the exploration of numerous techniques aimed at reducing the complexity associated with the PTS technique. Nevertheless, finding a favorable balance between reducing PAPR and minimizing search complexity remains an active and ongoing area of research. Therefore, our thesis will provide two contributions that focus on effectively mitigating PAPR and reducing the search complexity associated with the PTS scheme.

This work highlights the remarkable robustness of meta-heuristic algorithms in tackling complex and time-consuming problems. It explores the utilization of these optimization algorithms in conjunction with the PTS scheme to effectively reduce PAPR levels within a very low number of searches.

The first contribution of our research will focus on investigating an enhanced particle swarm optimization (PSO) algorithm. This investigation aims to address the primary challenges associated with the conventional PSO technique, such as premature convergence and susceptibility to local optima [6]. To overcome these issues, we introduce a novel coefficient, R_{best}, into the velocity formula. This inclusion promotes diversity and improves the accuracy of the solution. The enhanced PSO algorithm is then integrated with the PTS scheme, effectively searching for the optimal sequence of phase factors that minimize PAPR while maintaining reduced complexity. To demonstrate its efficacy, we compare the performance of our proposed algorithm against other established optimization techniques.

The second contribution introduces another new alternative PTS technique based on an improved whale optimization algorithm (IWOA). We compare the performance of the IWOA with other robust meta-heuristic optimization algorithms to evaluate its effectiveness in reducing PAPR. We analyze its convergence and complexity and compare it to conventional PTS scheme as well as to other optimization techniques.

Overall, our thesis is divided into three chapters, each of which is outlined in the following paragraphs.

In the opening chapter, we will offer an introduction to 5G technology, starting with a concise overview of the history of wireless communications. We will trace the significant advancements from Guglielmo Marconi's invention to the evolution leading up to 5G technology. Then, we will delve into the three main use cases of 5G, namely enhanced mobile broadband (eMBB), massive machine type communication (mMTC), and ultra-reliable low latency communication (uRLLC). Each use case is explained in detail. Next, we will explore the requirements of 5G, providing an explanation of each requirement. We will, then, discuss the key technologies that constitute the 5G system, including massive MIMO, Non-Orthogonal Multiple Access (NOMA), mmWave, IoT-based approaches, and Machine Learning (ML). Subsequently, we will outline several advancements of 5G over its predecessor, 4G. Additionally, we will emphasizes the importance of spectrum, numerology, and the waveform used in 5G NR networks, OFDM. We will, then, present the structure and mathematical model of OFDM, along with a mention of its inherent drawback, the PAPR. Overall, this chapter will provide an encompassing introduction to 5G technology, covering its historical context, use cases, requirements, key technologies, advancements, and the specific aspects of OFDM utilized in 5G NR networks, including its associated drawback.

In the second chapter, we will present a comprehensive overview of various well-known techniques employed in OFDM systems to reduce PAPR. Each technique will be described in detail, including its block diagram, mathematical model, and a thorough literature review that spans from early works to the most recent state-of-the-art contributions. Additionally, we will conduct a comparative analysis of these techniques to identify the most suitable approach among them. Through this analysis, we will conclude that the PTS technique emerges as the most suitable choice based on several criteria.

In the third chapter, we will present and discuss our contributions. In the first one we will introduce a novel PAPR reduction technique that combines the PTS scheme with an enhanced PSO algorithm. This approach leverages heuristics to efficiently find a near-optimal combination of phase factors, effectively minimizing

PAPR with minimal computational overhead. Moving on to the second contribution, we will suggest another innovative method for PAPR reduction. This contribution employ the IWOA within the PTS scheme, aiming to strike a balance between search complexity and PAPR reduction, providing an optimized solution. We will provide a detailed complexity and convergence analysis for both methods. MATLAB simulations and discussions will be conducted to assess the performance of each proposed method, further highlighting their potential for reducing PAPR in OFDM systems.

We wrap up our work by offering conclusions and future outlooks. In the concluding section, we'll provide a brief overview of each chapter and the findings derived from them. Our conclusion will highlight the effectiveness of both examined models in reducing PAPR levels and handling complexity. These models stand as viable options for mitigating PAPR levels in OFDM systems, ultimately enhancing the performance of the 5G system. The future prospects will primarily revolve around two key aspects. First, we will assess the effectiveness of various PAPR reduction techniques in improving system performance, considering crucial metrics such as spectral efficiency, coverage, and bit error rate (BER). Second, we will examine the efficiency of PAPR reduction methods and develop solutions to tackle the PAPR challenge in alternative waveform candidates designed to meet the specifications of 5G technology, including Filtered Multi-Carrier (UFMC), Filtered-OFDM (F-OFDM), and FBMC.

Contents

List of Abbreviations

IoT . . . . Internet of Things.

MIMO . . . . . multiple-input multiple-output .

mmWave . . . millimeter-wave.

3GPP . . . . . 3^{rd} Generation Partnership Project.

NR . . . . New Radio.

OFDM . . . . Orthogonal Frequency Division Multiplexing.

PAPR . . . . . Peak-to-average-power ratio.

PSO . . . . . . particle swarm optimization.

IWOA . . . . . improved whale optimization algorithm.

eMBB . . . . . enhanced mobile broadband.

mMTC . . . . massive Machine Type Communication.

uRLLC . . . . tra-Reliable Low-Latency Communication.

NOMA . . . . Non-Orthogonal Multiple Access.

ML . . . . Machine Learning.

QoS . . . . . . quality of service.

LTE . . . . . . Long Term Evolution.

GSM . . . . . . Global System for Mobile Communications.

5G . . . . fifth generation.

GPRS . . . . . General Packet Radio Service.

CDMA . . . . Code Division Multiple Access.

UAVs . . . . . unmanned aerial vehicles.

NFV . . . . . . network function virtualization.

SDN . . . . . . software-defined networking.

AR . . . . augmented reality.

ITU . . . . . . International Telecommunication Union.

RF . . . . radio frequency.

UL . . . . uplink.

DL . . . . downlink.

CDF . . . . . . cumulative distribution function.

KPI . . . . . . Key performance indicator.

RAN . . . . . . radio access network.

IMT . . . . . . International Mobile Telecommunications.

SU-MIMO . . Single-user MIMO.

MU-MIMO . . Multi-user MIMO.

UE . . . . User equipments.

OFDMA . . . orthogonal frequency division multiple access.

CSI . . . . channel state information.

M2M . . . . . machine-to-machine.

UDN . . . . . . ultra-dense networks.

GPS . . . . . . Global Positioning System.

RL . . . . Reinforcement learning.

QoE . . . . . . Quality of Experience.

POMDP . . . Partially Observable Markov Decision Process.

MDP . . . . . Markov Decision Process.

CRN . . . . . . Cognitive Radio Networks.

V2V . . . . . . vehicle-to-vehicle.

AAE . . . . . . Adversarial Auto Encoders.

SVM . . . . . . support vector machines.

MEC . . . . . . Mobile Edge Computing.

5GC . . . . . . 5G Core.

SA . . . . standalone.

NSA . . . . . . non-standalone.

NGC . . . . . . next-generation core.

TDD . . . . . . Time Division Duplexing.

FDD . . . . . . Frequency Division Duplexing.

TBCC . . . . . Tail-Biting Convolutional Coding.

LDPC . . . . . Low-Density Parity-Check.

RAT . . . . . . Radio Access Technology.

CA . . . . Carrier Aggregation

DC . . . . Dual Connectivity.

LTE-A . . . . . LTE-Advanced.

SCS . . . . . . subcarrier spacing.

CP . . . . cyclic prefix.

HPA . . . . . . high power amplifier.

IBO . . . . . . Input Back-Off.

OBO . . . . . . Output Back-Off.

CCDF . . . . . complementary cumulative distribution function.

MCM . . . . . multicarrier modulation.

TR . . . . tone reservation.

TI . . . . tone injection.

SLM . . . . . . selective mapping.

PTS . . . . . . partial transmit sequence.

BER . . . . . . bit error rate.

ICF . . . . . . iterative clipping and filtering.

CT . . . . clipping threshold.

CM . . . . . . cubic metric.

INI . . . . International Numeral Interface

NS-ICF . . . . noise-shaped ICF.

SNDR . . . . . signal-to-noise-plus-distortion ratio.

LMO . . . . . . Lagrange Multiplier Optimization.

DST . . . . . . discrete sine transform.

OOFDM . . . optical orthogonal frequency division multiplexing.

PRT . . . . . . peak reduction tones.

LSA . . . . . . leastsquares approximation.

DNN . . . . . . deep neural network.

NN . . . . neural network.

SFBC . . . . . spatial frequency block coded.

IPTS . . . . . . iterative PTS.
RC-PTS . . . . reduced-complexity PTS approach.
EM . . . . Electromagnetism.
RPSM . . . . . Random Phase Sequence Matrix.
RAM . . . . . random access memory.
DSI . . . . . . dummy sequence insetion.
CSS . . . . . . cyclic shift sequence.
SI . . . . side information.
CUPSO . . . . continuousunconstrained particle swarm optimization.
KKT . . . . . . karush-kuhn-tucker.
PSO . . . . . . particle swarm optimization.
WOA . . . . . whale optimization algorithm.
ABC . . . . . . artificial bee colony.
FA . . . . firefly algorithm.
IHS . . . . . . improved harmony search.
GWO . . . . . grey wolf optimization.
ACO . . . . . . ant colony optimization.
OPTS . . . . . ordinary PTS.
MOMF . . . . May Fly Multiobjective Algorithm.
IBO-MER . . IBO modulation error rate.
IBO-SDR . . . IBO signal-to-distortion ratio.
FWA . . . . . . fireworks algorithm.
GA . . . . genetic algorithm.
SA . . . . simulated annealing.
EGA . . . . . . elitist genetic algorithm.
SGA . . . . . . simple genetic algorithm.
BPSO . . . . . binary particle swarm optimization.
RS . . . . random search.

List of Figures

List of Tables

Life is like riding a bicycle. To keep your balance, you must keep moving...

— Albert Einstein

1
Review on 5G Technology

Contents

1.1 Introduction

The primary objectives of the fifth generation (5G) technology are to achieve substantially higher data speeds, remarkably low latency, enhanced base station efficiency, and significant improvements in quality of service (QoS) compared to existing 4G Long Term Evolution (LTE) networks. It aims to serve as a pivotal driver for future Internet of Things (IoT) implementations and address the limitations of previous telecommunications technologies. With the proliferation of advanced technologies and the increasing connectivity of IoT devices, smartphones, autonomous vehicles, virtual reality devices, and smart home systems, there has been a rapid surge in broadband data consumption. Waveform design plays a critical role in the development of 5G technology. The chosen waveform for the 5G New Radio (NR) system is orthogonal frequency division multiplexing (OFDM), which is a multicarrier modulation technique previously used in LTE. This waveform is employed in both the uplink and downlink transmission channels. OFDM has been selected as the preferred waveform for 5G NR due to its high spectral efficiency, robustness against interference, compatibility with existing systems, and ability to achieve high data rates in frequency selective fading channels. However, it is important to address the issue of peak to average power ratio (PAPR), which arises when a large number of time domain signals coherently combine through IFFT operations. Additionally, achieving high output power is crucial, particularly in scenarios such as vehicle-to-vehicle wireless communications and wireless communication systems. Nevertheless, power amplifiers with very high power capabilities often lack cost effectiveness and are prohibitively expensive. Therefore, practical implementations of OFDM must incorporate various techniques to mitigate the high PAPR.[1]

In this chapter, we have laid the foundation for our PhD research contribution by providing essential scientific background. Our exploration began with a concise overview of the history of mobile communications. We will then delve into an introduction to 5G technology, covering its various aspects such as technologies, use cases, requirements, spectrum, and numerology. Furthermore, we will emphasize the utilization of the OFDM waveform in 5G and highlighted the associated challenge of high PAPR.

1.2 Brief history of wireless communications

Telecommunication organizations as well as a variety of service providers across the globe are striving to provide the most up-to-date solutions to address the growing need for wireless data by households and business users.

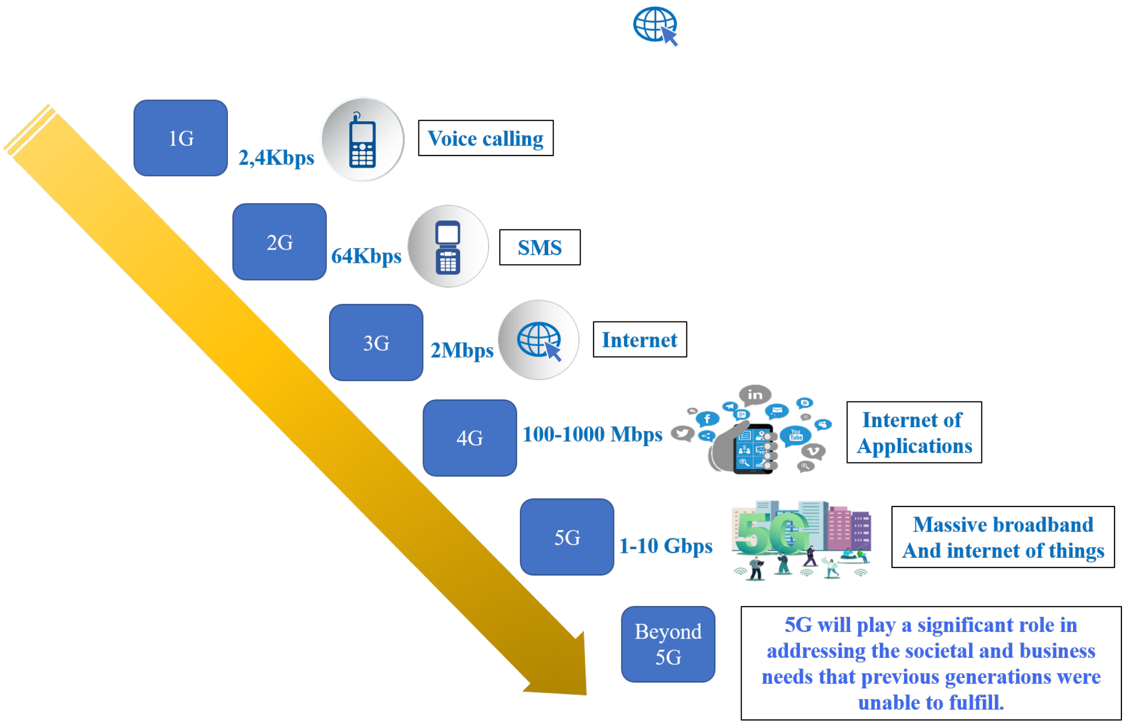

Figure 1.1: Overview of the principal stages of evolution in mobile communications.

The history of wireless communications dates back to 1895, when Macroni revolutionized long-distance communications by inventing the radio. The use of radio waves to communicate was a breakthrough in the history of technology. The Italian scientist was the first to be able to transmit radio wave signals in Morse code at a distance of 3.2 km [7]. The variety of new wireless devices that have been developed has necessitated an evolution of wireless standards [7]. During the past few decades, cellular networks have undergone several phases of evolution. Figure 1.1 provides a brief synopsis of the principal stages of evolution in mobile communications.

Based on analog technology, the first-generation (1G) cellular phone was developed in 1970 by Martin Cooper [1]. This generation suffered from signal attenuation, poor battery life, and its maximum speed was about 2.4 Kbps [8].

Based on digital technology, the second generation (2G) was launched, allowing short text messages, voice calls and emails at speeds between 14.4 kbps and 64 kbps [9]. The Global System for Mobile Communications (GSM) is an example of a 2G standard, introduced in 1991. Although it has been widely adopted, it suffers from several disadvantages such as limited coverage, compatibility issues, dependence on battery power and limited data transfer speeds. Transitional generations were introduced between 2G and 3G, namely 2.5G and 2.75G, which provided General Packet Radio Service (GPRS) and Enhanced Data Rates for GSM Evolution (EDGE) technologies respectively. These technologies offered faster data transfer and opened the way for the release of 3G technology [8]. In 2001, third generation (3G) was introduced [10]. 3G offered faster data transfer rates, better voice quality, global roaming and support for multimedia services. By the end of 2007, 3G had 295 million subscribers with high-speed Internet access from 200 kbps to a couple of megabits per second. Then, in 2009, researchers introduced Code Division Multiple Access (CDMA), which enables more than one user to use the same frequency channel to transmit data [11]. They played on controlling energy consumption and improving user QoS by employing cooperative game methods theory scoring user satisfaction. This allowed for the evaluation of several 3G applications such as Wireless Local Area Network (WLAN) and CDMA, their QoS expectations, power and resource allocation. 3G is also known as UMTS (Universal Mobile Telecommunications System). It gave birth to video calls for the first time and allowed mobile users to reach large amounts of data and internet features. Smartphones then went on to become very successful and gave rise to a new social life, games, multimedia experiences and health services [11]. As with 2G technology, 3G also includes intermediate mobile technologies that have been released between 3G and 4G. 3.5G technology, commonly referred to as High-Speed Packet Access (HSPA), is an enhanced cellular network technology that offers faster access to the Internet. Similarly, 3.75G, or High-Speed Packet Access Plus (HSPA+), is an enhanced variant of 3.5G that is faster and more powerful. The 3.5G and 3.75G technologies were important milestones in the evolution of mobile communications technology, improving capabilities and performance over 3G technology, while laying a basis toward future 4G and 5G technologies [8]. Although 3G technology created a revolution in the history of mobile communications, it suffered from several drawbacks, such as limited bandwidth, high cost, interference and security issues.

LTE, is an advanced mobile communication technology known as 4G. Compared to previous generations, 4G provides significant enhancements to data transfer speeds, latency rates, and multimedia support. Its advanced packet-switched network architecture and digital signal processing techniques enable superior data transfer rates. With 4G, users can experience upload speeds of up to 500 Mbps and download speeds of up to 1 Gbps, which is much faster than the speeds offered by 3G technology. One of the most significant advantages of 4G was its ability to be compatible with the previous generations [12].

The ever-increasing demand for high-quality multimedia services has raised the need for a global network that connects everything with more speed, reliability, massive network capacity and ultra-low latency. In the near future, 4G networks are not able to meet the demands of new technologies such as virtual reality, autonomous vehicles and unmanned aerial vehicles (UAVs). That's why researchers have proposed 5G and embraced emerging technologies such as network function virtualization (NFV) and software-defined networking (SDN). 5G can transmit data at 10 to 100 times the speed of 4G and 4G-LTE. The latter is expected to combine existing technologies such as cloud, IoT, big data, as well as blockchain and outperform superfast networks. In the 5G era, the delay is about a millisecond or less, which means there is no real-world response to real-time data; which represents a tremendous enhancement in comparison with the current services of the IoT. The broad introduction of 5G is expected to bring about massive IoT that can establish an ecosystem where "smart networks" would be employed to provide real-time interactivity. For the end user, 5G offers three main services: massive machine-type communication (mMTC), extreme mobile broadband (eMBB) and ultra-reliable low-latency communication (uRLLC). mMTC enables the interconnection of billions of devices and sensors and supports the high capacity of IoT devices. uRLLC is used to enable instant communication that requires minimal latency, such as remote surgery and autonomous vehicles. The eMBB uses ultra-fast speeds with greater capacity and therefore supports data-intensive applications such as live video streaming, augmented reality (AR) and high-precision medical applications.

1.3 Introduction to 5G

The development of communication technologies has come a long way since the introduction of Motorola's first cell phone in 1973. Today, with the introduction of 5G, we are witnessing another major shift in communication technologies. Figure 1.2 highlights the features of 5G. Its advantages include improved connectivity that covers both human-to-human and machine-to-machine communications, minimal latency (i.e., no signal delay or dropped calls) and significantly faster data rates ("10 times faster" than 4G). One of the key technical aspects of 5G systems is the use of higher frequencies than those used in current 4G systems. The 5G network will operate in two distinct frequency bands: a lower frequency band ranging from 3 to 6 GHz and an upper millimeter wave band ranging from 20 to 100 GHz. The first band is adjacent to the spectrum currently used by 4G systems. There will be some modifications made to the technology employed in the lower band of frequency band compared to 4G systems, but the changes will not be as significant as the technological adaptations needed for millimeter wave handsets and devices.

1.3.1 5G use cases

3^{rd} Generation Partnership Project (3GPP) and International Telecommunication Union (ITU) define application profiles for emerging wireless networks. In the case of 5G technology, it aims to enhance the network services of its predecessors in three key categories. These categories include:

1. Enhanced mobile broadband (eMBB)

   eMBB is a term used in 5G technology that describes the use of advanced wireless technologies to improve data rates, network capacity and latency. The main goal of eMBB is to improve the mobile broadband experience for consumers and businesses by enabling high-speed data transfer and supporting applications such as cloud gaming, augmented and virtual reality, and streaming video. This advancement is expected to enable previously unattainable services and experiences, making 5G a key driver of digital

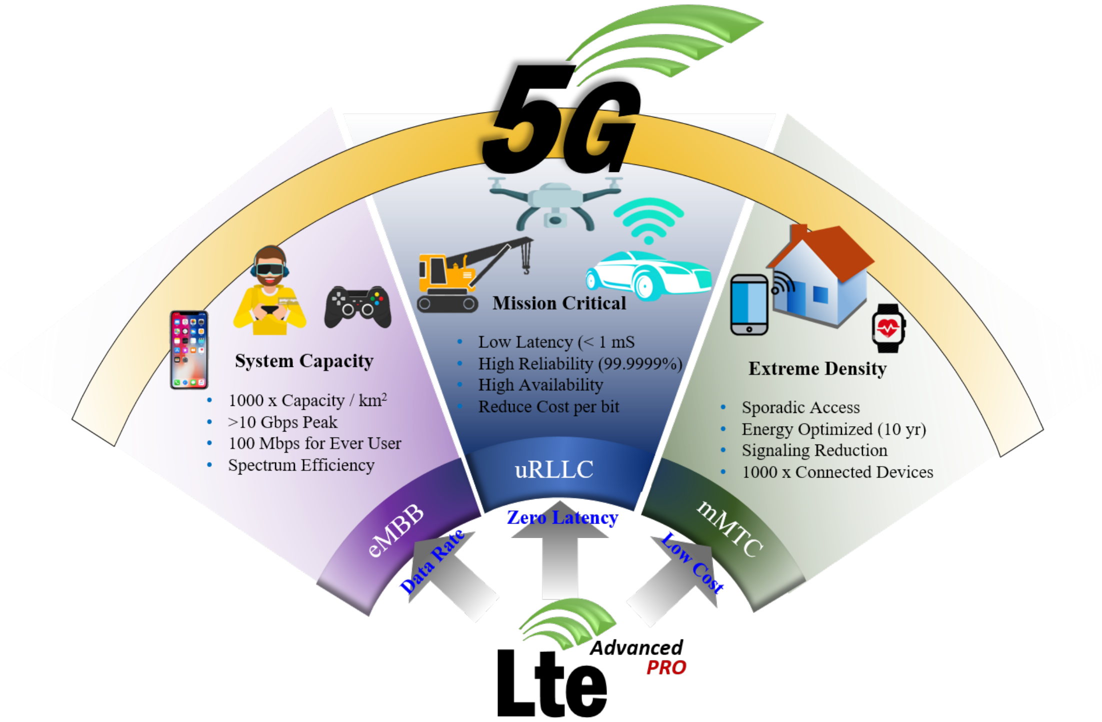

Figure 1.2: 5G system's advantages.

transformation in a variety of industries [13]. According to a report by Nokia Communication, there could be a significant surge in traffic demands for mobile broadband applications between 2020 and 2030, with requirements potentially increasing up to 10,000 times.

2. massive Machine Type Communication (mMTC)

   In 5G technology, mMTC describes communication between a multitude of devices that do not require either high data rates or low latency. Its main purpose is to facilitate the exchange of information between large numbers of power-saving appliances, as sensors, meters and other IoT devices. Such devices often transfer small data amounts for extended periods of time, underscoring the need for efficient use of network resources.

3. ultra-Reliable Low-Latency Communication (uRLLC)

uRLLC is a category of 5G technology that specifically caters to applications requiring extremely low latency. These include mission-critical applications such as factory automation, self-driving cars, and remote medical procedures where even the slightest communication delay could lead to dire consequences. Advanced technologies such as ultra-low latency transmission, high-reliability communication protocols, and network slicing are used in 5G networks to meet the high standards of reliability and low latency necessary for uRLLC applications. Ultimately, uRLLC is poised to open up a new frontier of critical applications that were once impossible, transforming the fields of industrial automation, transportation, and healthcare.

1.3.2 5G requirements

- Millimeter Wave (mmWave)

  The use of millimeter wave is a key technology in 5G systems because of the availability of a large amount of spectrum above 10 GHz. Therefore, bandwidth is not an issue. However, this open range of spectrum poses significant technical challenges. One of the most important is signal range, as attenuation increases with higher frequencies, reducing the distances that waves can travel. This has implications for 5G infrastructure deployment, as closely spaced base station towers are sufficient for systems operating below 3 GHz. For millimeter wave systems, the range would be much shorter, requiring smaller base stations or repeaters. A combination of centralized towers connecting base stations in the 3-6 GHz range and small decentralized base stations operating at millimeter wave frequencies can be used. Filtering is another challenge for 5G systems, especially for handset applications. Acoustic wave filtering is currently used for systems operating below 3 GHz, but a different type of filtering technology is needed for millimeter-wave applications in the 5G spectrum. It is too early to determine how 5G infrastructure will be deployed, but these technical considerations must be addressed to fully exploit the potential of 5G technology [14].

- Massive MIMO antennas

  In 5G systems, the antenna technology employed differs significantly from its predecessors. Rather than using a single antenna to transmit and receive signals in all directions, 5G systems utilize enhanced directionality. The adoption of a directional beam results in reduced power consumption because all radio frequency (RF) signals will be aimed toward the receiving unit rather than scattered in all directions. To achieve a directional beam, an array of antennas, known as MIMO, is used to guide the beam through a combination of constructive and destructive interference, thus conserving power and directing the signal towards a specific device. The effectiveness and bandwidth of an individual antenna are determined by its dielectric constant, with a lower constant material being more efficient [14].

- Peak data rate

  The term "peak data rate" denotes the highest possible data transfer rate achievable per user or device under optimal circumstances, measured in bits per second. The minimum required peak data rates for 5G networks are 10 Gbps for the uplink (UL) and 20 Gbps for the downlink (DL) [15].

- User experienced data rate

  Refers to the data rate that is consistently available throughout the coverage area to a device or mobile user, measured in bits per second. This performance metric is determined by the 5% point of the user's cumulative distribution function (CDF) of throughput and serves as a benchmark for the user's minimum experience in the coverage area. The International Telecommunications Union Radiocommunications Sector (ITU-R) has set this requirement at 50 Mbps on the UL and 100 Mbps on the DL [15].

- Peak spectral efficiency

  Peak spectral efficiency is a key performance indicator that measures the maximum achievable data rate normalized by the channel bandwidth, expressed in bps/Hz. The ITU-R has set a target of 15 bps/Hz in the UL and 30 bps/Hz in the DL. To meet these requirements, as well as the maximum data rate requirement mentioned above, 2 to 3 GHz of spectrum will be required [15].

- Area traffic capacity

  Area traffic capacity is a metric that measures the total traffic throughput provided per unit area in Mbps/m2. This Key performance indicator (KPI) has only been defined by ITU-R for indoor hotspot scenarios, with a DL target of 10 Mbps/m2 [15].

- Connection density

  Connection density refers to the number of devices connected or accessible in a given area. As an example, ITU-R has set a target of 1 million devices per square kilometer for mMTC services [15].

- Control plane latency

  The control plane latency represents the time required for a device to transition from the idle state to the active state, with the goal of achieving this transition in less than 20 ms [15].

- User plane latency

  Refers to the time taken by the radio network to transmit a packet from the source to the destination. It is measured as the time between when the source sends a packet and when the destination receives it. For eMBB services, the one-way end-to-end latency requirement is set at 4 ms, whereas for uRLLC services, the requirement is more stringent, at 1 ms [15].

- Area traffic capacity

  The ITU-R has defined the concept of area traffic capacity as the aggregate traffic volume serviced per unit geographic area, expressed in Mbps/m2. However, this metric has only been defined for the indoor hotspot scenario, with the goal of achieving a DL rate of 10 Mbps/m2 [15].

- Energy efficiency

  Energy efficiency is a critical consideration for both the network and the communication devices. The network-side metric is defined as the ratio of the amount of information bits transmitted or received to the power consumption of the radio access network (RAN), expressed in bits per Joule. On the device side, this measure is the ratio of the amount of information bits transmitted or received to the power consumption of the communication module, also expressed in bits per Joule. The ITU-R has specified that International Mobile Telecommunications (IMT)-2020 air interfaces should support high sleep rates and long sleep times to improve power efficiency [15].

- Connection density

  Connection density is a measure of the number of connected or accessible devices in a given area. For mMTC services, ITU-R has set a target of 1,000,000 devices per square kilometer [15].

- Mobility

  The mobility requirement in 5G refers to the maximum achievable speed while maintaining a certain quality of service and uninterrupted handover between different radio nodes and access technologies. In rural test scenarios, the user's average spectral efficiency must not fall below 0.45 bps/Hz in the UL when traveling at 500 km/h on a traffic channel link [15].

- Mobility interruption time

  The term "mobility interruption time" refers to the duration in which a device is unable to transfer data packets due to handover procedures. The ITU-R has set a minimum requirement of 0 ms for this metric, which implies that a make-before-break approach must be used. This approach involves establishing the connection to the new cell before dropping the old one [15].

- Reliability

  To define reliability in a 5G network, we refer to the probability of successfully transmitting a data packet prior to a specific cutoff time. The goal is to transmit 32-byte media access control (MAC) packets within 1 ms at the cellular edge of a busy urban area, with a success probability of 99.999% [11].

- Bandwidth

  The term "bandwidth" pertains to the highest attainable system bandwidth, wherein the capability to support a minimum of 100 MHz is required. Moreover, ITU-R advocates for a system that can support more than 1 GHz of bandwidth [15].

1.3.3 5G Technologies

There are several key technologies that make up the 5G system, including:

- Massive MIMO

  The MIMO technology has become a crucial element of wireless communication systems. Its primary purpose is to simultaneously send and receive multiple signals on the same radio channel, thus achieving high spectral and energy efficiency. However, early versions of MIMO proved to be insufficient in terms of throughput and connectivity reliability. To address these limitations, various MIMO technologies were developed, including Single-user MIMO (SU-MIMO), Multi-user (MU-MIMO), and networked MIMO, but none of them fully met the demands of end users. However, advances in massive MIMO, used in 5G networks, are solving this problem. This technology involves attaching hundreds or thousands of antennas to base stations to increase spectral efficiency and throughput. Using multiple transmit and receive antennas in massive MIMO raises the transmission rate. By shifting energy to smaller regions of space, massive MIMO allows for increased capacity, especially when multiple User equipments (UEs) are simultaneously generating downlink traffic. Unlike traditional systems, massive MIMO with beamforming and huge multiplexing techniques can collect data from different sensors with low latency, high data rate and higher reliability, streamlining the process for smart sensor implementations such as healthcare centers, self-driving cars, smart cities, smart grids, smart homes, smart highways, and smart companies. The main characteristics of massive MIMO technology in the context of 5G are the following:

1. **Number of user:** previous generations of wireless technology, ranging from 1G to 4G, employed only 10 antennas per cell. However, in 5G technology, each cell is equipped with over 100 antennas. This allows small cells to accommodate multiple users simultaneously [16], as depicted in Figure 1.3.

2. **Data rate:** massive MIMO is considered one of the leading technologies for providing high-speed wireless connectivity and achieving data rates that reach gigabit per second.

3. **MIMO role in 5G:** the application of massive MIMO technology is expected to be critical for the successful implementation of 5G wireless networks, since it can provide higher levels of spectral and energy efficiency.

4. **The relationship between the frequency of a wave and the size of the antenna:** the size of the antenna and the frequency of the wave have an inverse relationship, which implies that larger antennas are required for lower frequency signals and smaller antennas are needed for higher frequency signals.

- Non-Orthogonal Multiple Access (NOMA)

  NOMA is a critical radio access technique employed by next-generation of wireless networks. Unlike previous orthogonal multiple access methods, it provides several advantages such as low latency, high spectral efficiency, high reliability and massive high-speed connectivity. The main objective of NOMA

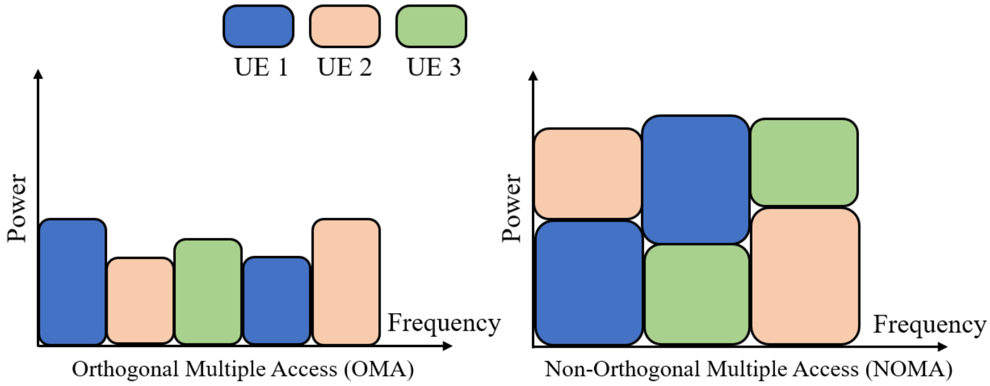

Figure 1.3: Major difference between OMA and NOMA.

is to accommodate multiple subscribers with identical resources regarding frequency, time and space. The NOMA's principle is illustrated in Figure 1.3. There are two major classifications of NOMA: code domain and power domain. NOMA in the power domain has become a popular choice for 5G wireless networks because of its compatibility with several wireless technologies, including beamforming, MIMO, cooperative communication, network coding, space-time coding, and full-duplex [17]. NOMA in the code domain is known to enhance the massive MIMO's spectral efficiency, thereby increasing the 5G's connectivity. Several multiple access techniques have been developed in code domain NOMA, including lattice partition multiple access, sparse code multiple access, patterned division multiple access, and multi-user shared access [18]. The 3GPP's conventional orthogonal frequency division multiple access (OFDMA) used in the 4G LTE network delivers poor spectral efficiency in cases where bandwidth assets were assigned to low channel state information (CSI) users. NOMA has been presented as a solution to this problem, allowing users to access all subcarrier channels, even those with low CSI, enabling users with high CSI to access the bandwidth resources allocated to users with low CSI, resulting in increased spectral efficiency. The forthcoming 5G network is anticipated to incorporate different architecture, wherein macro base stations and small cells cooperate to enable sharing the spectrum. NOMA has various applications, including machine-to-machine (M2M) communication, mMTC, and ultra-dense networks (UDN). Despite its many benefits, NOMA also faces some challenges. For example, executing CIS algorithms for a large number of users using high data rates requires significant computing power. In addition, managing NOMA's power allowance optimization gets difficult when users move from one network to another [19].

- millimeter Wave (mmWave)

  mmWave is a highly advantageous frequency band in 5G wireless networks due to its extremely high frequency range. This band uses a spectrum between 30 GHz to 300 GHz for transmission, which is known as mmWave since the wavelengths of these waves range from 1 to 10 mm. While satellites and radar systems already use millimeter waves, multiple cellular network companies have also begun to implement this technology to send and receive data across base stations. The use of millimeter wave technology is an effective way to increase the bandwidth of the spectrum and thus improve data transmission rates. The frequency band under 5 GHz is already heavily utilized, making mmWave technology an attractive option for 5G wireless networks [20]. By increasing the carrier frequency by 5% and utilizing frequencies between 28 GHz to 60 GHz, 5G wireless networks can achieve up to 2 GHz spectrum bandwidth. In comparison, 4G LTE only offers 100 MHz spectrum bandwidth with a 2 GHz carrier frequency. By increasing the spectrum bandwidth tenfold, mmWave technology significantly enhances transmission speeds [21, 22]. Further, low latency, massive data transfer, and high reliability have been shown to be provided by mmWave frequencies [23]. Despite the advantages offered by millimeter wave technology, there are a number of limitations that must be considered. First, its short range can be easily obstructed by common obstacles such as buildings, trees and even rain. In addition, the high penetration loss of mmWave signals through solid objects may result in lower interior coverage. In addition, the implementation of mmWave technology requires an expensive infrastructure that includes more base stations and antennas than lower

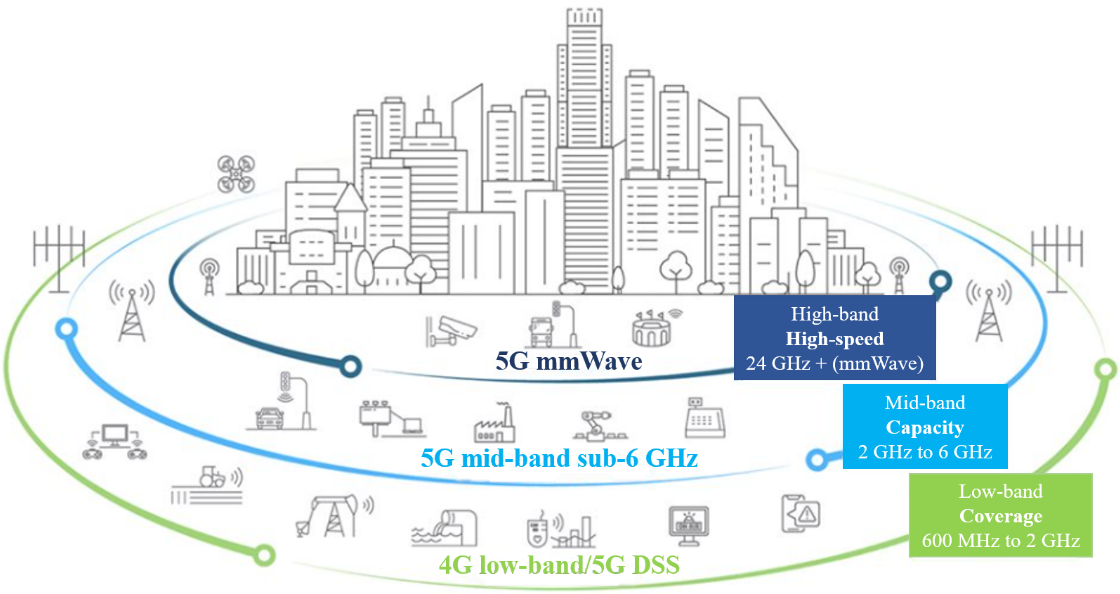

Figure 1.4: The frequency bands utilized in 5G technology [186].

frequency techniques, resulting in higher deployment costs. Finally, the higher power consumption of mmWave systems can reduce the battery life of mobile devices. Figure 1.4 represents the different frequency bands that are utilized in 5G network. The Figure illustrates three distinct frequency bands utilized in 5G technology: low-band, high-band, and mid-band. Each band presents its own set of advantages and challenges. These bands are defined as:

-The millimeter wave or high band: is characterized by its high speed and limited range. Operating within a frequency range of 24 GHz to 100 GHz, it enables multi-gigabit per second speeds, providing exceptional performance. However, its effectiveness is limited to short distances due to difficulties in penetrating buildings and walls.

-The 5G mid-band frequency range: offers a balance between speed and range. Operating between 2 to 6 GHz, it provides a wider coverage area compared to millimeter waves while still delivering gigabit per second speeds. The mid-band is commonly utilized in 5G technology, particularly in business campuses.

-The low band of 5G technology: offers long-range coverage but slower speeds.

Operating below 2 GHz, this band holds significant commercial importance for industries and experiences heavy congestion due to 4G LTE traffic. It is suitable for deploying IoT sensors in applications such as solar and wind farms spanning large areas

- 5G IoT-based approaches

  The IoT has experienced significant growth, thanks to advancements in wireless technologies, particularly with the emergence of the 5G network. Through IoT, sensors, appliances, objects, and devices are interconnected, enabling seamless communication. This connectivity facilitates the collection of substantial amounts of data from various sensors and devices. 5G offers ultra-fast connectivity speeds, making it ideal for efficient data collection, transmission, processing, and control in IoT applications. Moreover, 5G stands out as a favorable choice for IoT due to its cost-effective deployment options and the availability of unused spectrum [24]. Here are a few examples of IoT applications in 5G:

  1. **Smart homes:** the popularity of smart homes is growing rapidly, and 5G plays a crucial role in making them a reality. With its exceptional flexibility and ultra-fast monitoring capabilities, 5G enables seamless control of smart appliances within homes. The combination of low latency and high-speed connectivity offered by 5G makes it effortless to remotely manage home appliances.

  2. **Smart farming:** the agricultural sector also reaps the benefits of 5G technology. With the aid of Global Positioning System (GPS) technology and sensors, 5G assists farmers in real-time tracking of crop threats, enabling prompt management actions. Smart sensors utilized in this context can also facilitate pest and insect management, control of irrigation, as well as electricity consumption.

  3. **Smart cities:** the deployment of 5G wireless networks is instrumental in driving the development of various smart city applications. These applications

encompass automatic traffic management, local area broadcasting, real-time weather updates, efficient power supply, crowd management, smart lighting systems, energy conservation, emergency control, water resource management, and more.

4. **Autonomous driving:** the realm of autonomous driving heavily relies on the capabilities of 5G networks, which were unattainable with previous network technologies. This technology necessitates ultra-low latency and high-speed communication, which 5G readily provides. In the coming years, self-driving cars are expected to become increasingly prevalent with the advent of 5G networks. Leveraging 5G, vehicles will establish communication with other objects on the road, such as smart traffic lights, enabling enhanced coordination. The remarkable low latency feature of 5G plays a crucial role in making autonomous driving a reality, as split-second decision-making becomes crucial for avoiding accidents.

5. **Industrial IoT:** the integration of 5G technology into industrial settings brings forth a host of advantages, including enhanced energy efficiency, improved safety measures, optimized shipping processes, intelligent packaging solutions, automated equipment operations, and predictive maintenance capabilities. The implementation of smart sensors within industrial environments facilitates secure, intelligent, and cost-effective operations.

- 5G's machine learning (ML)

  ML techniques have seen increasing adoption in 5G networks, offering solutions to multiple complex problems that previously required manual tuning. ML methods can be categorized into three main types: reinforcement learning, unsupervised learning, and supervised learning.

  Reinforcement learning (RL) is particularly valuable for addressing uncertainties within the 5G network environment. Actor-critic reinforcement learning is employed for tasks like resource allocation and user scheduling. Quality of Experience (QoE)-based handover decision-making for HetNets utilizes Partially Observable Markov Decision Process (POMDP) and MDP. In HetNets, packet call admission is controlled, and in Cognitive Radio Networks (CRNs), channel access for secondary users is managed using ML techniques. Deep reinforcement learning (Deep RL) is leveraged to make decisions regarding mobility and communication channels, enhancing the learning rate of secondary users through anti-spam tactics. Various aspects of 5G network applications, including resource allocation and security, benefit from the implementation of Deep RL.

Unsupervised learning methods are employed to enhance network connectivity and performance seamlessly. Various aggregation techniques are utilized to minimize disruptions in the network by efficiently storing data center contents. In vehicle-to-vehicle (V2V) networks, handover optimization is achieved by analyzing mobility patterns. Detecting intrusions in wireless networks reduces network failures. Additionally, unsupervised soft clustering techniques help reduce latency. Nonparametric Bayesian methods, as a form of unsupervised learning, dynamically cater to user requests and demands, thereby reducing wireless network traffic. Other unsupervised learning methods, such as Affinity Propagation Clustering and Adversarial Auto Encoders (AAE), manage resources for ultra-dense small cells and identify abnormal behavior in the spectrum, respectively.

On the other hand, supervised techniques involve making decisions based on labeled training data. In this approach, the machine learns to predict and recognize patterns by generalizing from previously labeled examples. Various supervised techniques, such as logistic regression, support vector machines (SVM), random forest, decision trees, linear regression, and neural networks, are employed for tasks like regression and classification [25].

Machine learning is an integral component of artificial intelligence, focusing on the automated analysis and processing of data. By employing systematic models, ML identifies patterns and makes decisions with minimal intervention

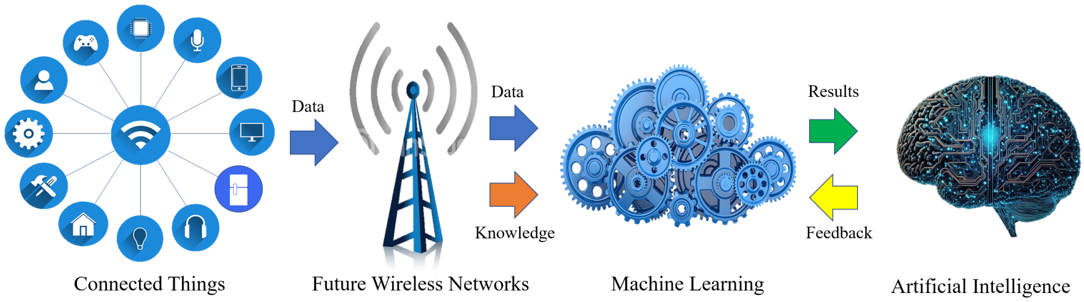

Figure 1.5: Machine learning with 5G.

of human. This enables efficient decision-making based on data-driven insights. Figure 1.5 illustrates this concept.

1.3.4 Advancements of 5G over 4G

This section provides descriptions of several novel features introduced in 5G technology compared to 4G. Specifically, it covers the concept of beamforming techniques, small cells, and Mobile Edge Computing (MEC).

1. **Beamforming**

   4G networks suffer from energy depletion and user interference due to the non-directionality of wireless signal waves. To solve this problem, 5G networks use beamforming technology, which provides directionality of signals, such as laser beams going from the base station to the user. This directional transmission gives the impression that signals are carried invisibly. Beamforming allows for faster data rates, which reduces interference and power consumption. Researchers have explored techniques [26], to improve system efficiency and reduce interference in the 5G mobile network.

   Beamforming technology enables the transmission of signals in a directional manner. Without beamforming, efficiently directing signals to specific locations in wireless systems, especially small cells, becomes challenging. By leveraging beamforming, small cells can effectively transmit signals towards desired directions, benefiting IoT systems, autonomous vehicles, laptops, and mobile phones. This technology improves the efficiency and energy consumption of

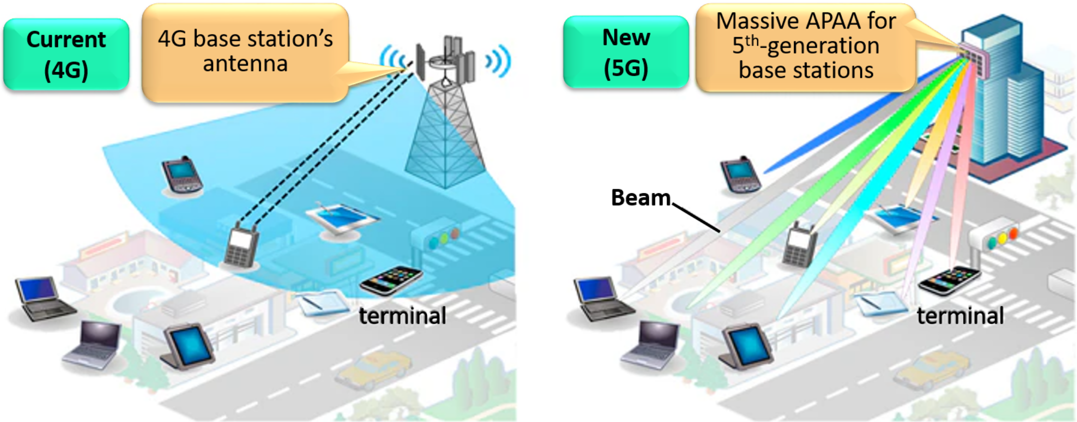

Figure 1.6: Difference between the beamforming in 4G and 5G.

5G systems. Beamforming can be classified into three types: analog, digital, and hybrid. Analog beamforming primarily focuses on enhancing coverage and mitigating the high path losses associated with mmWave frequencies in 5G NR. Digital beamforming, similar to multiuser MIMO in LTE Advanced Pro and 5G NR, enhances cell capacity by utilizing the same frequency to transmit data to multiple users. Hybrid beamforming, a combination of analog and digital approaches, is employed in 5G implementations using mmWave frequencies [27]. Figure 1.6 represents the beamforming's effect on the wireless transmission system.

2. **Small cells**

Small cells are cellular radio access nodes characterized by low power and operating within a range of 10 meters to several miles. Small cells have become a significant component of 5G technology, serving as low-power base stations that cover small areas. These cells stand out from their predecessors by their ability to handle high data rates while consuming minimal energy. In the 5G network, small cells facilitate low latency and high-speed functionality. They are compatible with advanced 5G technologies like beamforming, MIMO, and mmWave, which enable high-speed data transmission. The implementation of small cells is relatively fast and straightforward due to their simplified hardware design. In the market, three types of small cell towers exist: microcells,

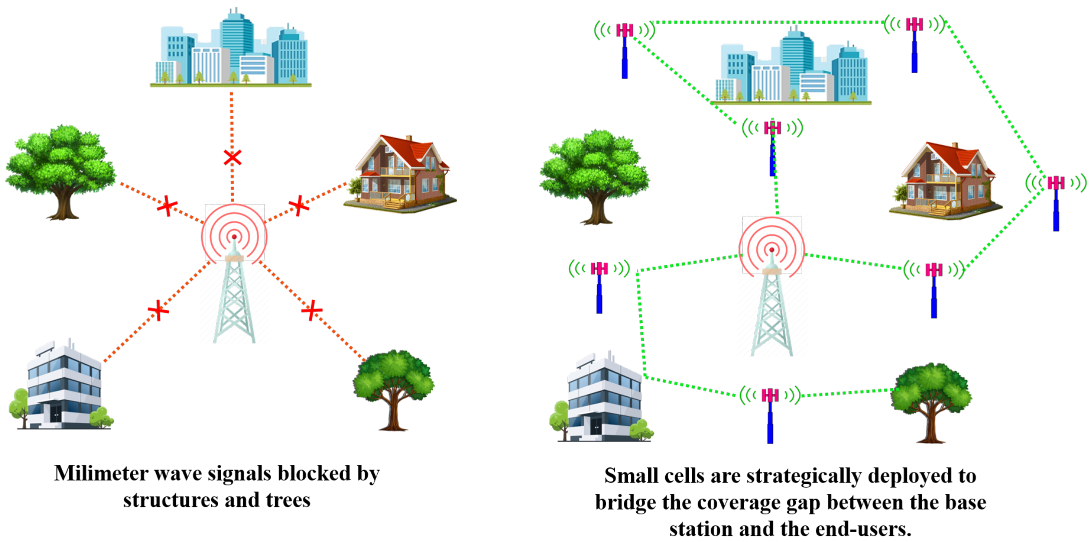

Figure 1.7: The important role of small cells in 5G communication systems.

picocells, and femtocells. To mitigate the challenges related to limited coverage, interferences, and energy loss in mmWave frequencies, a strategic deployment of multiple small cell stations has been employed. This approach aims to bridge the gap between base stations and end-users [28]. The implementation of small cells is contingent upon the population density of a given area, as their coverage range typically ranges from 10 to 90 meters. Researchers have also explored the simultaneous implementation of massive MIMO with small cells to enhance performance [29]. Figure 1.7 illustrates the positioning of small cells between base stations and users, effectively resolving signal blockage issues.

3. **Mobile Edge Computing (MEC)**

MEC represents an advanced iteration of cloud computing that brings cloud resources closer to end-users. While cloud computing offers numerous benefits, it is plagued by significant drawbacks such as high latency and remote data resources [30]. MEC addresses these limitations by establishing an edge infrastructure between the cloud server and user devices. With MEC, the need for users to download entire applications onto their devices is eliminated as the application is partitioned between the device and the cloud server. This

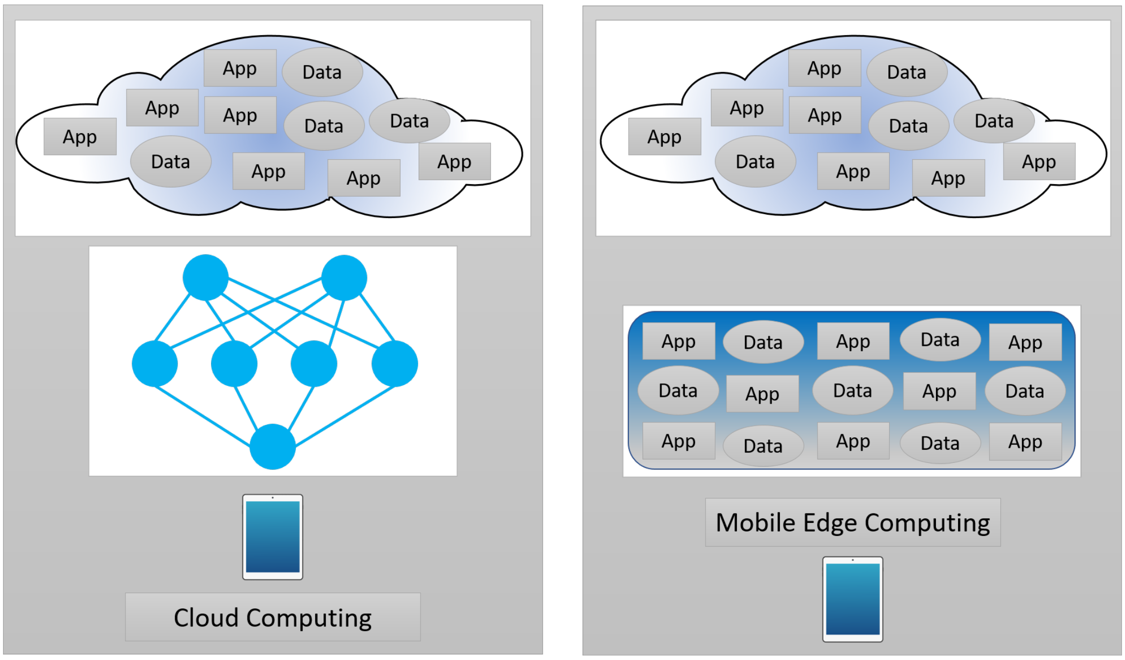

Figure 1.8: Key distinctions between MEC and traditional cloud computing.

approach enhances the performance of end-user devices. Extensive research [31, 32] has demonstrated the significant applicability of MEC within the 5G system. Figure 1.8 provides a visual representation of the key distinctions between MEC and traditional cloud computing.

1.3.5 5G NR: Spectrum, Numerology, and Waveform

As per 3GPP's Release 15, the initial version of 5G networks globally comprises two main components: the 5G NR serving as the air interface and the 5G Core (5GC). To fully deploy 5G NR, it is necessary to introduce new hardware while leveraging the existing infrastructure for reusability. The NR architecture provides for two deployment modes: standalone (SA) and non-standalone (NSA). SA architectures rely exclusively on the next-generation core (NGC) and operate on the basis of 5G specifications. In contrast, NSA mode uses existing networks and leverages current infrastructure, facilitating the seamless introduction of new technologies. To meet the requirements of 5G, certain attributes such as resilient numerology and spectrum integration are incorporated into the system. These attributes ensure a large number of UE connections and improved data rates. The 5G NR system uses the OFDM waveform, which employs unique numerology and spectrum that were not utilized in LTE. The adaptability of the physical layer in NR allows it to be implemented across a wide range of devices and applications. In contrast to LTE, the access procedures in NR differ in terms of signal reception. In NR, the indicated signal is transmitted specifically to the intended user rather than the entire cell. Furthermore, the transmission process is tailored to the user's needs, thereby enhancing the overall network performance.

In the 5G NR system, both Time Division Duplexing (TDD) and Frequency Division Duplexing (FDD) will be implemented for high and low frequencies, respectively. To dynamically allocate slots based on data traffic, NR utilizes dynamic TDD. Instead of Tail-Biting Convolutional Coding (TBCC) and turbo coding, NR adopts polar coding and Low-Density Parity-Check (LDPC) coding, respectively, to ensure transmissions with advanced data rates. The NR system maintains flexibility and mobility by incorporating interworking capabilities, allowing for the coexistence of different Radio Access Technologies (RATs). Enhanced Carrier Aggregation (CA) is provided to enable Dual Connectivity (DC), aiming to improve throughput and data rates through the combination of 5G NR and LTE's carriers [33, 34].

The 3GPP's release 15 encompasses fundamental elements of both 5G and LTE, commonly referred to as 5G NR. Within the 5G NR specifications, specific aspects such as synchronization, numerology, and waveform have been defined, further enhanced to better support diverse use cases and applications. The flexible architecture of 5G NR is designed to deliver high-speed data rates, low latency, seamless mobility, and enhanced reliability. The features enabling this flexibility are discussed in the following.

Spectrum

The 5G NR's flexibility stems from its architecture, which supports adaptable numerology and flexible spectrum allocation. In the context of 5G NR, the utilization of multiple frequency bands enables various communication functionalities. The focus of 5G NR is primarily on utilizing high-frequency bands, specifically mmWave,

Table 1.1: Major differences between the 5G NR's frequency layers [36, 37].

Designation	Frequency (GHz)	Bandwidth (MHz)	Spacing (kHz)	Coverage
FR1	<2	50/100	15	Wide
FR1	2-6	50/100/200	15/30.60	Medium
FR2	>6	200/400	60/120/240/480	small

to provide a wide capacity for traffic and improved quality of services. Moreover, the NR system is adaptable to support specific use cases such as uRLLC, eMBB, and MMTC. The primary modulation technique employed by 5G NR is OFDM. Unlike LTE/LTE-A systems with a subcarrier spacing of 15 kHz, the subcarrier spacing in 5G NR varies from 15 kHz to 240 kHz. The NR system operates in two frequency bands: FR1 (0.45 GHz to 6 GHz) and FR2 (24 GHz to 52.6 GHz), each serving specific frequency ranges [35]. Table 1.1 presents a breakdown of the spectrum into three frequency layers. The first layer comprises frequencies below 2 GHz, specifically dedicated to wide coverage and deep indoor scenarios. The second layer encompasses frequencies ranging from 2 GHz to 6 GHz, serving the purpose of capacity and coverage. These two frequency bands are part of the FR1 layer. The third layer involves frequencies above 6 GHz, primarily utilized for high-data-rate applications, and falls within the FR2 layer. Within the second layer, a range of frequencies, such as [3.3-4.2] GHz and [4.4-5] GHz, can effectively meet the majority of NR's use cases, offering optimal capacity and extensive coverage across KPIs [36]. It is advisable to attribute 100 MHz to each NR network from this frequency range. The below 2 GHz bands cater to uRLLC and mMTC applications, while the above 6 GHz bands are used for eMBB applications in 5G NR due to their higher capacity, lower latency, and faster data rates. In summary, the flexibility of the 5G NR spectrum is demonstrated through improved channel capacity, efficient bandwidth utilization, and the availability of narrower bandwidth options with reduced power consumption.

Table 1.2: The OFDM's subcarrier spacing with its modified parameters.

Spacing (kHz)	$T_{sym}(\mu s)$	$T_{cp}(\mu s)$	$T_{sym+cp}(\mu s)$	T_{slot}
15	66.67	4.69	71.35	1000
30	33.33	3.34	35.68	500
60	16.67	1.17	17.84	250l
120	8.34	0.585	8.92	125
240	4.17	0.293	4.46	62.5
480	2.08	0.146	2.23	31.25
$2^n\times$ 15				
(n=0,...,5)	66.67/2^n	4.69/2^n	71.35/2^n	1000/2^n

Numerology

The 5G NR prioritizes scalable numerology by increasing the spacing between OFDM subcarriers. The choice of spacing, ranging from 15 kHz to 240 kHz, depends on factors such as deployment scenario, carrier frequency, and service requirements. As indicated in the precedent table, the subcarrier spacing (SCS) of 15 kHz is supported in the frequency band below 2 GHz. In the frequency range of 2-6 GHz, the SCS can vary between 15 kHz, 30 kHz, and 60 kHz, depending on the specific service. For frequencies above 6 GHz, the employed SCS options are 60 kHz, 120 kHz, 240 kHz, or 480 kHz. The durations of OFDM slots, CP, and symbols also vary according to each SCS, as detailed in Table 1.2.

In the 5G NR system, the SCS is adjusted by multiplying the factor $2n$ by a base value of 15 kHz. The LTE system uses a fixed SCS of 15 kHz, whereas in 5G systems, n can take on integer values between 0 and 5. This allows for a range of available spacings, including 15 kHz, 30 kHz, 60 kHz, 120 kHz, 240 kHz and 480 kHz. For example, with $n = 0$, the spacing remains 15 kHz (15×2^0), while with $n = 1$, the spacing increases to 30 kHz (15×2^1). The 5G NR SCSs facilitate the creation of mini-slots, which improves the capabilities of the NR system. Successful transmission of extremely small packets is possible due to the presence of these mini-slots, which represent the smallest allocation of resource blocks (RBs) to users and carry the signal, enabling communication with low latency [37].

The NR's frame structure accommodates both TDD and FDD. The employed unit of time (T_b) is given as follows [35]:

$$T_b = \frac{1}{\delta f_s \times N_f} \tag{1.1}$$

The SCS in 5G NR is represented by the variable δf_s and can be adjusted using the factor $15 \times 2n$ kHz. The FFT size for 5G NR, denoted as N_f, is fixed at 4096. The frame duration (T_{fd}) is defined as:

$$T_{fd} = \frac{\delta f_s \times N_f}{100} = 10ms \tag{1.2}$$

The subframe duration (T_{sb}) is defined as:

$$T_{sb} = \frac{\delta f_s \times N_f}{1000} = 1ms \tag{1.3}$$

The 5G NR system divides each 10 ms frame into 10 subframes, each lasting 1 ms. Those subframes are autonomous units, allowing the decoding of information in a slot independently, without depending on other slots. Two half-frames of equal size are formed by combining five sub-frames. The number of slots and their duration in a subframe are flexible and determined by the value of $T_{sb}/2n$. For example, when $n = 0$, a subframe has a duration of 1 ms and contains only one slot. When $n = 1$, the slot duration is reduced to 0.5 ms and the subframe contains two slots. Each one of them contains 14 OFDM symbols having varying subcarrier spacing and CP length as listed in Table 1.2. The 5G NR system frame structure, including slot and subframe lengths, is shown in Figure 1.9. In the frequency domain, a resource block is formed by the combination of 12 subcarriers. The spacing between these subcarriers is flexibly determined based on the frequency range, according to the formula $15 \times 2n$ kHz. The flexible architecture of the 5G NR offers several advantages:

1. Low-latency enablement by offering mini slots.

2. Provision of large subcarrier spacing to mitigate inter-carrier interferences.

3. Improved power efficiency support for narrowband IoT.

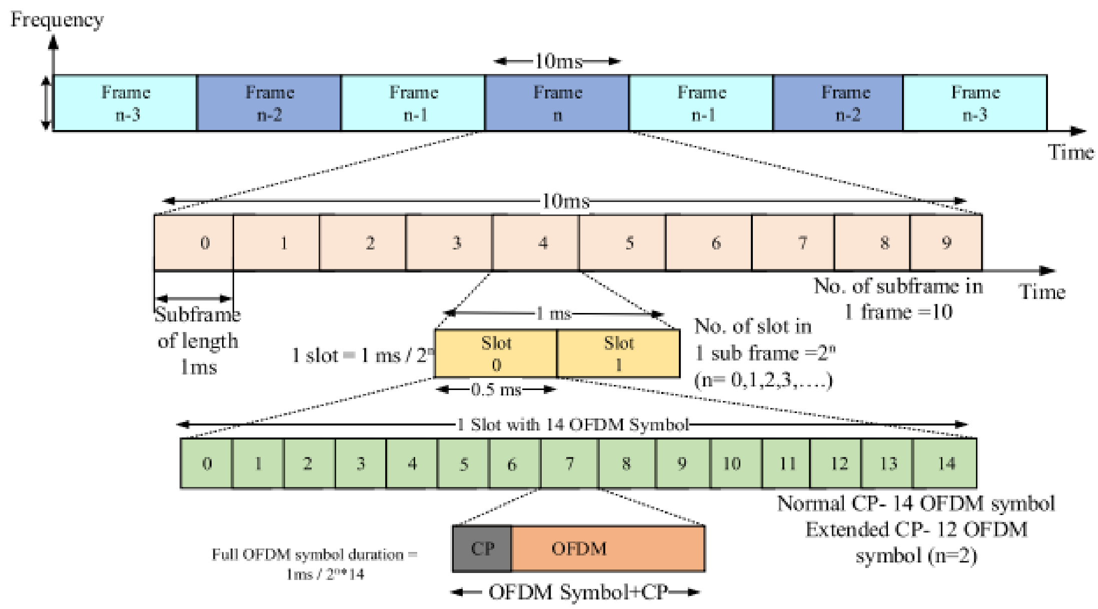

Figure 1.9: The 5G NR's frame structure.

Waveform

OFDM is the waveform chosen for the 5G NR system. It is a multi-carrier modulation technique widely used in various wireless communication technologies. OFDM has several advantages, including high spectral efficiency and the ability to achieve high bit rates even in frequency selective fading channels. In the NR architecture design, OFDM is used on both the uplink and downlink. OFDM was chosen as the primary waveform for the 5G NR system because of its significant advantages, such as:

1. **Spectral efficiency:** OFDM improves spectral efficiency by making efficient use of the available spectrum. To do this, the spectrum is broken down into a number of narrowly separated subcarriers, which can be attributed to different services or users. By allocating these subcarriers appropriately, the entire spectral efficiency of the system is maximized, allowing for optimal use of the available frequency resources.

2. **Scalability and flexibility:** this advantage is achieved through the flexibility to adapt to various bandwidth constraints and to accommodate various channel requirements. The OFDM waveform has the ability to easily adapt t,o and

support different frequency bands, as well as handle a wide range of data. As a result, it is well suited for deployment in various scenarios, providing the adaptability to meet varying network demands and requirements.

3. **Resistance to interference:** OFDM withstands both narrowband interference and multipath fading well. By using multiple subcarriers with orthogonal frequency spacing, it enables robust communication in environments characterized by changing the conditions of a channel, including city zones and domestic settings.

4. **Interoperability with Current Systems:** building on prior wireless transmission systems and leveraging accumulated expertise, researchers were able to capitalize on existing technologies and advance them for the 5G NR system.

5. **Optimal Resource Allocation:** In addition, data transmission will be optimized according to the user's needs and channel requirements using coding and modulation techniques and dynamic resource assignment support.

1.3.6 OFDM system model

The basic block diagram of OFDM is presented in Figure 1.10. In an OFDM system, the primary function of the transmitter is to map the initial message into a baseband sequence of modulated symbols. The data is divided into blocks of length N and converted into parallel streams. Each subblock undergoes an IFFT operation. To mitigate intercarrier and intersymbol interferences, a CP is added to each data block. At the transmitter side, the time domain signal is converted to analog using a discrete-to-analog converter and then amplified by an HPA. On the receiver side, the received signal is converted to digital, the CP is removed, and the FFT operation is performed. Finally, demapping is applied to reconstruct the original information.

The input block of symbols can be denoted as

$$\mathrm{X} = [X_1, X_2, X_3, ..., X_N]^T$$

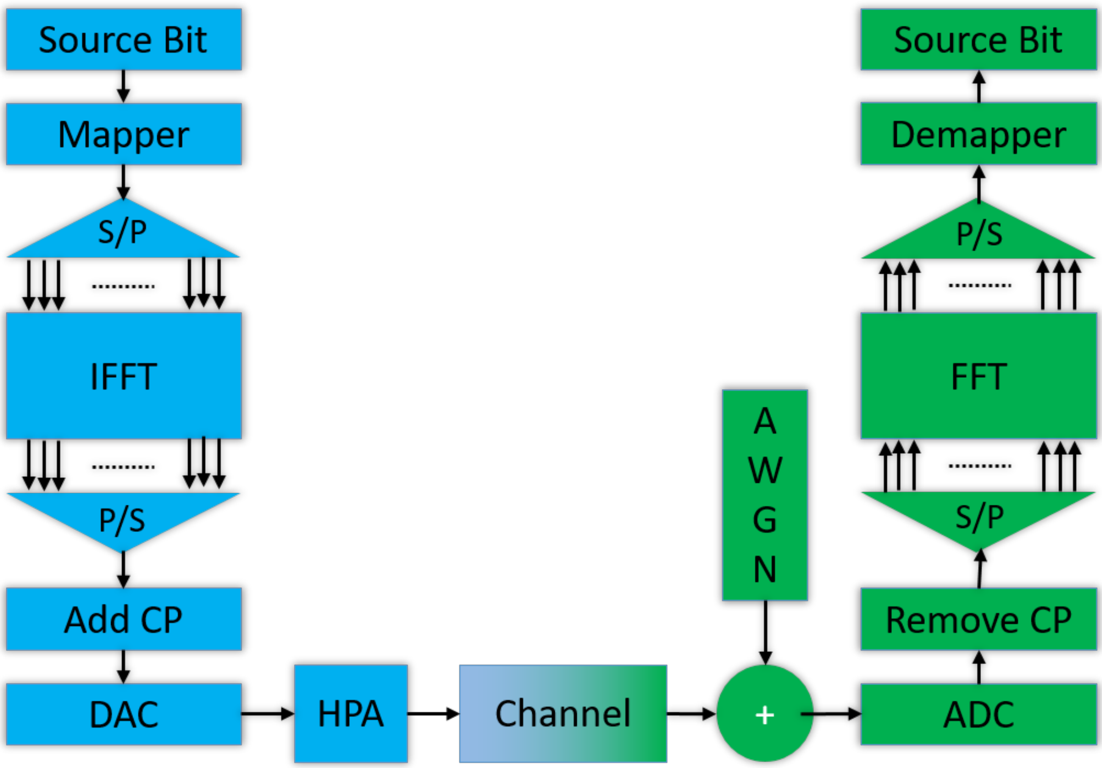

Figure 1.10: The basic structure of an OFDM system.

The duration of each symbol in the block X is denoted as T. The following equation expresses the transmitted OFDM signal.

$$X_n = \frac{1}{\sqrt{N}} \sum_{k=0}^{N-1} X_k e^{j\frac{2\pi}{N}kn} \qquad 0 \leq n \leq N-1 \tag{1.4}$$

- Peak to Average Power Ratio (PAPR)

  One of the challenges associated with OFDM waveforms is the high PAPR. System designers aim for high efficiency in RF power amplifiers, which is hampered by the high PAPR of OFDM waveforms. Although NR offers options such as CP-OFDM and discrete Fourier transform (DFT-S-OFDM) based schemes to mitigate PAPR, it remains relatively high, reaching up to 13 dB. This value increases further with larger bandwidths, which are often used in LTE-Advanced and 5G systems to improve data rates through carrier aggregation technology.

  Typically, amplifiers exhibit nonlinear distortion in their output signals when subjected to inputs that exceed their nominal values. This distortion arises

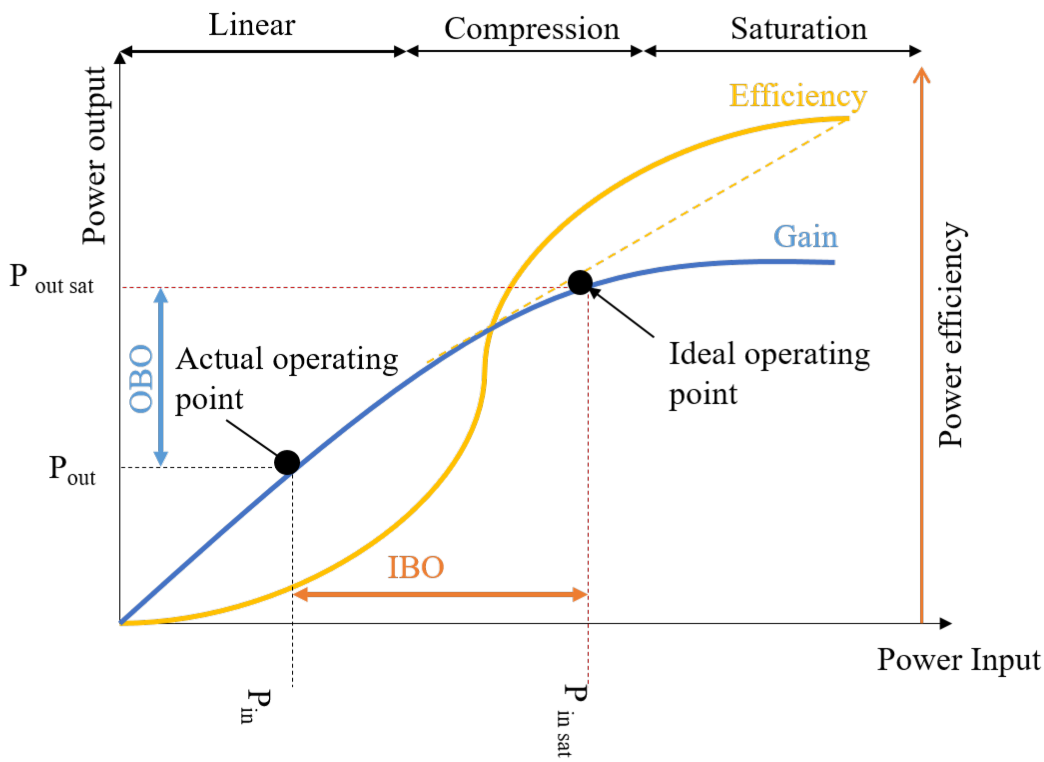

Figure 1.11: HPA's input/output characteristics.

from the saturation characteristics of the amplifiers when they process far higher input signals. The characteristics depicted in Figure 1.11 illustrate the relationship between the input power (P_{in}) and output power (P_{out}) of an HPA. The amplifier's saturation characteristic sets an upper limit on the output power, denoted as Pmax out, matching to a specific input power level, Pmax in. To ensure operation within the linear region, the input power needs to be reduced, which is commonly referred to as Input Back-Off (IBO) or Output Back-Off (OBO) [38].

$$IBO = 10log_{10}\frac{P^{sat\ in}}{P_{in}}, \qquad OBO = 10log_{10}\frac{P^{sat\ out}}{P_{out}} \tag{1.5}$$

The nonlinearity of the HPA can introduce in-band distortions that lead to rotation, attenuation, and offset in the received signal, as well as out-of-band radiation, affecting signals in neighboring frequency bands [39].

Defined as the fraction between the peak and the mean power, the PAPR of a transmitted OFDM signal can be given as follows:

$$PAPR = \frac{\max\{|x_n|^2\}}{E\{|x_n|^2\}} \tag{1.6}$$

Where $E\{.\}$ expresses the expectation operator. In order to estimate a veritable PAPR value of an OFDM signal, the oversampling factor L is commonly chosen as $L \geq 4$ [40].

- The CCDF of the PAPR

The OFDM signal's time domain representation, denoted as $x(t)$, is a complex-valued function. Given the assumption of independent and identically distributed imaginary and real components, with a Gaussian distribution characterized by zero mean and a variance of 0.5, as dictated by the central limit theorem for large values of N. A Rayleigh distribution will be followed by the amplitude $|x(t)|$ of the OFDM signal and its power distribution becomes exponential [39]. Thereby, we can derive the signal's corresponding CDF.

$$F(z) = 1 - e^{-z} \tag{1.7}$$

Assuming that the mean power of $x(t)$ is unitary ($E|x(t)|^2 = 1$), the distribution function of the probability that the PAPR ratio is below a given cutoff can be derived as follows:

$$Pr(PAPR < z) = (F(z))^K = (1 - e^{-z})^K \tag{1.8}$$

On the other hand, when evaluating the effectiveness of PAPR reduction techniques, it is common to evaluate the complementary cumulative distribution function (CCDF) of PAPR. The latter represents the probability that PAPR surpasses a specific cutoff value and is expressed as follows [39]:

$$Pr(PAPR > z) = 1 - Pr(PAPR \geq z) = 1 - (1 - e^{-z})^K \tag{1.9}$$

The high PAPR is a major drawback of OFDM systems. It causes a reduction in average power while requiring constant saturation power at the transmitter. The PAPR problem is most important on the uplink [41], which is the limiting connection with regard to range and coverage [42]. This becomes critical, as mobile terminals have limited battery power, making power amplifier efficiency crucial. In the context of 5G, there is a trend towards utilizing higher frequency bands to access more available spectrum. Extensive research [43] has already been conducted in this area. However, when deploying beamforming techniques in future 5G mobiles, and considering the low energy efficiency of power amplifiers, millimeter waves, and limited battery performance, the PAPR problem becomes even more severe [44]. In addition, achieving high output power is crucial, especially in V2V wireless communications and in wireless communication systems. However, power amplifiers with very high power capabilities tend to have low cost effectiveness and are cost prohibitive [45]. Therefore, in practical OFDM implementations, it is necessary to consider various measures to mitigate the high PAPR. Numerous PAPR reduction techniques have been proposed in the literature, which will be discussed in the upcoming chapter.

1.4 Conclusion

To facilitate comprehension and provide the necessary foundation for subsequent chapters, this chapter introduces the fundamental scientific background of 5G technology. It covers a range of topics including architecture, features and use cases of 5G NR, ensuring that readers have the appropriate knowledge and documentation to delve into the upcoming chapters. Firstly, a concise overview of the history of wireless communications is provided, tracing its evolution from the pioneering invention of the radio by Marconi to the revolutionary advancements leading up to the emergence of 5G technology. In the subsequent section, various use cases for 5G, which can be categorized into three major classes are explored. First, eMBB includes the application of advanced wireless technologies to improve data rates, network capacity, and latency, thereby improving the overall user experience. Second, we discussed mMTC, which is concerned with communication between a large number of devices not necessarily requiring high data rates or low latency, but focusing on connectivity and efficiency. Finally, we discussed uRLLC, which specifically addresses applications requiring extremely low latency, such as task and service critical. Following that, we emphasized the essential requirements of 5G and delved into its pivotal technologies, namely massive MIMO, NOMA, mmWave, IoT, and ML. Subsequently, we outlined the significant progressions brought about by 5G technology in comparison to 4G. These advancements can be succinctly summarized as beamforming, small cells, and MEC. Finally, we delved into the architecture and numerology of 5G NR, emphasizing the utilization of OFDM as the waveform of choice. We outlined the characteristics that make OFDM suitable for 5G, along with its major drawback, the PAPR, which needs to be mitigated before signal transmission. In the upcoming chapter, we will explore various PAPR reduction techniques employed in the OFDM system to minimize PAPR levels. Ultimately, we will select the most effective PAPR reduction technique, which will be thoroughly examined in chapter 3 and optimized using heuristic algorithms.

Success is Not Final;
Failure is Not Fatal;
It is the Courage to Continue that Counts.

— WINSTON S. CHURCHILL

2

Overview on PAPR reduction techniques in OFDM systems: Principle, Literature review, and Comparison

Contents

2.1 Introduction

OFDM is considered one of the most robust multicarrier modulation (MCM) techniques in wireless communication systems. This attractive transmission scheme offers high spectral efficiency and a strong immunity against multipath fading. However, the main drawback of this technique is the high PAPR. The latter occurs when a significant number of subcarrier components are coherently summed via IFFT operation [3]. Besides that, the power amplifier's nonlinearity degrades the systems' efficiency. Thus, applying a high-cost amplifier with sufficient dynamic range is essential [46]. Consequently, PAPR reduction is crucial in OFDM transmitters.

In the attempt to solve the PAPR problem, several approaches have been investigated. Such as clipping and filtering, tone reservation (TR), coding, tone injection (TI), selective mapping (SLM), and partial transmit sequence (PTS) [47]. Although clipping and filtering is an easy and simple implemented approach, it deteriorates the signal, and thus, it causes bit error rate (BER) degradation [41]. Compared with TR and TI, these two distortionless techniques aim to reduce the high PAPR by adding a data-block-dependent time domain signal to the original OFDM transmitted data. These two techniques are efficient in PAPR reduction, but their main drawback is increasing the energy of the transmitted signal [39]. The coding technique, introduced in [48] can diminish the PAPR of the transmitted OFDM signal. However, the high computational cost caused by the exhaustive search for the best codes is the major drawback of this approach. In the SLM method [49], a set of proper candidate data blocks representing the same information as the original data block is generated. Each data's aggregate is multiplied by a phase sequence after passing through the IFFT block. Then, the OFDM signal with the preferable PAPR is chosen for transmission. On the other hand, the main idea of the PTS approach is partitioning the input data block into several disjoint subblocks equal in size and located consecutively [5]. Each subblock is weighted by a phase factor. Those phase factors are chosen to reduce the high PAPR of the combined OFDM signal.

This chapter focuses on providing a comprehensive and in-depth description of various PAPR mitigation methods. The fundamental principles and modeling procedures of each method are thoroughly explained. A thorough literature survey is conducted for each technique, spanning from earlier approaches to the latest state-of-the-art schemes. Following that, a comparative analysis is performed, highlighting the advantages and disadvantages of each method, leading to the selection of the most promising one. The chosen technique will then undergo modifications and improvements, aiming to strike a favorable trade-off between PAPR reduction and the specific constraints imposed by the selected method.

2.2 PAPR mitigation techniques in OFDM systems

When dealing with dispersive channels, employing multicarrier transmission is indispensable to achieve high data rates. However, one crucial aspect that needs attention in the development of multicarrier transmission systems is the PAPR problem. Several PAPR mitigation methods have been extensively studied in the literature, including but not limited to:

2.2.1 Coding

The coding technique relies on choosing several specific codewords which lowers the PAPR [48]. This technique has several limitations such as its disability to provide a solution to the problem of error correction. Moreover, particularly when dealing with a large number of subcarriers, this approach is burdened by the requirement for an exhaustive search to find optimal codes and the necessity to use wide ranging lookup grids for encryption and decryption.

The researchers in [50] proposed a more appropriate technique, in which they involve the use of codewords derived from offsets of a linear code. This scheme combines the offset selection with the error correction characteristics of the selected code to decrease the PAPR of the transmitted signal. In [51], golay complementary sequence was employed for the modulation results monitoring in signals, which had a PAPR of up to two. In [52, 53, 54], additional improvements of this scheme were documented. Nevertheless, it is important to emphasize that these enhancements are specifically applicable to MPSK modulation. As N increases (N is the number of subcarriers), the feasibility of implementing these modifications diminishes due to the associated computational demands.

The practical advantages of coding for PAPR reduction are limited, as these methods are most effective for systems with only a limited subcarriers' number. Additionally, the exhaustive search required to find an optimal code is challenging. Therefore, the overall usefulness of coding for PAPR reduction in real-world multicarrier systems is restricted.

2.2.2 Clipping and Filtering

To mitigate PAPR, amplitude clipping is considered the simplest method [55]. The latter blocks the peaks of the input signal at a pre-set value while allowing the rest of the input signal to pass unaltered [56], expressed as

$$\begin{aligned} B(x) = \{x, \quad |x| \le A \\ Ae^{j\phi(x)}, \quad |x| \le A^{\intercal} \end{aligned} \tag{2.1}$$

In the above equation, $\phi(x)$ denotes the phase of x. The impact of amplitude clipping can be seen as an additional noise source, contributing to both in-band and out-of-band disturbances. In-band distortion, which cannot be mitigated by filtering, results in degraded error performance. On the other hand, out-of-band radiation decreases spectral efficiency, and thus, affecting whole spectrum usage. Out-of-band radiation can be addressed by filtering after clipping. However, this process can result in peak regrowth, leading to the signal exceeding the clipping threshold [39]. The latter can be lowered by repeating the process of clipping and filtering [57].

In the literature, several work have adopted the clipping and filtering technique to tackle the PAPR issue. In [58], authors have developed an optimized iterative clipping and filtering (ICF) technique in which, at each iteration, an ideal frequency response filter is determined using convex optimization schemes. The aim of the investigated design is to minimize signal distortion to ensure that the PAPR of the OFDM symbol remains below a predetermined threshold. In [59], an adaptive clipping and filtering method has been proposed. In this work, authors analyzed the conventional ICF technique's performance and proposed an adaptive alternative, in which, the signal is clipped with an adaptively modified clipping threshold (CT) during each clipping operation. Another study [60] focused on the clipping noise problem. The authors proposed an algorithm that solves the convex optimization task using various algebraic operations. In [61], an alternative clipping and filtering approach is introduced, which utilizes an optimized mapper based on artificial neural networks. The simulation results validate its superior performance, demonstrating favorable BER and cubic metric (CM) characteristics while requiring fewer computational resources. A modified PAPR reduction technique is proposed in [62], which uses a time-domain kernel matrix to generate the transmitted signal with reduced PAPR. This approach goes beyond the conventional assumption of uncorrelated parabolic pulses for clipping noise, making it suitable for a wider variety of situations. Another work [63] merges the clipping and filtering method with the selective mapping technique to mitigate PAPR and avoid signal distortion. A related work [64] investigated a new iterative flipping technique for mixed numerology systems. Initially, it was shown that due to repeated execution, extending the ICF method directly led to the build-up of inter-numerical interference (INI). To solve this problem, a noise-shaped ICF (NS-ICF) method was offered, using the clipping noise instead of the clipping signal. This approach effectively attenuated the INI without introducing additional interference. Additionally, the research tackled the problem of minimizing in-band distortion while adhering to the problem of PAPR. In [65], the performance of OFDM with the clipping and filtering scheme is reviewed and a closed-form simplified expression of the signal-to-noise-plus-distortion ratio (SNDR) is proposed. In addition, a new analyzer for the time-domain distortion compensation technique is studied. In [66], the study centers on an enhanced optimization algorithm combined with the clipping and filtering technique. The system uses the Lagrange Multiplier Optimization (LMO) approach, which was chosen for its ability to find the best solution efficiently within a minimum number of searches. In [67], the authors propose two effective techniques to mitigate PAPR. One of these includes a new clipping and filtering method. The latter is partitioned into two parts : in the first part, a set of cancellation signals is precomputed based on

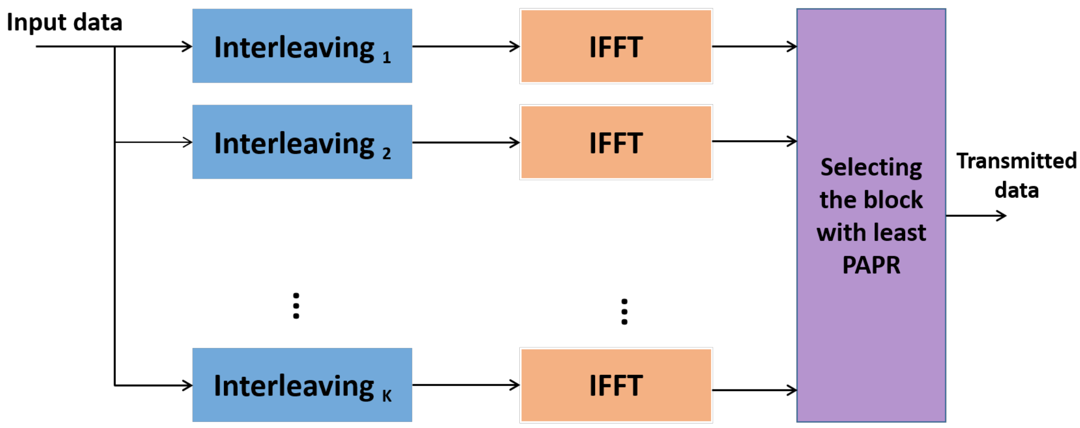

Figure 2.1: block diagram of an interleaver.

the OFDM system's configuration. These cancellation signals are designed to cancel out signals that exceed a predefined threshold. The second part of the scheme utilizes the precomputed cancellation signals to mitigate the peaks that appears in the signal.

2.2.3 Interleaving

As shown in Figure 2.1, an aggregate of interleavers is applied in this technique so that the arrangement of the symbols is reorganized. This results in a homogenized distribution of power [47]. To do this, we split the input data sequence into K blocks and then swap them, which helps to spread high-power symbols and reduce the PAPR ratio. Then, the PAPR is determined for both the original and the exchanged data blocks. Next, we select the data block with the least PAPR to be transmitted.

At the transmitter side, the original information is recovered by knowing the interleaver used. Here, the number of bits required to be transmitted as secondary information is $log_2 K$. However, the receiver may present an additional complexity.

Some studies have been devoted to the development of the interleaving technique such as, in [68], an interleaving method with no secondary information to be transmitted to the receiver has been presented. The method aim to increase the spectral efficiency and enhance the performance of the BER. In [69], the authors focused on improving the complexity of the interleaving technique. Another [70] merged the interleaving technique with the companding technique. The performance of the studied technique was compared with that of the original system, and

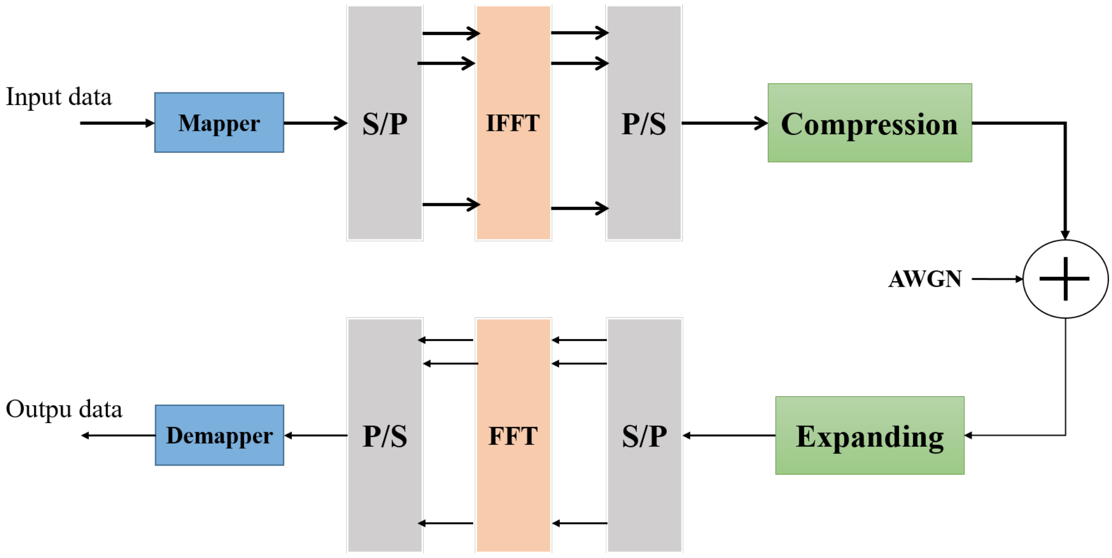

Figure 2.2: The principle of the companding system.

its effectiveness was proven. Further work on improving this approach can be found in the literature.

2.2.4 Companding

In this technique, the dynamic range, defined as the difference between the upper and lower signal peaks, is reduced. This method consists of compression and expansion. Compression is performed on the transmitter side, where a non-linear function is used to process the input signal. By using the A-law or the µ-law compression, the power of the high peaks can be reduced. While expansion is carried out on the receiver side, the reverse operation is performed using the inverse of the compression function used previously. With these functions, reduced peaks are maintained and originally weak peaks are expanded. In this way, the application of this technique helps to attenuate the PAPR. The block diagram illustrating its principle is depicted in Figure 2.2.

Similar to the previously discussed PAPR reduction methods, the companding technique has also been extensively explored and documented in the existing research literature. Jiang and Yang in [71] solved the problem of broadening only small signals using the µ-law function. They therefore proposed a new technique called exponential companding, which helps to enlarge both small and large signals with equal efficiency. In [72], Jeng and Chen proffered an efficient PAPR reduction technique involving the use of a trapezoidal distribution. Their technique offered good PAPR levels and BER performance. In order to compensate for the problem of the standard µ-law function discussed earlier, an attempt was made by Anoh et al in [73]. Their technique is based on using the roots of the envelope of the Rayleigh distribution in the companding technique. This technique achieves an acceptable balance between BER and PAPR. In [74], a compound between the nonlinear A-law compression method and discrete sine transform (DST) precoding has been realized and maintained for PAPR reduction in Filter Bank MultiCarrier with Offset Quadrature Amplitude Modulation (FBMC/OQAM) systems. This approach has reduced the PAPR by a rate of 84%. In [75], the authors developed and analyzed several companding methods, which maitain a resistant BER and a good level of PAPR. They also evaluated different compression functions and chose the best among them. Another technique studied in [76] merged the companding method with the PTS technique, benefiting from the advantages of both techniques, the PAPR diminishing ability is enhanced. In [77], a non-linear companding scheme has been investigated for optical orthogonal frequency division multiplexing (OOFDM). By proposing a new hybrid compensation scheme, remarkable PAPR and BER values were obtained.

2.2.5 Active constellation extension (ACE)

In the ACE [78], the PAPR ratio is minimized simply by pushing the outlying constellation points outwards from their original limits. Using QPSK modulation, the ACE principle can be explained simply. According to this fundamental, we have four constellation points, each positioned in a distinct quartet; these points have equal distances to the imaginary and real axes. The four quartets are regarded as decision regions, so the further a point is from the nominal limits, the greater the margin and therefore the lower the BER. Figure 2.3 highlights this concept. In the first quartet, the colored area indicates the area where the margin is extended, i.e.

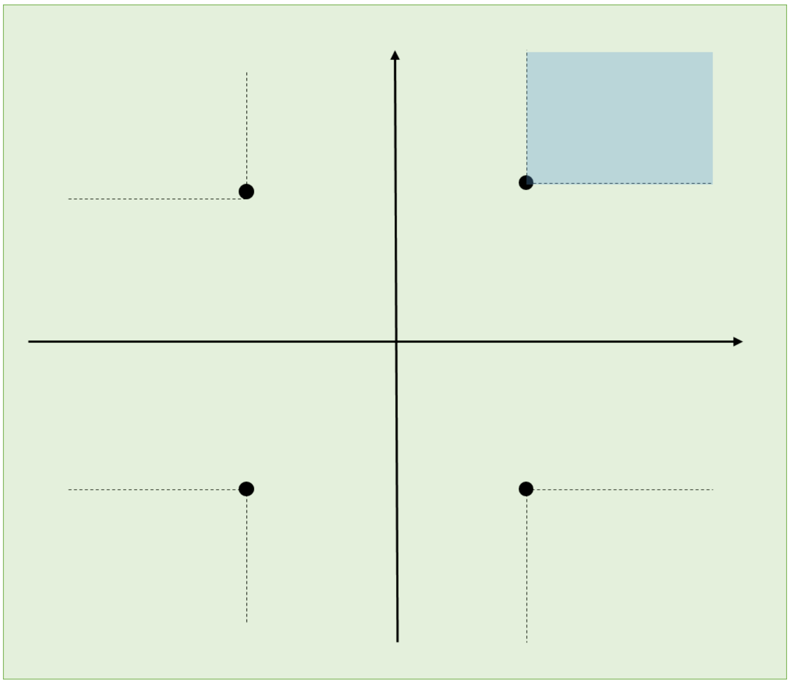

Figure 2.3:]
The principle of the ACE scheme using QPSK modulation [79]

the additional data symbols, which will be used to adaptively eliminate peaks in the transmitted signal.

ACE technology does not require the transmission of secondary information to the receiver. However, it does suffer from an increase in transmitted signal power. As a result, this system is particularly useful for high-sized constellation modulations.

Numerous resrach focused on the use of the ACE scheme to mitigate the PAPR phenomenon. In [79], the authors have introduced an ACE technique that adaptively extends the additional symbols in a dedicated channels for data transport. Another work [80] have dealt with the deterioration of ACE performance when the targeted clipping point is not known. In this context, an alternative ACE method with adjustable clipping monitoring have been investigated. In [81], a low-complexity ACE scheme is presented. In this method, a technique involving subcarrier clustering is adopted to improve the amount of liberty in the workflow of the optimization. In [82], a new chaotic ACE technique is investigated for OFDM systems. The presented scheme uses multiple data encryption in OFDM symbol interlacing. The technique enables safe transmission by means of a massive key space in the order of

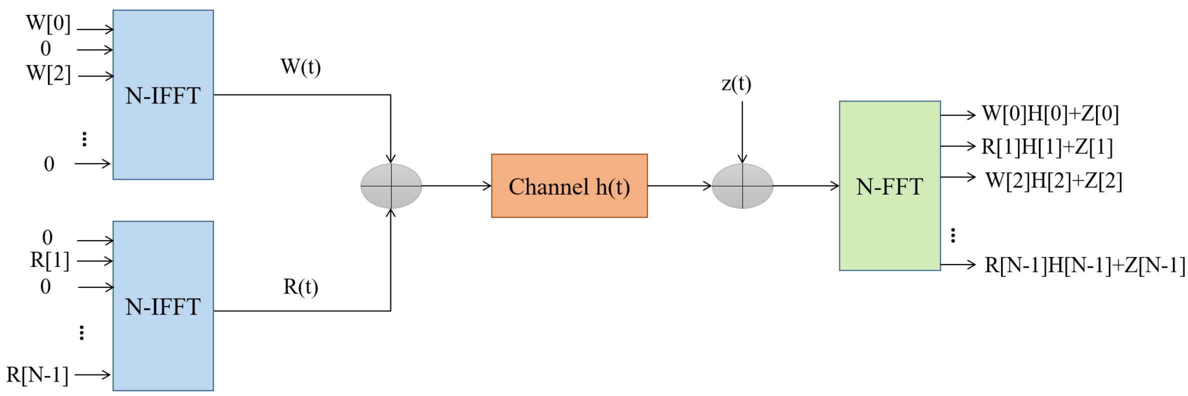

Figure 2.4: The principle of the TR scheme

2048. In [83], the authors attempted to fill the gaps in the literature and extend the applications of ACE by investigating a mathematical model for a standardized 2D constellation waveform. In [84], ACE has been used to shape the spectrum and precoding of the massive MIMO.

2.2.6 Tone reservation (TR)

The TR [85] technique consists of adding a time signal to the original waveform, depending on the data segment. At the receiver, this signal can be easily removed. The principle of this system is to allocate particular subcarriers for the transmission of extra signals, which are intended to attenuate the PAPR ratio. Figure 2.4 presents the TR's block diagram. Exclusively, the input signal undergoes the addition of a temporally added signal, also known as peak reduction tones (PRT). Subsequently, the input data sequence is divided into two distinct sequences: the data sequence W and the peak reduction sequence (PRT) R. The input data sequence is then designated as follows

$$\begin{aligned} If \;\; j \in M, \quad & W[j] + R[j] = W[j] \\ elseif \;\; j \in M^c, \quad & W[j] + R[j] = R[j] \end{aligned} \tag{2.2}$$

Where $W[j]$ represents the data tones and $R[j]$ represents the PRT. M and M^c represent data tones and PRT components respectively. Next, the IFFT is performed for each symbol as follows

$$w[n] + r[n] = \frac{1}{N} \sum_{k \in R^c} W[n] e^{j2\pi kn/N} + \frac{1}{N} \sum_{k \in R} R[n] e^{j2\pi kn/N} \tag{2.3}$$

In the previous equation, we note that the added signal $R[j]$ does not interfere with the data tone signal $W[j]$ thanks to the orthogonality of the subcarriers. If we suppose that the length of the CP is greater than that of the impulse response of the channel, the signal obtained at the receiver is noted as follows

$$\begin{aligned} H[k](W[k]+R[k])+Z[k] &= H[k]R[k]+Z[k] \qquad k\in M \\ &= H[k]W[k]+Z[k] \qquad k\in M^c \end{aligned} \tag{2.4}$$

In the above equation, the channel response is denoted by $H[j]$, and the additive noise DFT is expressed by $Z[j]$. Decoding is performed only for the tone of the data included in $M^c(k \in M^c)$. The TR system requires extra power to transmit the added symbols (PRT), as these function as a load, and the associated efficient rate of data is therefore reduced.

Several techniques have been investigated for reducing PAPR levels using the TR method. In [86], researchers developed a combined TR-OFDM method. The aim of the study was to address the complexity of the TR scheme using the compressive detection technique. In [87], an alternate TR method offering speedy convergence properties has been investigated. The latter is centered on the least-squares approximation (LSA) algorithm, which calculates the optimization ratio to be multiplied by the filtered clipping noise to obtain the peak nulling signal. Another study [88] focused on PAPR reduction by investigating a new TR scheme that uses cross-entropy to search for a sub-optimum PRT aggregate. In [89], Jiang et al presented a new technique, called CF-TR, which creates a peak attenuation waveform through the matching of the peak attenuation waveform with the clipping noise signal. Next, in [90], Tosato and Sandell studied a method that outperforms the active set method, which is known to have fast convergence and does not cause additive power to the original signal power. The method consists of an algorithm based on the sphere encoding and decoding principle, known as the tree search algorithm. In another publication by Li et al. [91], a study focused on applying deep learning to the TR technique has been reported. The authors investigated each layer of the deep neural network (DNN) and treated it as a trial for the TR. Recognizing that neural networks require learning, the proposed DNN has been trained to

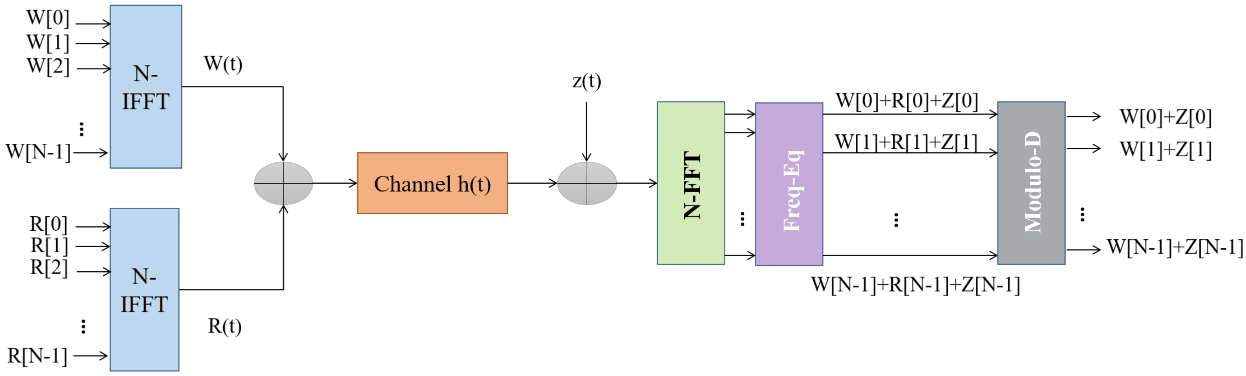

Figure 2.5: The TI 's block diagram

acquire the clipping ratio for each individual trial within the system. Later, El hassan et al [92] offered a detailed analysis of the TR scheme, its performance in reducing PAPR and the signal distortion that occurs at the end of the transmission system. Further, in [93], Tu and Chang proposed a new technique consisting of two phases for alleviating PAPR using the TR scheme.

2.2.7 Tone injection (TI)

Despite the effectiveness of the TR method in reducing PAPR, it does result in a reduction in data rate. In contrast, the TI [85] scheme allows PRT symbols to be superimposed on the data tones, so the data rate will not be altered. The TI's block diagram is presnted in Figure 2.5. The TI technique guarantees an additional freedom's degree that could be deployed to lower the PAPR factor, as it relies on increasing the size of the constellation. The equation below denotes the transmitted reduced-PAPR time-domain signal

$$\tilde{w} = w[n] + r[n] = \frac{1}{\sqrt{N}} \sum_{k=0}^{N-1} (W[k] + R[k]) e^{j2\pi kn/NL} \tag{2.5}$$

Where $r[n]$ expresses PAPR's attenuation sequence in the time domain and $R[k]$ its corresponding waveform in the frequency domain.

We can note that, in the frequency domain, PRT sequences and data tones are not orthogonally separated. Consequently, at the receiver level, the impact of $R[k]$ can be suppressed as follows : $R[k] = p[k].D + jq[k].D$. Where $p[k]$ and $q[k]$

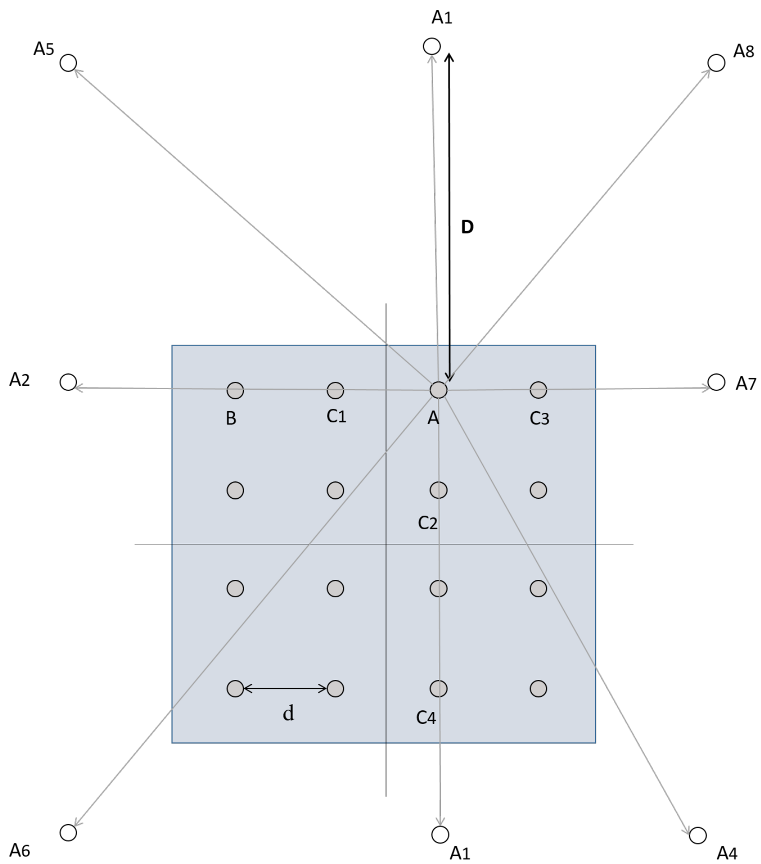

Figure 2.6: Expansion example for 16 QAM constellation

are factors used for PAPR reduction. D represents a predefined coefficient, a real number and positive. Consequently, at the frequency-domain exit of the equalizer, the modulo-D procedure is carried out on both the imaginary and real fractions to suppress $R[k]$. The below equation demonstrates this process

$$W[k] + R[k] + Z[k] = W[k] + p[k].D + q[k].D + Z[k] \tag{2.6}$$

A more sophisticated example can be exploited by showing the expansion effect in a constellation diagram. Figure 2.6 illustrates this example. In this figure, 16 QAM modulation is used. The grey dots represent the original QAM symbols, while the white ones indicate the extended symbols. Extended QAM symbols can be then designated by :

$$\tilde{W}[k] = W[k] + R[k] = W[k] + p[k].D + jq[k].D \tag{2.7}$$

The TI scheme does not suffer from data loss, as the PRT use the same data tones' subcarriers. However, it may require an increment in power in order to transmit the extended symbols.

To our best knowledge, work on TI dates back to 2005, when Wattanasuwakull and Benjapolakul [94] combined TI and TR techniques to create a new PAPR reduction variant. Then, in 2006, Han et al [95] published research on TI in PAPR reduction. The article tackles the TI's problem of power rising using a hexagonal constellation. In 2010, another work [96] addressed the problem of the high temporal spikes by reporting the cross-entropy scheme as a solver of a combinatorial optimization task that was principally provided by the TI scheme. Then, in 2013, Jacklin and Ding [97] highlighted the usefulness of the investigated linear scheduling for decreasing the intricacy of the TI approach. Next, Hou et al [98] proposed a new TI scheme offering lower intricacy. The authors of this work used the clipping noise method to seek the best constellation points (size and positions) in a minimal number of computations. In 2015, Lee et al [99] reported a modified TI approach, in which the authors used the genetic algorithm to optimize both PAPR and power augmentation. In 2016, researchers sought to minimize the complexity of the TI technique by limiting the investigation space, then, based on the distortion signals, the system identifies each subcarrier disturbance [100]. In [101], Hou et al attempted to solve the problem of TI complexity and BER deterioration by proposing two alternative approaches to the TI technique. The first applies clipping noise to determine the best constellation components. The second mitigates the non-linear distortion caused by the high-power amplifier. Next, in 2018, Chen et al [102] sought to improve the performance of single-carrier frequency-division multiple access in terms of PAPR reduction by developing a new scheme that merges TI and TR techniques. The main objective of this combination is to support the inherently poor data rate of the TR method. An iterative flipping algorithm was also used to handle the resulting massive computations. In 2020, Wang et al [103] grasped the revolution of the neural network (NN) in solving many tasks and employed it in the TR scheme to boost its capabilities. The technique involves setting aside a

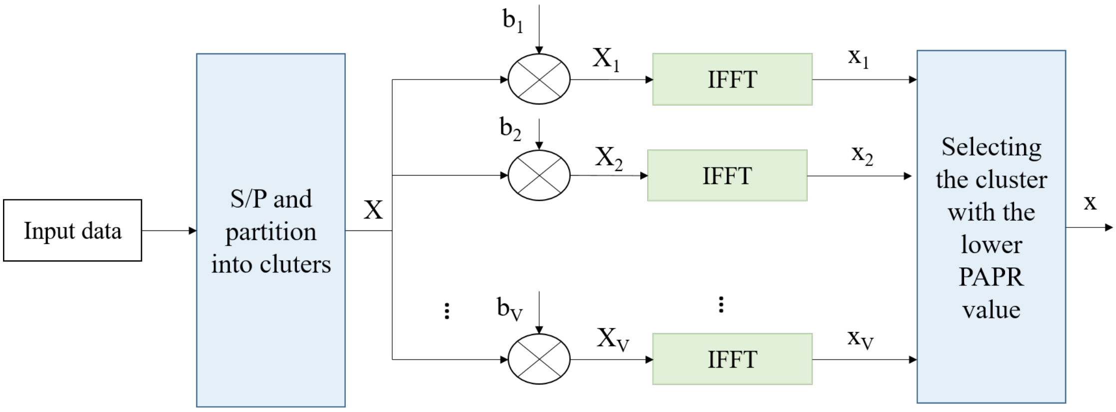

Figure 2.7: The SLM technique' block diagram

fraction of the data used to create a peak-deletion waveform. Then, on the basis of the feed waveform's properties, the approach studied uses a feedforward neural network to dynamically build up a spike cancellation waveform.

2.2.8 Selected mapping (SLM)

The SLM [49] is considered a robust, distortion-free system that relies on scrambling the signal to reduce its high temporal peaks. More precisely, in the SLM-OFDM transmitter system, several data clusters containing identical data as the input cluster are generated, then the cluster with the lowest PAPR is selected.

As shown in Figure 2.7, V different rotation factors are multiplied by V different SLM clusters. Each rotation factor compound is given as $b_v = [b_{v,0}, b_{v,1}, ..., b_{v,N-1}]^T$, where N represents the length of the rotation factor compound, and $v = 1, 2, ..., V$. The first cluster can be defined as the original cluster, for which purpose we define the rotation factor compound multiplied to it as a ones vector b_1 .

After scrambling the data clusters, the signal can be expressed as follows

$$X_v = [X_0 b_{v,0}, X_1 b_{v,1}, ..., X_{N-1} b_{v,N-1}]^T \tag{2.8}$$

After the IFFT block, the alternating time SLM signals are expressed as follows

$$x_v(t) = \frac{1}{\sqrt{N}} \sum_{n=0}^{N-1} X_n b_{v,n} e^{j2\pi\delta ft}, \qquad 0 \leq t < NT, \ v = 1, 2, ..., V \tag{2.9}$$

Next, the candidate signal with the lowest PAPR is selected for transmission. Secondary information must be transmitted to the receiver, as the phase factors compound used to scramble the signal must be re-used to reconstruct the original signal. The SLM technique therefore requires the transmission of $[Log_2 V]$ bits of information for each cluster. The number of phase factors can have an impact on the SLM performance.

Since the creation of the SLM scheme, a variety of methods have been dedicated on its development or modification as a means of mitigating PAPR in RF networks. The authors of [104] have introduced a new SLM method for coded OFDM to tackle the PAPR phenomenon. The principle of this method lies in inserting the peaks reduction compound into the coded OFDM control information symbols. In [105], the investigators described an SLM method that has no secondary information to send to the receiver, as this is known to result in a waste of data throughput and raise the computational load of the system. In [106], the authors used new rotation factors, introduced in the form of regularized Riemann matrices. The system achieved a PAPR value of 2.3 dB. In [107], the SLM approach was modified by the use of standard linear block programming matrices. In [108], an alternative SLM scheme that uses Alamouti coding and has a less optimal signal reconstructor installed at the receiver. The technique has mainly been studied for OFDM systems with spatial frequency block coded (SFBC). In [109], another variant of the SLM method is studied. In this technique, the peak-cancellation signal index is integrated into the data being transmitted. The results obtained are identical to those of the traditional SLM method, whilst the data rate has been enhanced. In [110], by merging SLM and chaos, the vector of rotation factors is obtained through chaotic vectors. This study enhanced the BER over the regular SLM scheme. Another work [111] used the Hadamard sequence in the SLM scheme to reduce high time peaks without requiring the transmission of secondary information. This study achieved a significant reduction in PAPR and a considerable improvement in BER. In [112], the analysts invoked the inverse of the fast Fourier transform (U) to produce U2/4 of candidate symbols . They underline the efficiency of their work compared to the state-of-the-art methods. In [113], a modified SLM approach has been presented. Its principle is based on the integration of pre-established interlacing modules

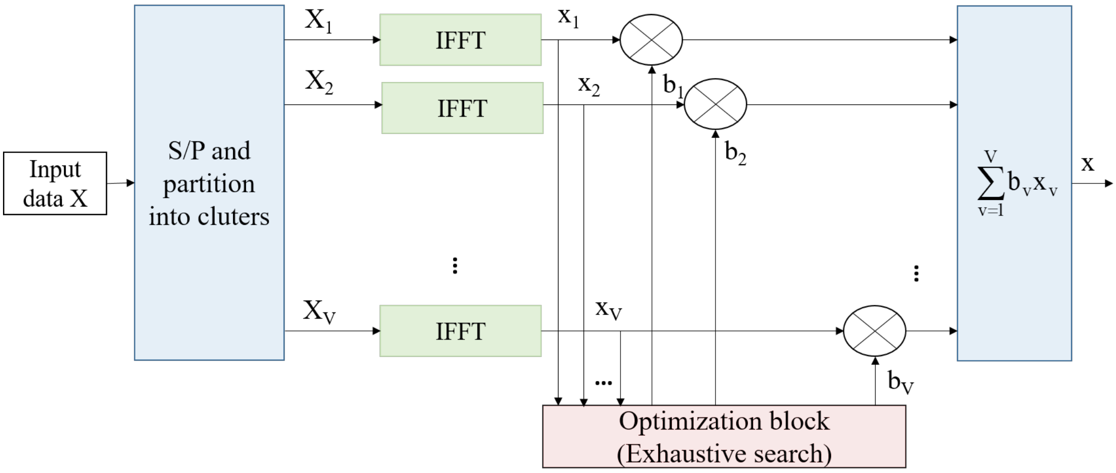

Figure 2.8: Ordinary PTS block diagram

in-between the mapper and the weight factor multipliers. The scheme has for advantages : performance improvement and secondary information exemption. In [114], an examination of the 5G candidate waveform has been carried out and an efficient SLM variant has been introduced. The results of the study were practical in the context of BER and PAPR capacity. In [115], an altered SLM scheme which uses multiple phase compounds has been deployed. The authors argue the suitability of their method for 64 QAM implementations for its good performance. Recently, in [116], the researchers investigated a closed-form algorithm in the SLM approach for attenuating PAPR measurements via component phase shifts. In [117], The PAPR mitigation for the OFDM-NOMA has been performed using a new SLM alternative.

2.2.9 Partial transmit sequence (PTS)

Figure 2.8 provides the principal structure of the PTS scheme [5]. In this approach, the N OFDM symbols in each X block of data are sorted into V separate identically sized groups.

$$X_v = [X_{v,1} \quad X_{v,2} \quad X_{v,N-1}]^T \qquad 1 \leq v \leq V \tag{2.10}$$

Such that

$$\sum_{v=1}^{V} X_v = X \tag{2.11}$$

After performing an IFFT operation for each group, a multiplication by an optimal rotation factor is provided. The latter is employed to reduce the high peaks appearing in a transmitted OFDM signal. The expression of the resulting signal is

$$x = IFFT\left\{\sum_{v=1}^{V} b_v X_v\right\} = \sum_{v=1}^{V} b_v IFFT\left\{X_v\right\} = \sum_{v=1}^{V} b_v x_v \tag{2.12}$$

The best-fit weighting factor vector, chosen to minimize the high peak levels in the transmitted OFDM signal, is introduced as

$$[\tilde{b_1}, ...\tilde{b_V}] = argmin_b = \left\{\max\left|\sum_{v=1}^{V} b_v x_v\right|\right\} \tag{2.13}$$

The expression of the resulting signal after the PAPR minimization process is as follows

$$x = \sum_{v=1}^{V} \tilde{b_v} x_v \tag{2.14}$$

The permitted set of weighting factors $\{b_v\}$ is provided below

$$b = \left\{e^{j2\pi i/W} \quad |i = 0, 1, ..., W-1\right\} \tag{2.15}$$

Where W represents the permitted number of weighting factors.

The PTS technique has as disadvantage, an exponentially rising complexity with the number of clusters. Thus, several researchers have developed in-depth techniques to solve the exponentially growing complexity problem.

In 2000, Jayalath et al [118] investigated a simplified PTS technique in which the optimization process is provided only for alternative partitions. Cimini and Sollengerger [119] developed an iterative PTS (IPTS) technique to reduce complexity. Nevertheless, the PAPR reduction performance has degraded. Likewise, L yang et al [120] sought to minimize the computational cost of the PTS method by introducing a new reduced-complexity PTS approach (RC-PTS). However, a degradation in the system's efficiency was perceived. A reduced complexity PTS scheme based on the study of the correlation between candidate signals was introduced in 2007 by Xiao et al [121]. In 2008, Ghassemi and Gulliver [122] developed a new PTS method based on the Radix FFT. The latter has considerably reduced the number of additions and multiplications the OPTS technique undergoes.

In 2010, Chen [123] proffered a new PTS scheme to diminish PAPR and computation intricacy using the Electromagnetism-like technique (EM). In 2017, Vittal and Naidu [124] presented an optimized PTS technique using a Random Phase Sequence Matrix (RPSM). In the same way, the authors of [125], and [126] attempted to solve the PAPR phenomenon, respectively, by proposing a PTS technique without side information and thus enhancing the BER performance and investigating an improved harmony search (IHS) algorithm. Another [127] proffered linear codes with the tiniest trellis to choose the transmitted waveform with the lowest value of PAPR. Additionally, a new method focusing on examining the available random access memory (RAM) data was introduced by Merah et al [128]. In 2019. Similarly, Al-jawhar et al [129] discussed a new low-complexity algorithm through merging gray code with left-feedback shift register operation using a particular mapping principle. In another effort to solve this problem, Zhou et al [130] proposed a novel PTS scheme based on two newly developed parameters for selecting the best time domain samples to further reduce the search complexity. Likewise, another research [131] suggested the insertion of a dummy sequence (DSI) in addition to a cyclic shift sequence (CSS) to overcome the high complexity problem without degrading the BER performance.

In 2022, Alameri et al [132] reported a new algorithm for clusters segmentation to minimize high PAPR levels in OFDM signaling. Similarly, Naidu et al [133] studied the different PTS segmentation schemes and provided a novel hybrid partitioning model that mitigates the computational intricacy phenomenon. In [134], fuzzy neural network was employed in the PTS method to mitigate the PTS' complexity. The technique combines the learning and reasoning abilities of the neural network and the fuzzy control scheme, respectively, to properly choose the signal' processing parameters. The results obtained demonstrate the validity of the studied technique as regards search complexity and PAPR reduction.

Another research [135] developed a new PTS scheme based on a centering phase sequences matrix algorithm. This technique provides an enhancement in the OFDM system' performance as it significantly lowers high PAPR levels. In [136], Goel and Gupta introduced a new PTS scheme, which addresses the transmitter' side information (SI) free transmission and the exhaustive search' complexity mitigation. The technique is based embedding the side information on the high power subcarriers' locations using particular segregations. On the other hand, at the receiver side, the SI is extracted using power disparity. This technique provides a reduced bit error rate (BER) degradation and have lesser computations compared to the ordinary PTS scheme. A hybrid PTS method was presented in [137]. The technique applies the Mu-law expanding and compressing techniques in the PTS scheme. A continuous-unconstrained particle swarm optimization (CUPSO-PTS) method was proposed in [138] to search for a suboptimal combination of phase factors. These are obtained by introducing several continuous-phase PTS methods, and a continuous-unconstrained investigating space is employed to determine the theoretical boundaries. The simulations prove the effectiveness of the method in providing good PAPR levels while saving 84.74% of the ordinary PTS' search complexity.

Another PTS technique based on the MIMO was proffered by Naidu et al in [139]. The latter investigates a reduced-complexity hybrid subblock segmentation for the PTS technique. In [140], Nguyen et al presented a novel PTS scheme, which applied phase quantization to lower the high peaks levels in OFDM systems, and permit the detection of the data without the need for side information. The technique utilizes a convex relaxation scheme, which converts into groups of convex programming the primary optimization task. A convergence to a suitable solution, which satisfies, in polynomial time, the karush-kuhn-tucker' (KKT) conditions is then provided.

2.3 Critical considerations in selecting PAPR reduction approaches

Selecting the most suitable PAPR mitigating scheme for system's implementation relies on several considerations. Diverse research papers have been devoted to review the PAPR mitigation approaches, describing their advantages, disadvantages, and drive comparisons between their performances, complexity, alignment with established standards, ...etc. In [141], investigators deployed a substantial work, in which they described several PAPR lowering schemes and cite several criteria of choosing the adequate technique for the situation. In [142], numerous methods for solving the PAPR problem have been examined. The analysis led to the finding that the balance between the added overhead of the PAPR reduction and the cost of energy inefficiency tilts towards favoring the initial approach. In [143], some of the effective PAPR attenuators were surveyed and several key factors to consider when choosing a suitable method were highlighted. In [144], researchers overviewed the traditional methods of PAPR minimizing and inferred that no one of the overviewed methods could be universally regarded as the benchmark for communication employments. Nonetheless, modified low complexity alternatives could be used for OFDM systems operating at elevated data rates. In what follows, we briefly review the key considerations of PAPR reduction methods:

1. **PAPR lowering performance** This is the primary consideration to examine when choosing a specific PAPR diminishing technique. However, it is crucial to be cautious about the potential drawbacks associated with certain methods, such as the clipping technique. The latter efficiently lowers the PAPR rates, but at the expense of the increase in the BER.

2. **Computational load (CL)** When evaluating PAPR reduction techniques, it is important to consider their complexity. Highly complex techniques, such as the partial transmission sequence (PTS) method, are effective in reducing PAPR. However, their computational burden makes them impractical. Consequently, researchers have explored various techniques to reduce complexity. Modified versions of the PTS have therefore been developed to strike a balance between PAPR reduction efficiency and computational complexity, making them effective on both counts.

3. **Bit Error Rate degradation (BER)** The BER is a crucial metric that requires careful consideration during the selection process. If a PAPR reduction method exhibits a higher BER compared to the conventional system, it becomes ineffective, and practical attention should be redirected accordingly.

Table 2.1: PAPR reduction techniques and their key comparative aspects [146].

Scheme	PAPR reduction	Distortionless	CL	BER Degradation	PR	LDT
TR	High	Yes	High	No	No	Yes
TI	High	Yes	High	No	Yes	No
SLM	Medium	Yes	Medium	No	No	Yes
PTS	High	Yes	High	No	No	Yes
ACE	High	Yes	High	No	Yes	No
Coding	Medium	Yes	High	No	No	Yes
Companding	High	No	Low	Yes	No	No
Interleaving	Low	Yes	Medium	No	No	No
Clipping and Filtering	High	No	Low	Yes	No	No

Additionally, techniques that rely on secondary information at the receiver demand extra attention since an error in the side information can potentially corrupt the entire data frame. In such cases, the use of coding and encryption methods can provide necessary safeguards to attenuate the impact of errors and preserve data accuracy.

4. **Power rise (PR)** Increased power is another important factor to consider in wireless systems. The more power the PAPR reduction technique requires, the more BER is degraded through the power normalization process.

5. **Loss in data rate (LDT)** Many PAPR mitigation methods require additional processing overhead or signaling, leading to a deterioration in data throughput. It is therefore essential to consider the trade-off between PAPR attenuation and loss of data throughput when considering an appropriate PAPR attenuation design.

Table 2.1 considers and compares the reported PAPR mitigation schemes in this chapter.

Among the precedent approaches mentioned for reducing PAPR, we find the PTS technique particularly intriguing. PTS is a scrambling scheme that effectively attenuates PAPR without introducing signal distortion or degrading bit error rate (BER). Its outstanding PAPR reduction performance has made the method particularly attractive. In addition, the PTS technique offers the advantage of adaptability, as it can be customized to suit specific system constraints by adjusting the number of subcarriers and rotation factors. This flexibility gives it an advantage over other techniques such as TR and SLM. Although the PTS technique is known for its high computational load, many low-complexity variants have been studied in the literature, in order to strike a balance between PAPR reduction and computational requirements. On the other hand, techniques such as SLM and ACE tend to impose a higher computational load due to the need for inverse Fast Fourier Transforms (IFFTs) or additional processing steps. Another remarkable aspect of the PTS technique is its precise selection of phase weighting factors to minimize performance degradation (such as BER degradation), thus maintaining signal quality. In contrast, techniques such as clipping can introduce distortion, which has a negative impact on signal quality. The suitability of the PTS method in an OFDM system generally depends on various factors associated with the communication system, including specific implementation, cost considerations, complexity, weight, quality requirements and data transmission rate. For example, a system designed for high data rates may prioritize low computational complexity, while a system emphasizing high-quality transmission would require an outstanding reduction in PAPR. Consequently, a compromise exists between PAPR lowering efficiency versus computational difficulty within the PTS approach [145].

2.4 Conclusion

In this chapter, various PAPR mitigation approaches have been reported, such as clipping and filtering, companding, coding, interleaving, TR, TI, SLM, and PTS. The principle of each method is discussed and its corresponding literature work are also included. This chapter is for reason to select the most adequate PAPR reduction method. Each PAPR reduction method has its advantages as it has its disadvantages and the choice of the appropriate method depends on the specific system requirements, constraints, and trade-offs. The PTS technique has proved very interesting. It effectively attenuates the PAPR ratio without introducing signal distortion or degrading the bit error rate (BER). In addition, this technique has the advantage of being adaptable, as it can be customized to meet the requirements of a specific system by adjusting the number of subcarriers and rotation factors. This flexibility gives it an advantage over other techniques.

The high complexity of the PTS scheme can be reduced using different modifications and adjustments. However, on the other hand, techniques such as SLM and ACE tend to impose a higher computational load due to the need to perform IFFT or additional processing steps. The PTS technique maintains signal quality, thanks to the precise selection of phase weighting factors that minimize performance degradation. Conversely, techniques such as clipping can introduce distortion, adversely influencing signal quality.

In the following chapter, two new PTS-based PAPR reduction techniques have been investigated to mitigate the high complexity related to PTS, resulting in a beneficial compromise between reducing PAPR and complexity.

do not say a little in many words,
but,
a great deal in few...

— PHYTHAGORAS

3

Contribution Models : Two Efficient PTS-based Meta-heuristic Algorithms for PAPR Reduction in OFDM Systems

Contents

3.1 Introduction

Having carried out a comprehensive review and comparison in the previous chapter of PAPR reduction methods, we determined that the PTS technique was of great interest. This technique has an inherent PAPR reduction performance, adaptability to different numbers of subcarriers and modulation types, and the advantage of preserving signal integrity. The approach involves combining scrambled signals from groups of partial transmission sequences. Scrambling is achieved by multiplying each sub-block of the ordinary PTS (OPTS) technique by an appropriate phase factor chosen to minimize the PAPR of the transmitted signal. Finding the optimal set of phase factors involves an exhaustive search, which poses significant complexity. In particular, as the number of sub-blocks (V) increases, a significant number of W^{V-1} searches must be performed to identify the optimal solution. Undoubtedly, as the values of V and W are raised, the quantity of available alternative signals rises, resulting in enhanced PAPR measurement. Nevertheless, when $W \geq 4$ and $V \geq 8$, the number of required searches to obtain a solution exceeds 4^{15}, equivalent to 16384 searches. This renders the technique impractical due to its excessively high computational burden. Extensive research in this field has led to the exploration of numerous techniques aimed at reducing the complexity associated with the PTS technique. Nevertheless, finding a favorable balance between reducing PAPR and minimizing search complexity remains an active and ongoing area of research.

In this chapter, we will develop two approaches for reducing the complexity of the PTS technique. These involve combining the PTS technique with a naturally inspired meta-heuristic algorithm. The rationale behind this combination lies primarily in the ability of the meta-heuristic to tackle non-linear, complex and time-consuming tasks efficiently, while at the same time exhibiting properties of speed and accuracy.

In order to tackle the intricate nature of the PTS system, our initial contribution will revolve around the investigation of an enhanced particle swarm optimization

(PSO) algorithm. The enhanced PSO is developped to address the main issue encountered with the conventional PSO technique, which is premature convergence and the inclination to become stuck in local optimal solutions. In our proposed algorithm, we introduced a novel coefficient, Rbest, into the velocity formula to promote diversity and enhance the solution's accuracy. This improved PSO algorithm will be subsequently integrated with the PTS scheme to efficiently search for the optimal sequence of phase factors that minimizes the PAPR, while keeping the complexity at a significantly reduced level. To showcase its superior efficiency, we compared the performance of our proposed algorithm against other effective optimization techniques.

Our second contribution will relove around a new PTS technique based on an improved whale optimization algorithm (IWOA). As far as we know, the IWOA-PTS technique has not been the subject of any prior research. The whale optimization algorithm (WOA)[146] is a highly robust algorithm that has been extensively employed in various research studies to effectively optimize complex problems. In this study, we will employ the IWOA proposed by Chakraborty et al [147] in the OPTS technique, primarily due to its superior capabilities in addressing issues like stagnancy in local optima, rapid convergence, and a well-balanced exploration-exploitation trade-off. We will compare the performance of IWOA with other robust meta-heuristic optimization algorithms to assess its efficiency in reducing PAPR.

3.1.1 PTS technique and problem formulation

The PTS technique utilizes a scrambling approach to mitigate PAPR in the transmitted signal. As depicted in Figure 3.1, the technique involves dividing the input data block into multiple V subblocks using a suitable type of segmentation, such that $X = [X_1, X_2, ..., X_V]^T$. Subsequently, scrambling is applied to each subblock individually. To elaborate further, every X_v subblock within the PTS scheme undergoes an IFFT operation, followed by multiplication with a phase factor b_v. It should be noted that b_v is defined as $e^{j\phi v}$, where v ranges from 1 to V.

The transmitted signal with least PAPR can be then given as:

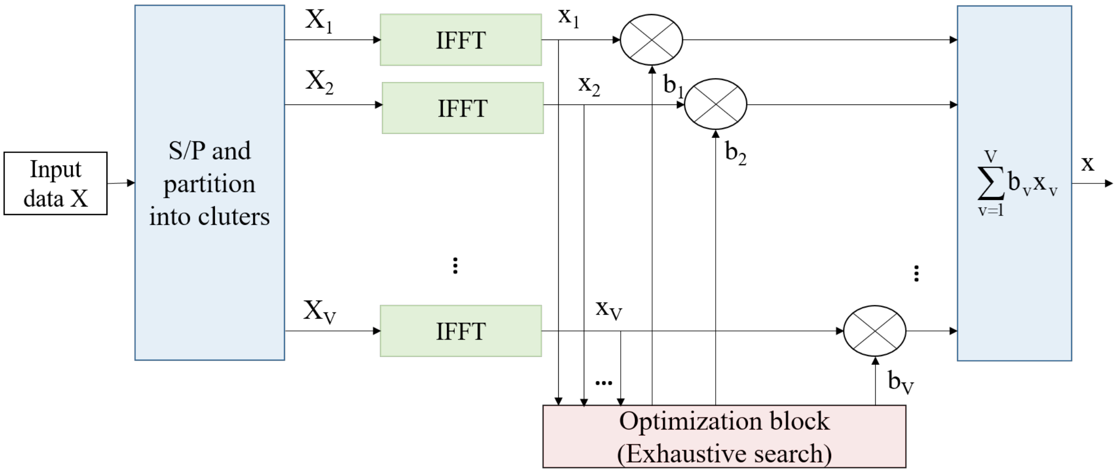

Figure 3.1: Ordinary PTS block diagram

$$x = IFFT\left\{\sum_{v=1}^{V} b_v X_v\right\} = \sum_{v=1}^{V} b_v IFFT\left\{X_v\right\} = \sum_{v=1}^{V} b_v x_v \tag{3.1}$$

The sequence of phase factors is selected in such a way that it minimizes the PAPR.

$$[\tilde{b_1}, ...\tilde{b_V}] = argmin_b = \left\{\max\left|\sum_{v=1}^{V} b_v x_v\right|\right\} \tag{3.2}$$

Where $[\tilde{b}_1, \ldots\ldots, \tilde{b}_v]$ denotes the optimal phase factors sequence by which the minimum PAPR is achieved. The term "$argmin$" indicates the "lowest value" achievable through the use of phase rotation factors. The obtained waveform with the minimal PAPR is given as follows:

$$x = \sum_{v=1}^{V} \tilde{b_v} x_v \tag{3.3}$$

Generally, the phase factors are commonly taken constant to avoid further complex multiplication operations. The set of phase factors $\{b_v\}$ is provided below

$$b = \left\{e^{j2\pi i/W} \quad |i = 0, 1, ..., W-1\right\} \tag{3.4}$$

Where W represents the permitted number of weighting factors.

In the optimization process performed by the exhaustive search, if we set the first element of the phase factors to 1, the number of searches performed by the technique is W^{V-1}, representing a complexity that grows exponentially with the increase in the number of subblocks. As we know, the PAPR reduction performance of the OPTS improves with the increase in the number of subblocks (see Fig. 3.2), mainly due to the increase in the number of alternative signals. This method is then considered impractical, especially for $W \geq 4$ and $V \geq 8$, since ≥ 16384 searches will be performed to obtain the optimal combination of phase factors. Thus, this study presents two novel PTS techniques with reduced complexity. Their concept will be disclosed in what follows.

Figure 3.2 shows the CCDF curves for PAPR reduction of the OPTS technique for different sets of phase factors (W) and numbers of sub-blocks (V), as well as the CCDF curve of the OFDM signal without PAPR reduction.

As can be seen, the PAPR reduction performance of the OPTS improves by increasing V and W, mainly due to the increase in the number of alternative signals since W^{V-1} candidates are there. Clearly, for $W = 2$ and $V = 4$, $2^3 = 8$ alternative signals are present; while for $V = 16$, there are $2^{15} = 32768$ candidates. For $V \geq 8$ and $W \geq 4$, the problem space becomes large and difficult to handle. Therefore, the investigated techniques are studied for $V \geq 8$ and $W \geq 4$, where the OPTS technique becomes impractical due to its extreme complexity. In scenarios characterized by large-scale, complex, and time-consuming problems, the utilization of meta-heuristic algorithms becomes indispensable to attain near-optimal solutions while significantly reducing the computational burden.

3.2 PTS-based meta-heuristic algorithms: literature review

Contemporary literature pays attention to meta-heuristic algorithms to solve time-consuming problems. Several works have been devoted to using meta-heuristic algorithms in the PTS technique to lower its complexity.

A hybrid partial transmit sequence (PTS) scheme based on the artificial bee colony (ABC) was presented in [148]. Although the exploration space provided by this method is ample, the convergence speed of the algorithm is slow. Another

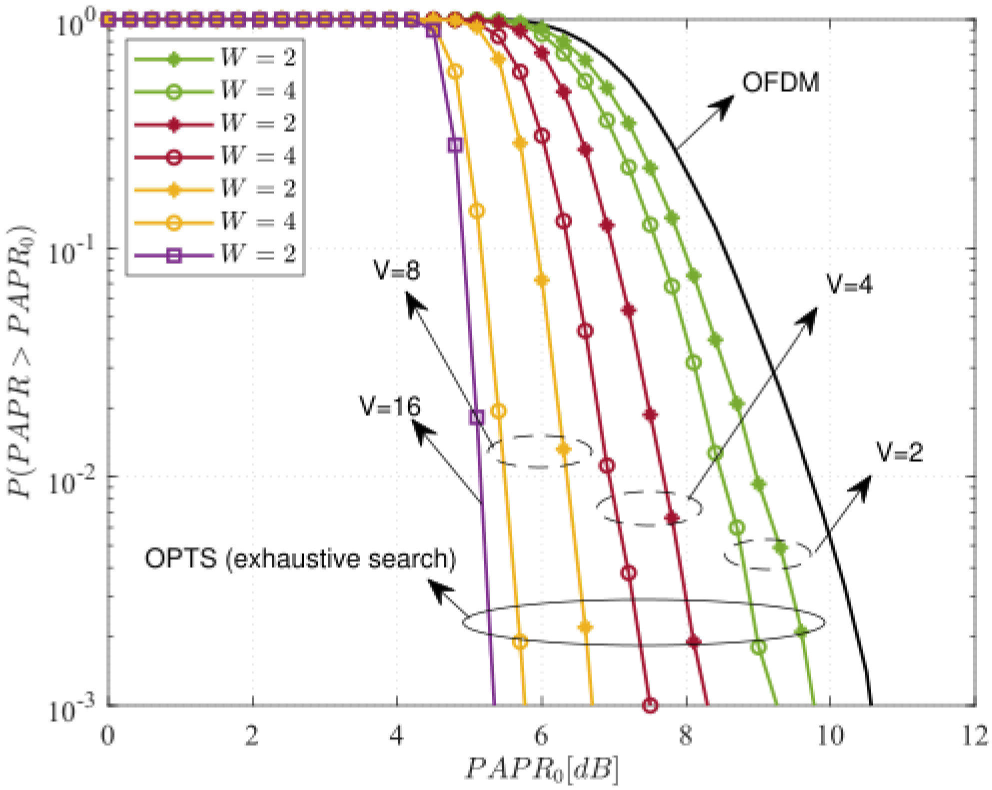

Figure 3.2: OPTS with different V and W sets.

work [149] uses the firefly algorithm (FA). The latter requires less number of computations; however, its performance is degraded

An improved harmony search (IHS) was studied in [150]. While the results of the PAPR are approximately the same as the ABC, the complexity is comparatively high.

In[151], a new PTS scheme based on gray wolf optimization (GWO) was proposed. Regardless of the fast convergence of the algorithm, the resulting PAPR is not worthy. The ant colony optimization (ACO) algorithm, first introduced in [152] by Dorigo and Caro, was used in [153] to reduce the complexity of the OPTS method. However, the convergence rate of the ACO is slow.

In other work [154, 155, 156], PSO was incorporated to search for the best-fitting phase factors sequence. PSO is a real-valued optimization technique known for its robustness in solving nonlinear optimization tasks. Nevertheless, it can easily fall into the trap of local optimization, which affects its performance. Thus, [154] suffers from a low convergence rate, [155] has a degraded performance compared to the state-of-the-art techniques, and [156] has a doubled inertia weight which may jeopardize the stability of the algorithm [6].

In [157], fuzzy neural network was employed in the PTS method to mitigate its complexity. The technique combines the learning and reasoning abilities of the neural network and the fuzzy control scheme, respectively, to properly choose the signal' processing parameters. The results obtained demonstrate the validity of the studied technique as regards search complexity and PAPR reduction. Another research [158] developed a new PTS scheme based on a centering phase sequences matrix algorithm. This technique provides an enhancement in the OFDM system' performance as it significantly lowers the high PAPR levels.

In [159], Goel and Gupta introduced a new PTS scheme, which addresses the transmitter' SI free transmission and the exhaustive search' complexity mitigation. The technique is based embedding the side information on the high power subcarriers' locations using particular segregations. On the other hand, at the receiver side, the SI is extracted using power disparity. This technique provides a reduced bit error rate (BER) degradation and have lesser computations compared to the ordinary PTS scheme.

A continuous-unconstrained particle swarm optimization (CUPSO-PTS) method was proposed in [160] to search for a suboptimal combination of phase factors. These are obtained by introducing several continuous-phase PTS methods, and a continuous-unconstrained investigating space is employed to determine the theoretical boundaries. The simulations prove the effectiveness of the method in providing good PAPR levels while saving 84.74% of the ordinary PTS' search complexity.

A related work [161] uses a well-balanced algorithm, called the May Fly Multiobjective Algorithm (MOMF) to optimize the phase factors. The technique's performance is tested on the PTS scheme. The investigated technique effectively enhances the performance of the PTS technique compared to other existing optimization methods.

An alternative PTS method was presented in [162]. Based on continuous unconstrained particle swarm optimization (CUPSO), the latter addresses high peak levels in FBMC. The CUPSO-PTS is considered alongside the input-back-off modulation error rate (IBO-MER) to select the boundaries and improve the convergence rate in the unconstrained continuous investigation area. Furthermore, the MER computations were decreased using CUPSO with IBO signal-to-distortion ratio (IBO-SDR).

A new PTS system, which uses PSO, was presented in [163]. This technique does not require the transmission of side information because it inserts dummy subcarriers into the transmitted data. The idea consists of adding six adaptive sequences of subcarriers to input data, prior to the IFFT, and then measure the PAPR after the IFFT block. The proposed algorithm then decides the send of data based on the values of PAPR to a specific threshold.

Another work [164] submitted a PTS scheme that employs firefly algorithm (FF) and a hybrid ACO. The provided method noticeably lowers the PAPR. Likewise, Amhaimar et al [165] compared the PTS techniques that are based on swarm intelligence (SI) algorithms. The study was done based on algorithms such, PSO, ACO, fireworks algorithm (FWA), genetic algorithm (GA), and simulated annealing (SA). The performance is assessed based on the accuracy of the solution and the convergence speed.

Another PTS technique based on the MIMO was proffered by Naidu et al in [166]. The latter investigates a reduced-complexity hybrid subblock segmentation for the PTS technique. In [167], Nguyen et al presented a novel PTS scheme, which applied phase quantization to lower the high peaks levels in OFDM systems, and permit the detection of the data without the need for side information. The technique utilizes a convex relaxation scheme, which converts into groups of convex programming the primary optimization task. A convergence to a suitable solution, which satisfies, in polynomial time, the karush-kuhn-tucker' (KKT) conditions is then provided. In [168], the authors developed a PTS system based on an enhanced elitist genetic algorithm (EGA). The EGA-PTS is then compared to the simple genetic algorithm (SGA), binary particle swarm optimization (BPSO), and the ordinary PTS technique. Simulation outcomes show its effectiveness compared to its counterparts.

3.3 The 1^{st} Contribution: A Low-Complexity PTS Technique based-Improved PSO Algorithm for PAPR Reduction in OFDM Systems

Our work [187] is dedicated to mitigating the exponential growth in search complexity inherent in the PTS approach. We have integrated and enhanced the effectiveness of a highly efficient meta-heuristic algorithm called particle swarm optimization (PSO) within the PTS scheme. The primary objective of the enhanced PSO is to systematically explore and discover a sequence of phase factors that is near-optimal, leading to the attainment of the lowest achievable PAPR within the least of complexity.

3.3.1 Why PSO?

PSO, introduced by Kennedy and Eberhart in 1995 [169], is a highly effective heuristic evolutionary algorithm for addressing optimization problems that are both high-dimensional and time-consuming [170, 171]. It draws inspiration from the collective behavior of real bird swarms, employing an evolutionary computing approach. The algorithm mimics the movement of birds within a search space as they navigate towards the best location of food, adjusting their positions based on connections with other birds. This enables both local and global optimization exploration. The inherent search capability of PSO facilitates the convergence of the swarm towards the optimal location. According to [170], PSO embodies the five principles of Swarm Intelligence (SI) as well as the four principles of self-organization introduced by Millonas [172] and Bonabeau et al [173], respectively. In comparison to other optimization algorithms such as GA, a study [171] has demonstrated that PSO exhibits comparable effectiveness in discovering global optimal solutions while achieving significantly improved computational efficiency (requiring fewer function evaluations). This conclusion was drawn based on a series of benchmark test problems.

3.3.2 Motivation behind enhancing the PSO

Several investigations have highlighted the robust performance of PSO algorithms in handling nonlinear optimization tasks [174, 175, 176, 177, 178]. Nevertheless, the ordinary version of PSO commonly encounters the issue of being susceptible to local optima [176, 177, 178]. To address this issue, this section introduces an enhanced PSO algorithm that leverages heuristics to efficiently identify the optimal weighting factors complex with reduced computational requirements.

3.3.3 The Proposed Solution: An Improved PSO-PTS Technique

In this study, we have presented an effective PSO algorithm that conducts a comprehensive investigation for an optimal sequence of phase factors, resulting in effective reduction of PAPR within the minimum of search's number. A new term, R_{best}, is integrated into the velocity formula to improve the algorithm's efficiency and avoid local optima stagnancy. This approach strikes a good balance between attenuating PAPR and managing computational load.

In in context, the population is represented by a swarm composed of individuals referred to as particles. Each particle maintains a set of phase factors with a dimension of V, where V is denoted by the number of the PTS's clusters. These particles explore the search area in order to find the best solution. During the exploration process, the positions of the particles are adjusted based on the following criteria:

- P_{best} , which designates the best location frequented by a particle.
- G_{best}, which designates the best location frequented by all particles in each trial.
- R_{best}, which designates a randomly chosed particles's position from the G_{bests} sets.

Hence, in the context of an optimization of dimension V, the j^{th} search agent (particle) adapt the location by applying the velocity formula as shown below:

$$\begin{aligned} v_{jp}(t+1) = w_t.v_{jp} + c_1.rand(P_{best_{jp}}(t) - x_{jp}(t)) \\ +c_2.rand(G_{best_p}(t) - x_{jp}(t)) \\ +c_3.rand(R_{best_p}(t) - x_{jp}(t)) \end{aligned} \tag{3.5}$$

$$x_{jp}(t-1) = x_{jp}(t) + v_{jp}(t+1) \tag{3.6}$$

Here, $p = 1, \ldots\ldots, V$ denotes the dimension's index, and t corresponds to the number of trials. Meanwhile, the coefficients c_1, c_2, and c_3 represents the acceleration factors that guides each search agent towards P_{best}, G_{best}, and R_{best}, respectively. To guarantee the algorithm's stability and responsive performance, the cognitive coefficient (c_1) and the social coefficient (c_2) were set to $c_1 = c_2 = 2$ [179]. In the present study, an additional coefficient c_3 is introduced to improve the efficiency of the algorithm. The parameter w_t stands for the inertial weight, which characterizes the fluidity of the search space explored by the particles to find the best solution. It is advisable to initialize w_t with a significant value. By allowing the particles to widely explore the global space and gradually reducing w_t to a smaller value, the system converges towards local optima [179]. Appropriate tuning of this rate facilitates a harmonious balance between local and global search, while allowing convergence to an optimal solution with a minimum of computations.

The inertial weight is configured as a linearly decreasing function, starting from 0.95 and gradually reducing to 0.4.

$$w_t = w_{max} - \left(\frac{w_{max} - w_{min}}{max_{iter} - 1}\right) \tag{3.7}$$

The symbol *rand* represents random numbers uniformly scattered across the interval [0,1]. These random numbers are generated for each iteration and for each particle. The purpose of introducing this variable is to emulate the erratic comportment observed in natural swarms. The velocity of each particle is adjusted based on Equation 3.5 at each iteration, allowing the particles to oscillate randomly around P_{best}, G_{best}, and R_{best}. After updating the velocity, the particles proceed to update their position using Equation 3.6. To evaluate the PAPR value of each sub-block of the PTS scheme, a fitness function is introduced:

$$fitness(x) = PAPR(x) \tag{3.8}$$

As shown in Figure 3.3, the process begins by generating a swarm of particles whose positions are randomly assigned, with the position of each particle representing a potential compound of rotation factors (one possible solution). Then, the PAPR ratio is evaluated for each potential compound of phase factors using a predefined fitness function, iteratively, until the specified number of iterations is reached. Finally, the system outputs the sequence of rotation factors that produces the minimum PAPR, indicating the best solution obtained. The proposed improved PSO process is summarized in the below Algorithm 1.

Algorithm 1 Pseudocode for the PSO-PTS

Initialize with the proper values: c_1, c_2, c_3, w_{max}, w_{min}, max_{iter} , and Pop.
Initialize in the rotation factors area particles with random positions
Let t=0
while $t <= max_{iter}$ **do**
    for each particle **do**
        Compute the fitness function
        Update P_{best}
    end for
    Update G_{best}
    Update R_{best}
    for each particle **do**
        update the velocity according to Equation (3.5)
        update the position according to Equation (3.6)
    end for
    t=t+1
end while
Return the best-found compound of phase factors (best solution) obtained thus far

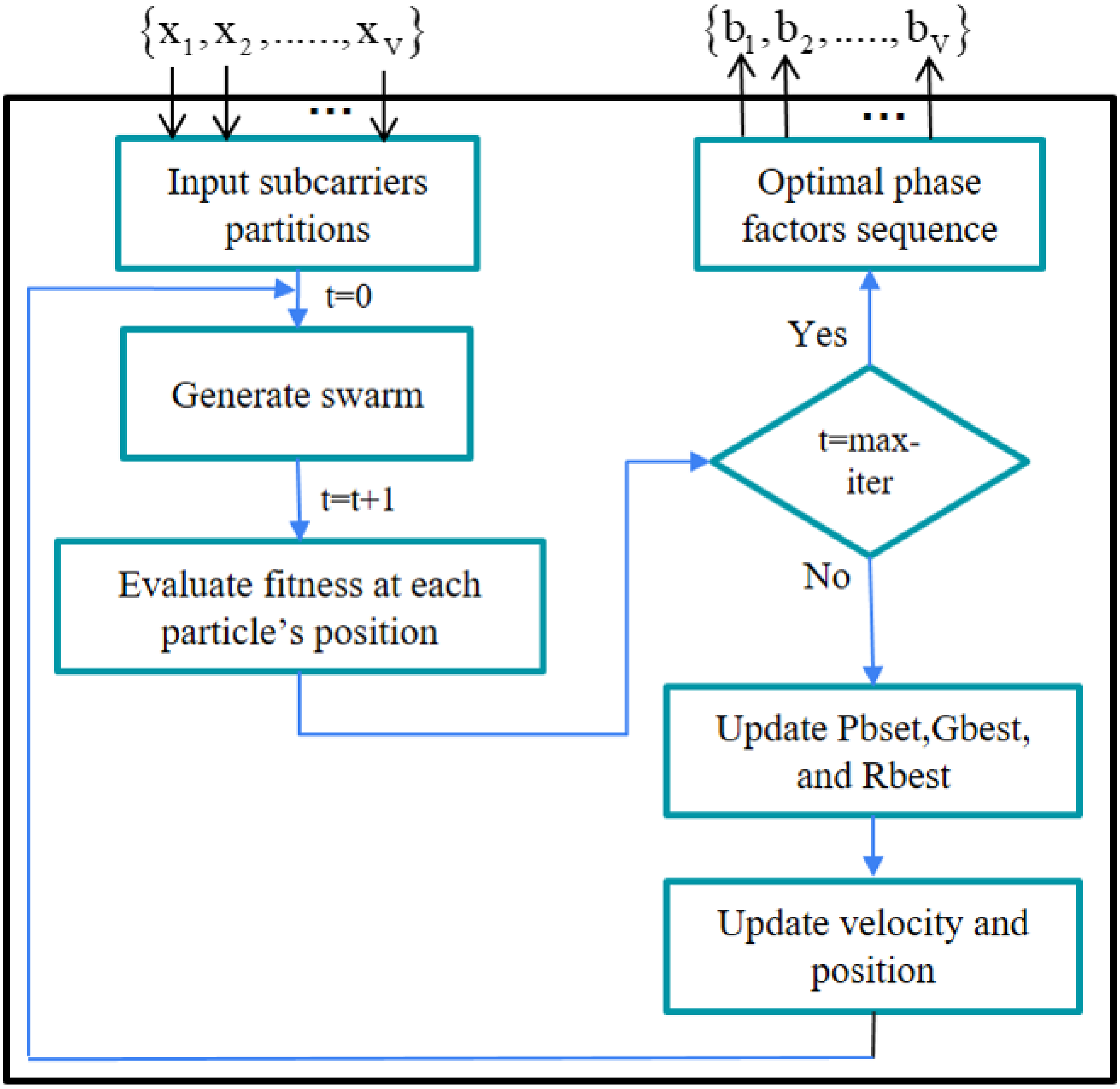

Figure 3.3: Block diagram of the proposed PSO.

3.3.4 Simulation results

To assess the proposed PSO-PTS approach's efficiency, we carried out MATLAB simulations. A total of 10 000 randomly generated OFDM frames were used, with a modulation type of 16 QAM. The simulation employed N=64 subcarriers and an oversampling factor of L=4. Also, a comparison with other well-known optimization algorithms, namely the GA, Random Search (RS) and Harmonic Search Algorithm (HSA) has been conducted. The phase weighting factors were chosen from a set of $b_v \in \{\pm 1, \pm j\}$ (W=4). Table 3.1 illustrates the simulation parameters.

Table 3.1: Simulation paramaters, search intricacy, and PAPR values for different simulated algorithms

Algorithm	Parameters	Computational load	PAPR (dB)
Exhaustive search	–	$W^V = 2^16 = 65536$	5.32
PSO	$c_1 = c_2 = 2$, $c_3 = c_1 \times (1 - e^{-c_1 \times t})$	$max_{iter} \times pop = 30 \times 20 = 600$	5.73
GA	crossover=single point, mutation=0.001	$max_{iter} \times pop = 30 \times 20 = 600$	6.05
HSA	HMCR=0.95, PAR=0.8	$max_{iter} \times pop = 30 \times 20 = 600$	6.37

According to Muller and Huber [5], the efficiency of the PTS system can be altered by the type of segmentation used in cluster partitioning. This is mainly due to autocorrelation between subcarriers. Three main types of segmentation can be used in PTS: random, adjacent and interleaved, of which random is the most efficient and best known to offer better performance. Consequently, the random segmentation has been chosen as the most appropriate one for our system.

Figure 3.4 shows the comparison of PAPR reduction performance between the proposed technique using different numbers of clusters (V), the conventional PTS, and the original OFDM signal. The figure clearly shows that performance improves as the number of clusters increases. This improvement can be attributed to the exploration of higher-dimensional vectors, which in turn leads to a higher probability of finding more exact solutions.

Observing Figure 3.4, it is evident that the CCDF curve of the reported approach utilizing a number of subblocks of 16 (V=16) exhibits a minor decline compared to the case of V=32, with a difference of 0.14 dB. Given this observation, the model will be further analyzed using 16 clusters. For the simulation of the PTS technique, a set of phase factors was utilized, selected from $b_v \in \{\pm 1\}$ (W=2), along with a total of 16 partitions (V=16). This choice of parameters is driven by the impracticality when employing extensive sets of phase factors and sizable clusters. In the scenario of V=32 and W=4, the number of required searches would amount to 1.84×10^{19}, which is impractical. At the CCDF clip of 10−3, the exhaustive search substitutes a value of PAPR of 5.32 dB. On the other hand, the proposed system achieves a PAPR of 5.73, degraded with only 0.41 dB than the OPTS, and prevailed over the conventional OFDM by a value of 5.11 dB, representing a 47.75% enhancement.

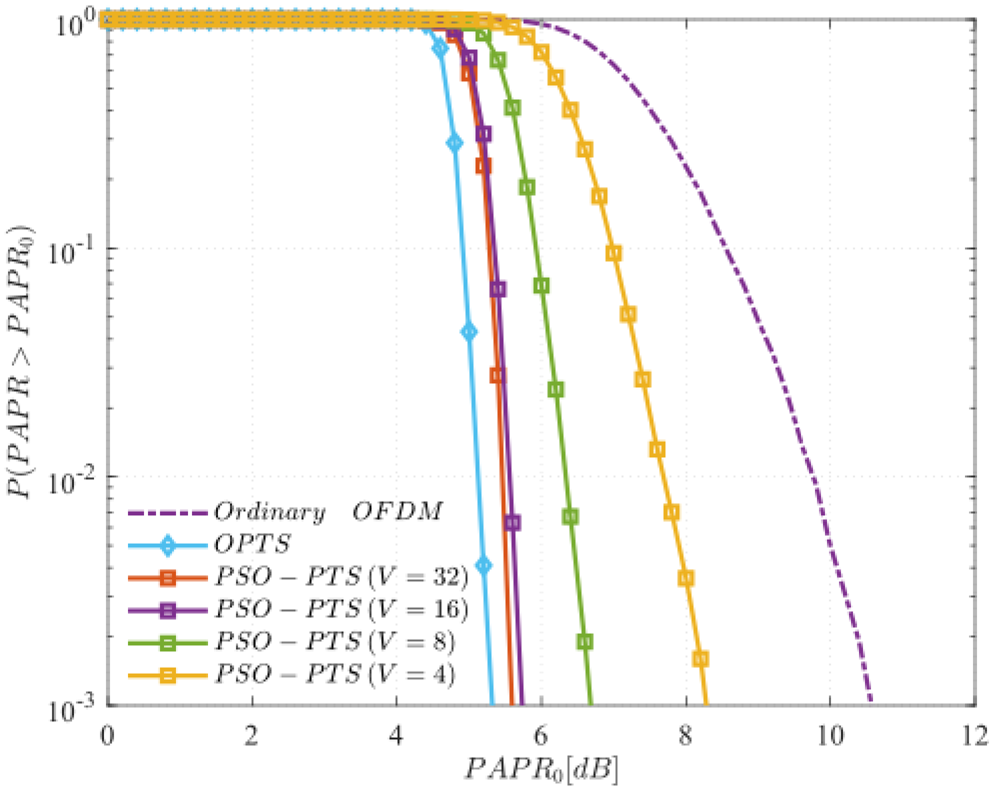

Figure 3.4: CCDF comparisons between the OPTS technique and the proposed PSO-PTS method

Figure 3.5 presents a comparative analysis between the proposed technique and other PTS techniques based on meta-heuristic algorithms. The complexity of the evaluated population-based algorithms, including PSO, GA, and HSA, is determined by the product of the maximum number of iterations (max_{iter}) and the population size (pop), resulting in a value of 600 (20×30). In contrast, the complexity of the RS algorithm is equal to the maximum number of trials (max_{iter}), which is 20. The superiority of the proposed PSO-PTS technique over HSA, GA, and RS is clearly evident in the graph. With a predefined probability of 10^{-3}, the PSO-PTS achieves a PAPR value of 5.73 dB, surpassing GA, HSA, and RS by 0.32 dB, 0.64 dB, and 1.07 dB, respectively. These results conclusively demonstrate the superior effectiveness of the proposed method.

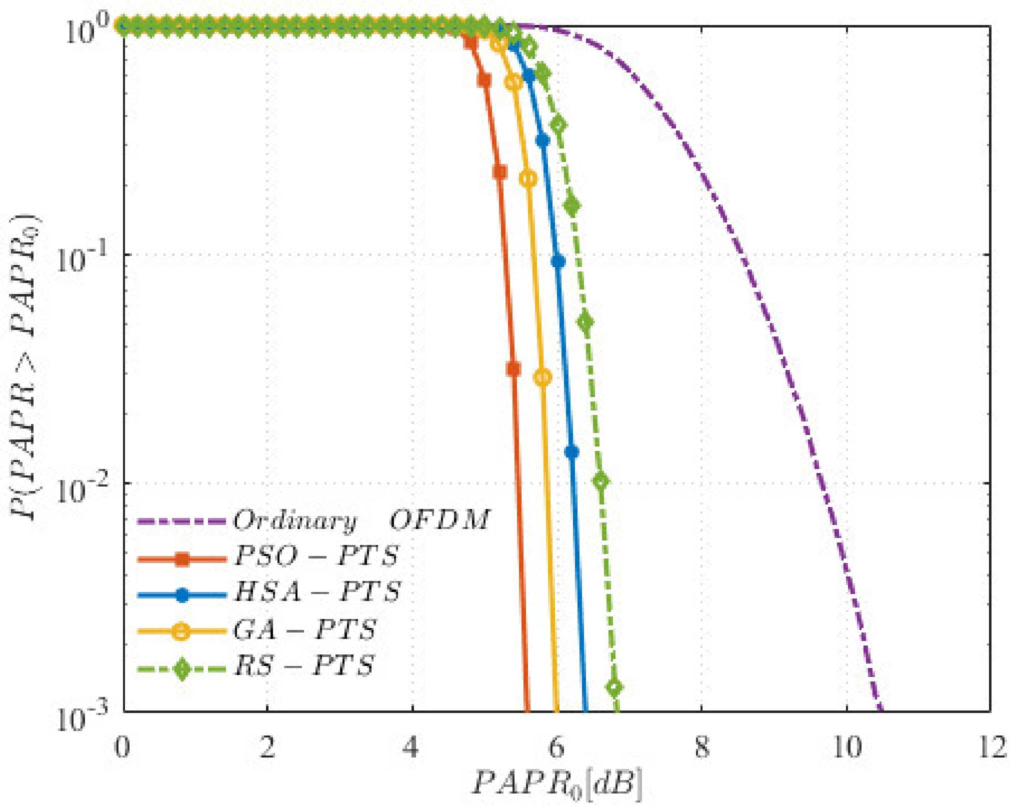

Figure 3.5: CCDF comparisons between the proposed PSO-PTS method and other efficient heuristic algorithms

Complexity analysis

The primary aim of this study is to attain a desirable balance between minimizing complexity and reducing PAPR. The proposed model exhibits a complexity of $max_{iter} \times pop$=20 $\times$ 30=600, which is significantly lower compared to the standard PTS scheme (0.92%) within only a marginal degradation of 0.41 dB in the PAPR value.

Convergence analysis

To assess the convergence performance of our PSO, we conducted 100 experiments using a one-symbol OFDM. Figure 3.6 depicts the curves of convergence of the PSO-PTS system, showing the mean of best PAPR values. Various population sizes and trials numbers has been employed to carry out the analysis. It is obvious from the Figure that after the first 20 iterations, the algorithm's convergence progressively

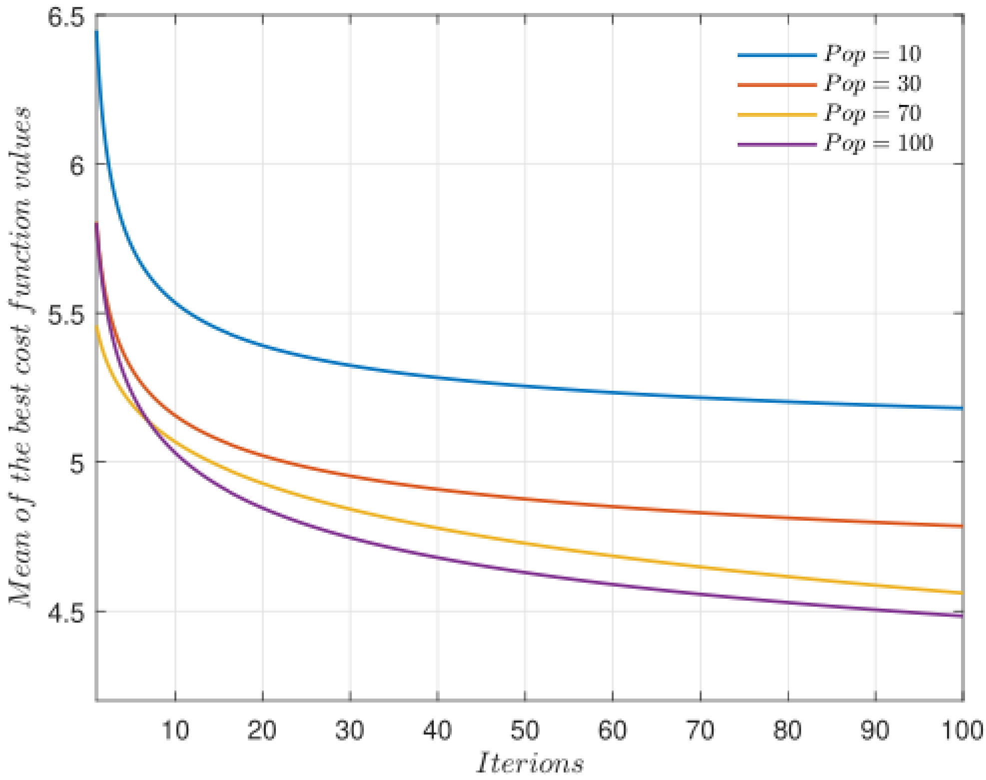

Figure 3.6: Convergence curves of the proposed PSO-PTS technique with different population sizes and iteration numbers.

decelerates and becomes less apparent. Thus, we made a compromise by prioritizing competitive search complexity over further minimizations. However, if additional reductions in PAPR value are desired at the cost of increased search effort, the number of iterations can be set to 100.

Likewise, as Figure 3.6 illustrates, within a population of 30 (Pop=30), the system exhibits a notable convergence towards the mean of the optimal PAPR values. Overall, we can ensure the convergence of our system within 20 iterations and 30 particles, demonstrating a favorable trade-off between reducing PAPR and search complexity.

Figure 3.7 demonstrates the fast convergence of the algorithm in contrast with other models. At 20 iterations, the mean of the best PAPR values of our algorithm is better than that of RS, HSA, and GA by 0.71 dB, 0.6 dB, and 0.4 dB, respectively.

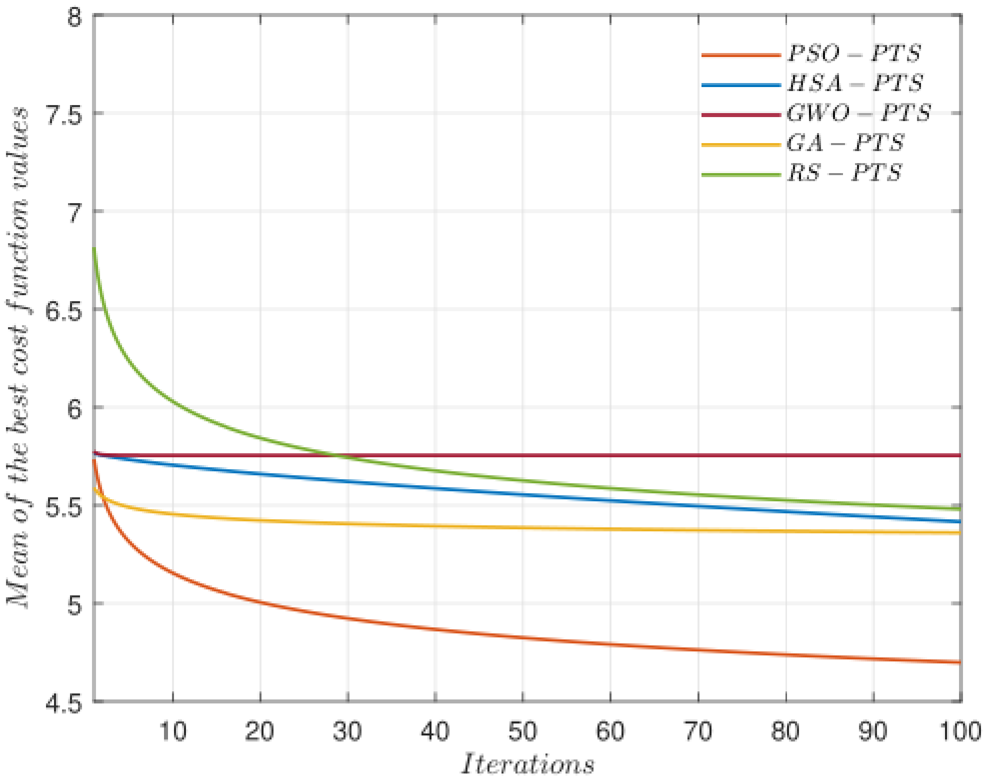

Figure 3.7: Convergence curves comparison between the proposed PSO-PTS and the compared methods.

3.4 The 2^{nd} Contribution: IWOA-PTS: an Improved Whale Optimization Algorithm-based PTS Technique for PAPR Reduction in OFDM Systems

An innovative PTS based on an improved whale optimization algorithm is presented in this study to lower the OPTS' complexity. To our knowledge, no previous research has reported the IWOA-PTS. The whale optimization algorithm is a meta-heuristic algorithm proposed in 2016 by Mirjalili and Lewis [146] and enhanced in 2021 by Chakraborty et al [147] to handle continuous optimization tasks with fast and accurate convergence properties. The principal inspiration behind the creation of the WOA is the unique hunting behavior of the humpback whales, "bubble nets". In this attacking mechanism, whales aim to herd their prey (krill or small fish flocks) by creating spiral bubble-nets captured as 9-figured paths as shown in Figure 3.8. In this study, the IWOA of Chakraborty et al is employed in the OPTS technique, mainly due to its superiority in addressing local optima stagnancy, fast convergence, and its balanced exploration-exploitation capabilities.

The IWOA is compared with other robust meta-heuristic optimization algorithms to measure its efficiency in PAPR reduction. The simulation findings ascertain the superiority of the proposed IWOA-PTS method over the OPTS technique in terms of computational load and prevailing over the compared algorithms in terms of PAPR performance and convergence rate.

At the whole, the principle interventions of the presented work are:

- We introduce a novel technique, namely IWOA-PTS to minimize the PTS' technique massive computational load.
- We combine the IWOA algorithm with the PTS technique to create a new hybrid variant of the PTS scheme.
- We analyze the complexity of the search; the IWOA-PTS reduced the OPTS' complexity by 93.9%.
- We compare the proposed system' performance with other efficient techniques. The comparative analysis prove the superiority of the IWOA over random search (RS), harmony search algorithm (HSA), particle swarm optimization (PSO), and WOA in terms of PAPR mitigation.
- We evaluate the performance of the system against some effective state-of-the-art techniques, [180], [181], [182], [183], [184]. The comparative analysis demonstrates the effectiveness of the IWOA-PTS.

3.4.1 The proposed IWOA-PTS technique

In this work, the IWOA of Chakraborty et al [6] is used in the OPTS scheme to cope with the time loss and impracticality of the OPTS technique when the number of sub-blocks increases. Figure 3.10 identifies the IWOA-PTS process.

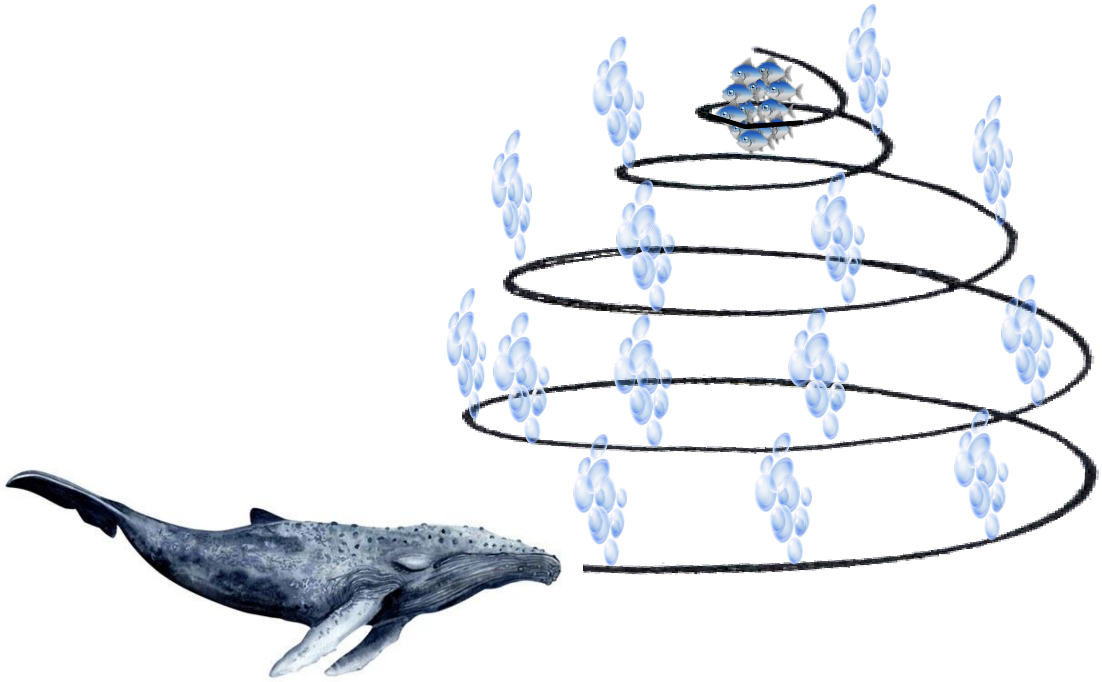

Figure 3.8: Bubble-net hunting mechanism of humpback whales.

The proposed method's main compounds and mathematical modeling are noted and explained in the following.

Initially, we define the objective function by which the PAPR evaluation of the system is performed. The goal is to minimize the PAPR by searching for the best combination of phase factors. Thus, the best value of the objective function is taken as the lowest value of the PAPR.

$$Obj_{fun}(x) = PAPR(x) \tag{3.9}$$

The main objective is to emulate humpback whales' tracking and attack mechanisms during their foraging behavior. The IWOA is primarily initialized by a population (P) with random whales positions. The huge sea represents a massive search area filled with small schools of fish (humpback whales' prey); these are considered potential combinations of phase factors of length V (V denotes the problem' dimension). The best whale position is assumed as the target prey's position, which refers to the combination of phase factors that results in the best objective function value (lowest PAPR). Whales swim through the search area looking for prey, and their positions are updated according to the cornerstones of their foraging mechanism, namely exploration, and exploitation.

3.4.2 Exploration phase

In order to obtain the global sequence of phase factors that effectively reduces PAPR without getting trapped in less efficient suboptimal local solutions, a modified mutualism phase is first introduced, which strengthens the exploration phase and balances the exploration-exploitation capabilities of the algorithm[6].

Modified mutualism phase

- **Background of the mutualism phase of the symbiotic organism search (SOS) algortihm**

  Mutualism, part of the SOS algorithm introduced by Chang and Prayago in 2014 [29], is a kind of interdependent, symbiotic connection that benefits both interacting entities. A simple example of a mutualistic relationship is the bee and the flower. Bees fly into flower fields, collect nectar, and convert it into food. Through this process, the bees benefit from the food; in return, the flowers benefit from pollination. The mathematical modeling of mutualism is as follows:

$$X^j(t+1) = X^j(t) + rand * (X^{best} - MV + BF^1) \tag{3.10}$$

$$X^{rand}(t+1) = X^{rand}(t) + rand * (X^{best} - MV + BF^2) \tag{3.11}$$

  where "X^j" denotes the j^{th} element of the imposed population, whereas "X^{rand}" represents another element randomly chosen to interoperate with X^j. Both entities interact and mutually benefit to persist in the environment."t" represents the iterations' number, "$rand$" denotes random numbers regularly distributed in the range [0,1],"X^{best}" represents the t^{th} iteration' best solution. "MV" refers to the mutual vector, expressed as

$$MV = \frac{X^j + X^{rand}}{2} \tag{3.12}$$

"BF" denotes the benefit vector, it is defined as

$$BF = round(1 + rand) \tag{3.13}$$

The above formula employs a "$round$" function to adjusts the "BF" value to either 1 or 2. "BF" determines the benefit rate of each interacting entity among the constituents of the considered population.

- **The IWOA' modified mutualism**

After initializing the random population of whales, the objective function is evaluated at each whale position to select the best solution (X^{best}). Then, a modified mutualism is executed at each iteration, as described in the following steps

- For each whale (X^j) select two other random whales $\{X^{r1}$ and $X^{r2}\}$ from the considered population, such that $j \neq r1 \neq r2$.
- If $Obj_{function}(X^{r1}) < Obj_{function}(X^{r2})$, then the positions of the currently considered whale (X^j) and the one with inferior performance (X^{r2}) will be updated as shown below.

$$X^j(t+1) = X^j(t) + r(X^{r1} - MV + BF^1) \tag{3.14}$$

$$X^{r2}(t+1) = X^{r2}(t) + r(X^{r1} - MV + BF^2) \tag{3.15}$$

Otherwise

$$X^j(t+1) = X^j(t) + r(X^{r2} - MV + BF^1) \tag{3.16}$$

$$X^{r1}(t+1) = X^{r1}(t) + r(X^{r2} - MV + BF^2) \tag{3.17}$$

Where "MV" is denoted as the average of $\{X^j, X^{r1}\}$ when the first condition is true ($Obj_{function}(X^{r1}) < Obj_{function}(X^{r2})$), else, "$MV$" is the average of $\{X^j, X^{r2}\}$."$rand$" and "BF" are defined as previously.

Obviously, by simultaneously updating the position of two whales using the one with the best objective function among the two previously randomly selected whales, greater diversity in solution is obtained, and guidance to the best global solution is provided. Subsequently, the exploration capability is enhanced. After the modified mutualism, the IWOA evaluates and updates the global best solution if it is better than the existing one.

Search for prey

To search for prey, humpback whales explore the search area in a haphazard way. As they explore, their locations are updated based on their shared knowledge of their positions. This tracking behavior can be mathematically imitated as follows

$$D = |C.X^r(t) - X^j(t)| \tag{3.18}$$

$$X^j(t+1) = X^r(t) + A.D \tag{3.19}$$

Where "X^r" is a randomly considered whale from the existing population, "D" is the range between the current and randomized whales. The "." refers to the vectorized multiplication (element by element), and "||" computes the absolute distance value.

"A" and "C" are known as coefficient vectors, they are calculated as follows

$$A = 2a \times r - a \tag{3.20}$$

$$C = 2 \times r \tag{3.21}$$

In the latter equations, "a" denotes a linearly decreasing value in the interval [2-0].

3.4.3 Exploitation phase

Interestingly, humpback whales have a particular hunting mechanism known as bubble-net feeding. The whales dive to a depth of about 12 m [6], then create spiral bubbles around their prey and rise to the surface. The mechanism consists of two simultaneous behaviors, namely shrink-wrap, and spiral-update.

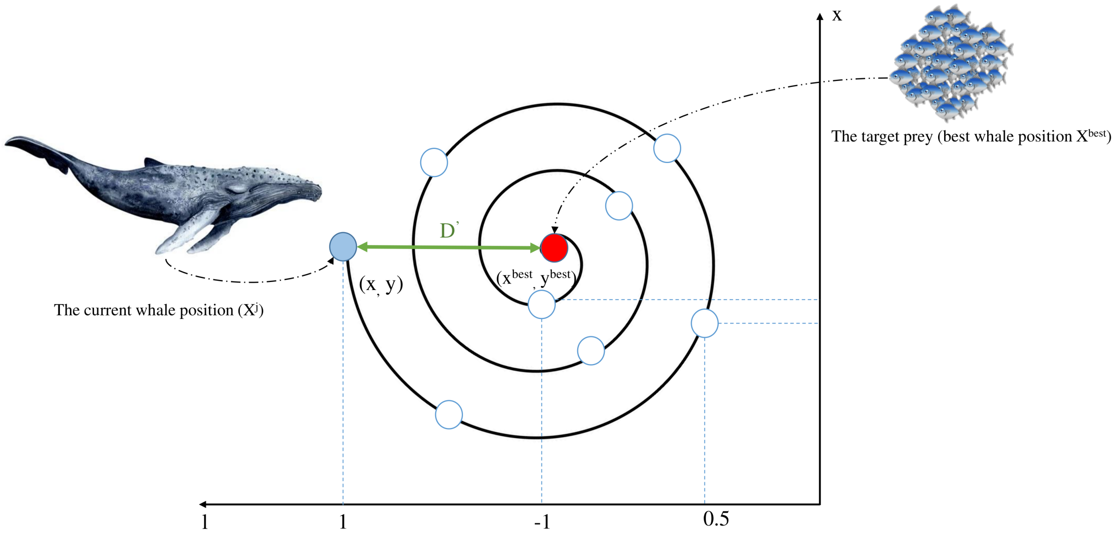

Figure 3.9: Spiral-updating position.

Shrink-wrap behavior

During this stage, the whales tend to gather the school of fish in a single area. Using the shrink-wrap mechanism, the whales update their positions in the neighborhood of the best solution found so far (X^{best}). This natural behavior is mathematically modeled as follows

$$D = |C.X^{best}(t) - X^j(t)| \tag{3.22}$$

$$X^j(t+1) = X^{best}(t) + A.D \tag{3.23}$$

Spiral-update behavior

In addition to the shrink-wrap maneuver, whales update their position based on the best whale position in a helix-like motion. As shown in Figure 3.9The technique calculates the difference between the whale's best position X^{best}, or, more precisely, the position of the target prey that is located at (x^{best}, y^{best}), and that of the current whale positioned at (x, y). The spiral equation representing this motion is expressed as follows

$$D' = X^{best}(t) - X(t) \tag{3.24}$$

$$X^j(t+1) = D'.e^{bl}.cos(2\pi l) + X^{best}(t) \tag{3.25}$$

In the above equations, "b" is a constant that defines the logarithmic helix shape, "l" represents a stochastic number defines as

$$l = (a_1 - 1)r + 1 \tag{3.26}$$

Where "a_1" is considered as a linearly decreasing value in the range [-1,-2] with the number of iterations.

3.4.4 The IOWA' exploration-exploitation transition process

During the IWOA optimization cycle, the transition from exploration to exploitation is mainly determined by the value of A. In other words, we establish a kind of condition explained as follows

- If $|A| \geq 1$ then, the whales head for the exploration phase; new regions in the search space are visited using Equation 3.19.
- Otherwise, they choose the exploitation phase; obviously, whales in this state tend to update their positions close to the target prey position. It is worth mentioning here that the position-updating process of humpback whales involve the two behaviors mentioned above, namely shrink-wrap and spiral-update, performed simultaneously. Imitating these two behaviors ends with the assumption of a probability ($Prob$) of 50% to designate one of them. If $Prob < 0.5$ then the position of X^j is updated using Equation 3.23, else it is updated using Equation 3.25.

The pseudo-code representing the process of the IWOA-PTS technique is presented in Algorithm 2.

Algorithm 2 Pseudocode for the IWOA-PTS

```
initialize the population (P)
compute the objective function at each whale position (Obj_fun(X^j)) to find the best whale position (X^best)
Let t=0
while t <= I do                    ▷ "I" denotes the maximum number of iterations
    for each whale do
        randomly select two other whales (X^r1 and X^r2) such that j ≠ r1 ≠ r2
        compute the objective function of the random whales
        if Obj_fun(X^r1) < Obj_fun(X^r2) then
            update the position of X^j and X^r2 according to Eq. (3.14) and Eq. (3.15) respectively
        else
            update the position of X^j and X^r1 according to Eq. (3.16) and Eq. (3.17) respectively
        end if
        compute the objective function of X^j(t+1) and X^r1(t+1) or X^r2(t+1)
        update X^j, X^r1 or X^r2 if a better objective function value is found
    end for
    update X^best if a better objective function value is found
    for each whale do
        update A,C,l, and Prob
        if Prob < 0.5 then
            if |A| >= 1 then
                update the current whale position according to a randomly selected whale using Eq. (3.19)
            else
                update the current whale position according to Eq. (3.23)
            end if
        else
            update the current whale position according to Eq. (3.25)
        end if
    end for
    t=t+1
end while
Return X^best
```

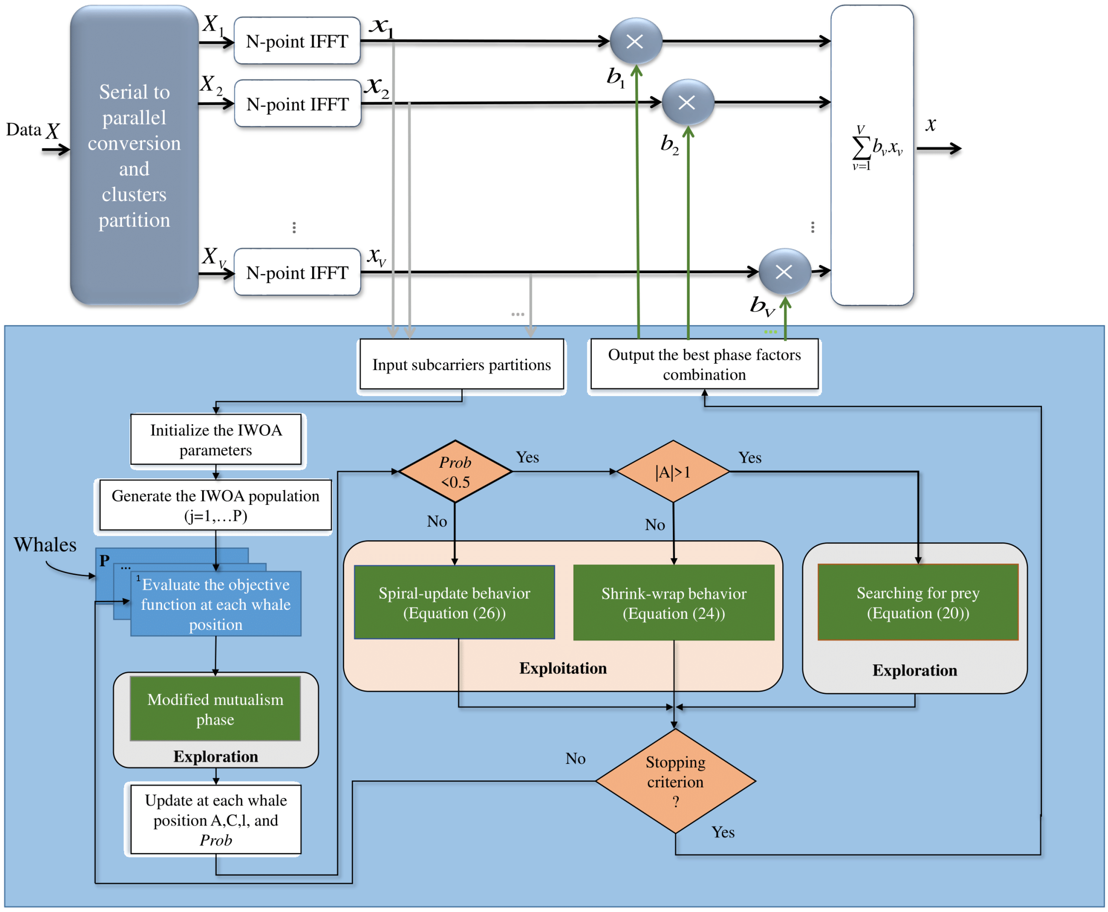

Figure 3.10: Block diagram of the proposed IWOA-PTS technique.

3.4.5 IWOA-PTS general workflow and solution building

The general process of the proposed IWOA-PTS technique is illustrated in Figure 3.10. The workflow starts with randomly generating the whales population. Then, the algorithm evaluates and finds the best whale position (best phase factors combination) in the current iteration. After that, the algorithm performs a modified mutualism to the whales population to balance the exploration-exploitation phases. Thereafter, depending on the value of A, the algorithm switches from searching for a new potential best solution (exploration) to updating the whale positions according to the best solution found so far (exploitation). Finally, if the process performs the predefined number of iterations (stopping criterion), it returns the best phase factors combination found; otherwise, the tracking and attack mechanisms of whales are repeated until the stopping condition is met.

3.4.6 Computational load of the IWOA-PTS

As shown in Figure 3.10, at each iteration, the objective function is evaluated for each whale from the considered population (P). Thus, for a predefined number of iterations (I), the computational load of the IWOA-PTS technique is $P \times I$. Compared to this, the conventional PTS technique requires W^{V-1} function evaluation to output the solution.

3.4.7 Compared methods and their complexity

PSO is a swarm intelligence, nature-inspired algorithm. It is based on the observations of birds moving in the search space toward the best location of food at a particular speed and changing their positions according to the connections they have between them. The swarm represents a population based on individuals, known as particles. A set of phase factors of dimension V is performed for each particle. These particles explore the search area to find an optimal solution. Primarily, PSO requires the tuning of two parameters: the acceleration coefficients (c_1 and c_2) and the inertia weight (w), by which, if well chosen, the algorithm will have balanced exploitation-exploration capabilities. Thus, in this paper, the parameters of the PSO are set according to [154]. Like the IWOA, the computational load of the PSO is equal to $I \times P$. HSA is a metaheuristic optimization algorithm based on music. The idea comes from the observations of musicians searching for a perfect state of harmony, which is equivalent to the search for the optimal state in an optimization problem. HSA has two probabilistic tuning parameters: the harmony memory consideration rate (HMCR) and pitch adjustment rate (PAR). These two parameters vary between 0 and 1, and their values are taken as in [185]. As with any population-based algorithm, the complexity of the HSA is equal to $I \times P$. RS is an iterative algorithm that consists, in the OPTS technique, of evaluating a random combination of phase factors at each iteration. Unlike swarm intelligence algorithms, RS has no tuning parameters, and its complexity is equal to the number of iterations imposed.

Table 3.2: Simulation parameters.

Parameters	Values
modulation type	16-QAM
number of subcarriers (N)	64 ,128,256
oversampling factor (L)	4
allowed phase factors set (W)	2$\{\pm 1\}$,4 $\{\pm 1, \pm j\}$
number of subblocks (V)	2,4,8,16,32
number of iterations (I)	20,30
number of whales population (P)	50,100

3.4.8 Simulation results and discussions

To evaluate the performance of the IWOA-PTS model, MATLAB simulations have been performed. 10^4 OFDM frames are randomly generated. 16 QAM modulation is employed, and different numbers of subcarriers are used (N=64, 128, 256). An oversampling factor of 4 is chosen for the simulation for a veritable estimation of PAPR. IWOA requires only setting two internal parameters, called coefficient vectors ("A" and "C"), whose equations and values are defined in subsection 3.4.2. The "A" coefficient contributes to the conditioning of the exploration-exploitation balance. It improves the local search using the best whale position as a reference in the updating process, simulating encircling prey (exploitation $|A| > 1$), as well as the global search using a random whale position as a reference in the update process, simulating searching for prey (exploration $|A| <= 1$). While the "C" coefficient represents a random vector used to diversify the solution [147]. The values of theses parameters are taken as in [147]. Further, the proposed work is compared with WOA-PTS, PSO-PTS, HSA-PTS, and RS-PTS. Obviously, each algorithm has a predefined set of parameters that must be adjusted appropriately for optimal rendering. Therefore, for a fair comparison, the parameters of the algorithms are selected as reported by their authors. Different numbers of iterations and populations are used to analyze the algorithm's performance. Pseudo-random partitioning is used for sub-block partitioning as it provides the best performance in PAPR reduction [4]. Table3.2 summarizes the parameters of the simulation.

In order to accurately select the population size and the iterations' number for the next analysis of the IWOA using 8 subblocks and 4 phase factors, a convergence analysis is first provided, shown in Figure 3.11. The latter is performed by running 100 experiments for one OFDM symbol and then computing the average of the best values of the objective function. As illustrated in Figure 3.11, for all fixed population sizes, after 20 iterations, the average of the best PAPR values has barely improved; thus, 20 iterations is the appropriate choice for the simulation. It is evident from Figure 3.11 that the PAPR reduction performance improves with the increase in the size of population; more clearly, the higher the number of whales, the higher the diversity of solutions. At $I = 20$, and for the $P = 10$ and $P = 30$ populations, the difference between their best average PAPR and that of $P = 100$ is considered non-negligible. Compared to that, The $P = 50$ population has only a marginal difference of 0.07 dB compared to the $P = 100$ population. Furthermore, with the $P = 50$ population, rapid convergence to an appropriate average PAPR is achieved in only 20 iterations. Therefore, $P = 50$ and $I = 20$ are the proper choices for subsequent simulation.

Figure 3.12 shows the CCDF curves of the ordinary OFDM signal (without PAPR reduction), the OPTS technique using exhaustive search, the proposed IWOA-PTS scheme, and other compared methods, namely WOA-PTS, HSA-PTS, PSO-PTS, and RS-PTS. To the readers' knowledge, the computational load of WOA, HSA, and PSO is the same as that of IWOA ($P \times I = 50 \times 20 = 1000$). While that of RS is equal to the number of iterations (I). Obviously, the compared algorithms improved the PAPR of ordinary OFDM by the following values: 6.6 dB, 6.7 dB, and 6.8 dB for WOA-PTS, PSO-PTS, and RS-PTS respectively; however, the gap between their performance and that of exhaustive search is considerable. In comparison, IWOA has approximately the same performance as the exhaustive search (5.77 dB) with a marginal difference of 0.07 dB that can be considered negligible. Thus, IWOA-PTS has the same performance as exhaustive search while only accounting for 6.1% of its complexity. ($Computational\ load\ of\ IWOA\ -$

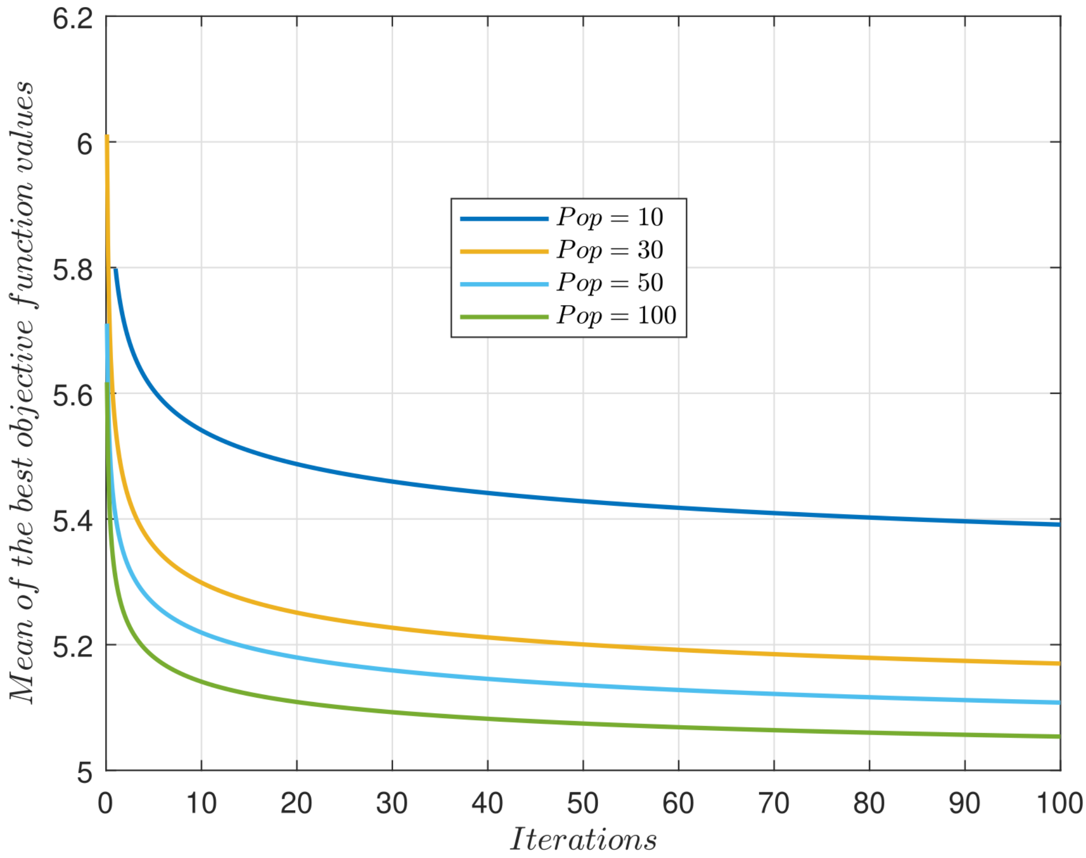

Figure 3.11: Convergence analysis of the IWOA-PTS with $V = 8$ and $W = 4$.

$PTS/Computational\ load\ of\ OPTS = (P \times I = 50 \times 20)/(W^{V-1} = 4^{8-1}) = 1000/16384 = 6.1\%)$.

Figure 3.13 shows the PAPR reduction performance of the IWOA-PTS compared to other approaches using 16 subblocks ($V = 16$). After performing a convergence analysis, the appropriate selection of I and P using $V = 16$ and $W = 4$ is as follows: I=30 and P=100. As shown in the Fig, for the same computational complexity ($I \times P$), IWOA-PTS has the best performance compared to other methods. The proposed technique gives a PAPR of 5.45 dB which is improved over WOA, PSO, HSA, and RS with 0.5 dB, 0.85 dB, 0.5 dB, and 1.15 dB, respectively. The CCDF curve of the OPTS is obviously ignored due to its huge complexity since $W^{V-1} = 4^{15} = 1.07 \times 10^9$ searches must be performed to reach the optimal solution. Notably, the complexity of the IWOA is negligible compared to OPTS since it is

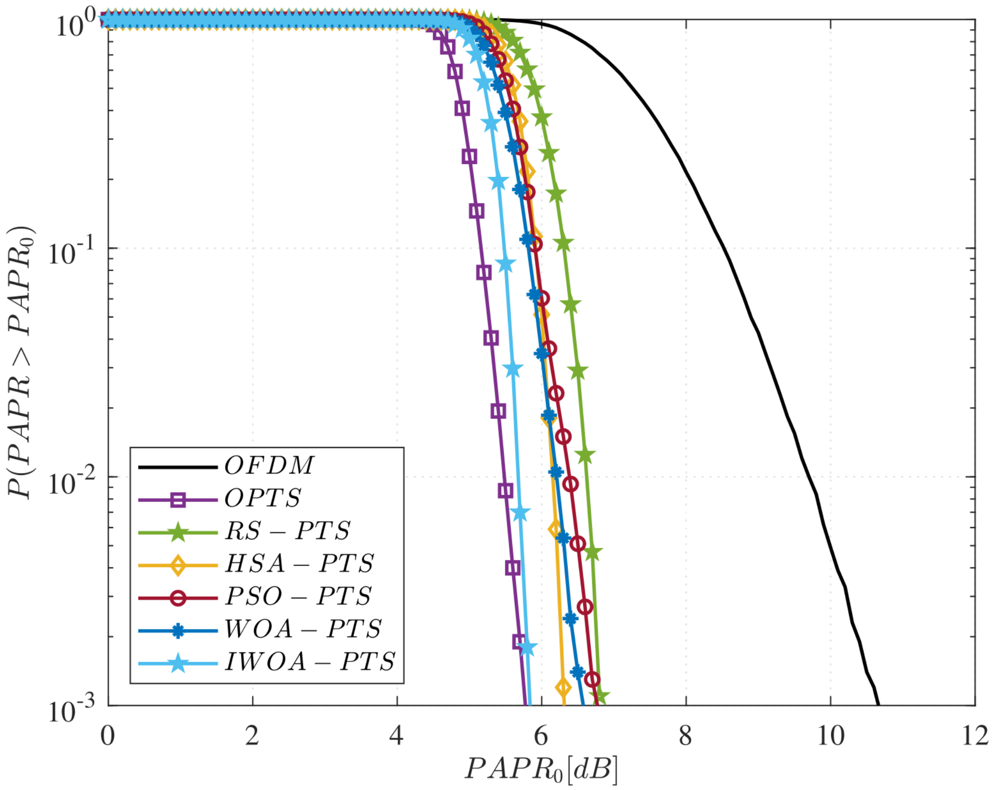

Figure 3.12: PAPR reduction comparisons using $V = 8$ and $W = 4$.

only $(I \times P)/W^{V-1} = (30 \times 100)/4^{16-1} = 2.8 \times 10^{-4}\%$ of its complexity.

In general, as the number of subcarriers in the OFDM system increases, the PAPR increases. Obviously, the more subcarriers are there, the greater the addition of components with the same phase, and, therefore, the more peaks will appear in the signal. Fig. 3.14 represents the PAPR performance of the IWOA-PTS with different numbers of subcarriers. As can be seen, as the number of subcarriers increases, the PAPR increases. However, for N=256, using 16 subcarriers (V=16), the PAPR of the OFDM signal is reduced by 3.9 dB. Thus, the IWOA-PTS demonstrates its performance efficiency for larger numbers of subcarriers ($N \geq 64$).

At the CCDF clip of 10^{-3}, Table 3.3 compares the PAPR reduction performance of the IWOA-PTS against the ordinary WOA-PTS for different numbers of subblocks. It is clear from the results presented therein that the performance improves as the

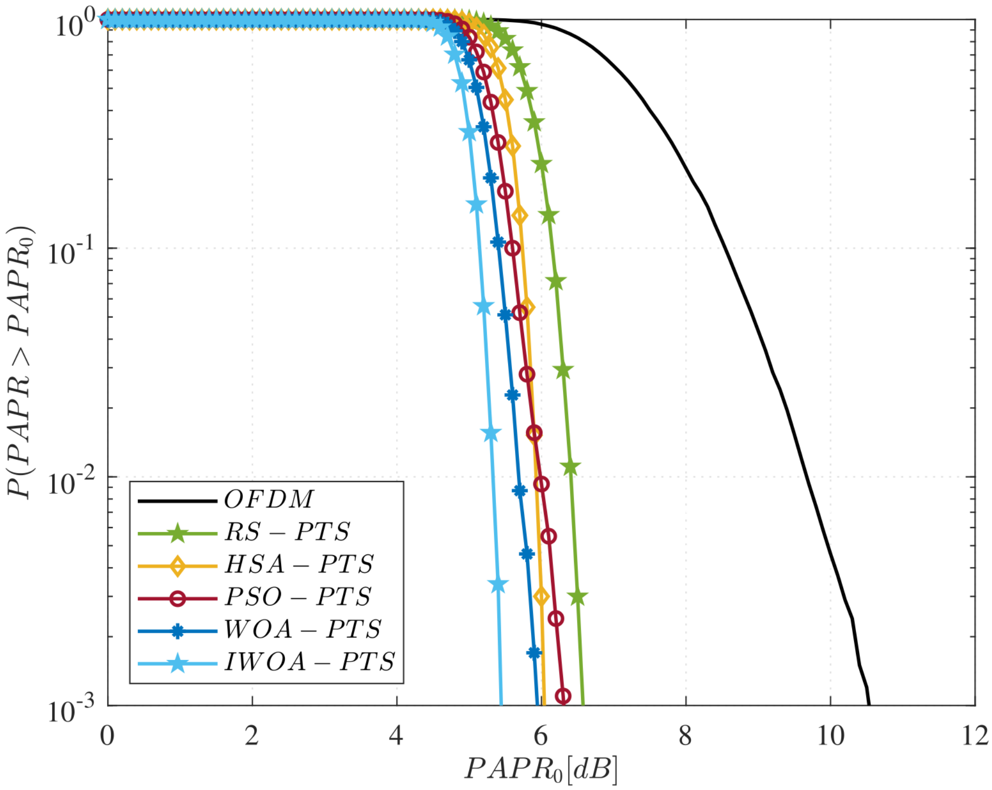

Figure 3.13: PAPR reduction comparisons using V=16 and W=4.

Table 3.3: PAPR performance comparisons of IWOA-PTS against ordinary WOA-PTS for different numbers of subblocks (at the CCDF clip of 10^{-3}).

Method	V=8	V=16	V=32
WOA-PTS	6.6	5.9	5.62
IWOA-PTS	5.84	5.45	5.3

number of subblocks increases. However, the IWOA has better PAPR values than the ordinary WOA. Therefore, the IWOA-PTS proves its superiority over WOA-PTS.

Table 3.4 lists the PAPR and computational complexity of the proposed IWOA-PTS technique and that of OPTS, WOA-PTS, PSO-PTS, HSA-PTS, and RS-PTS. The results obtained confirm the superiority of the IWOA-PTS over the compared methods. The IWOA-PTS has approximately the same performance as the OPTS (marginal difference of 0.07 dB) with a complexity that is only 6.1% of that by the

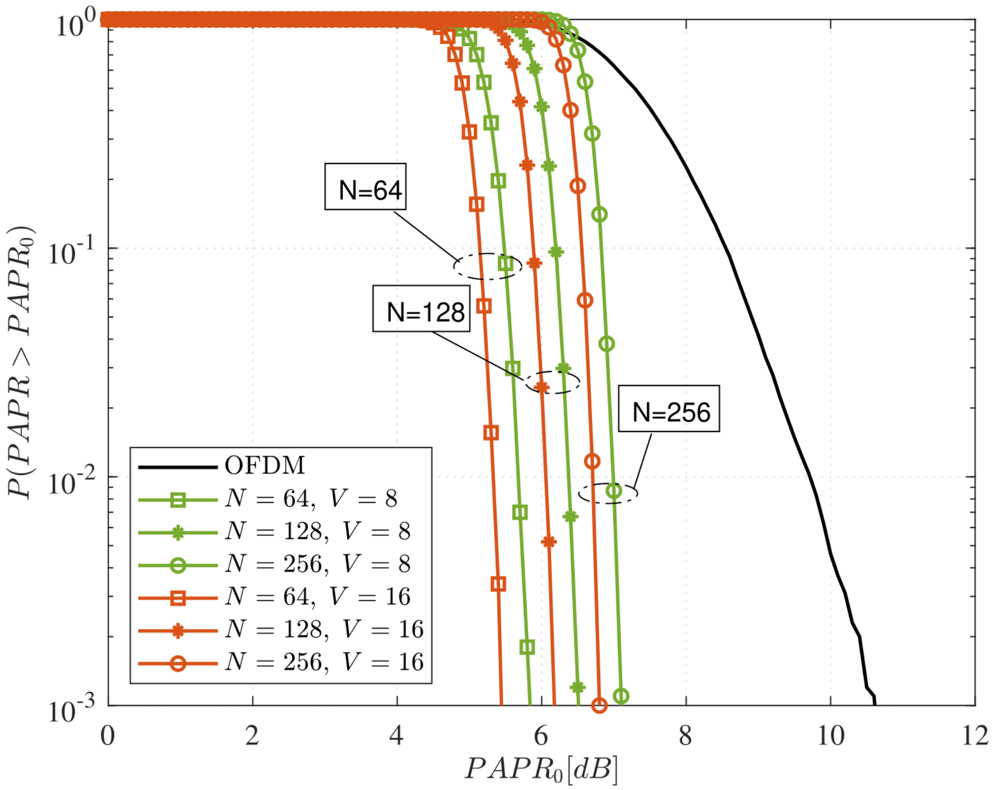

Figure 3.14: CCDF comparisons of PAPR reduction performance of IWOA-PTS using different numbers of subcarriers and subblocks.

Table 3.4: PAPR performance comparisons of the IWOA-PTS against other techniques with V=8 and W=4 (at the CCDF clip of 10^{-3}).

Method	Computational load	PAPR value (dB)
Conventional OFDM	–	10.7
OPTS	$W^{V-1} = 4^7 = 16384$	5.77
RS-PTS	$I = 20$	6.8
HSA-PTS	$I \times P = 20 \times 50 = 1000$	6.3
PSO-PTS	$I \times P = 20 \times 50 = 1000$	6.7
WOA-PTS	$I \times P = 20 \times 50 = 1000$	6.6
IWOA-PTS	$I \times P = 20 \times 50 = 1000$	5.84

OPTS. Furthermore, IWOA-PTS prevails over the swarm intelligence algorithms (WOA, PSO, and HSA) in PAPR reduction for the same computational load.

Table 3.5 shows the PAPR performance comparisons of the IWOA-PTS against the state-of-the-art techniques. For proper comparison, the simulation parameters of

Table 3.5: PAPR performance comparisons of the IWOA-PTS against the state-of-the-art techniques (at the CCDF clip of 10^{-3})

Method	PAPR[method]	Cl[1][method]	PAPR[IWOA-PTS]	Cl[IWOA-PTS]
Side Information Embedding[180]	9.2	8192	8.18	1000
EA-PTS[181]	6.4	1200	5.8	1000
HGA-PTS [182]	5.6	1200	5.55	1200
ACO-PTS [183]	6.52	1200	6.3	1200
GWO-PTS [184]	6.7	1200	5.45	1200

[1] Computational load.

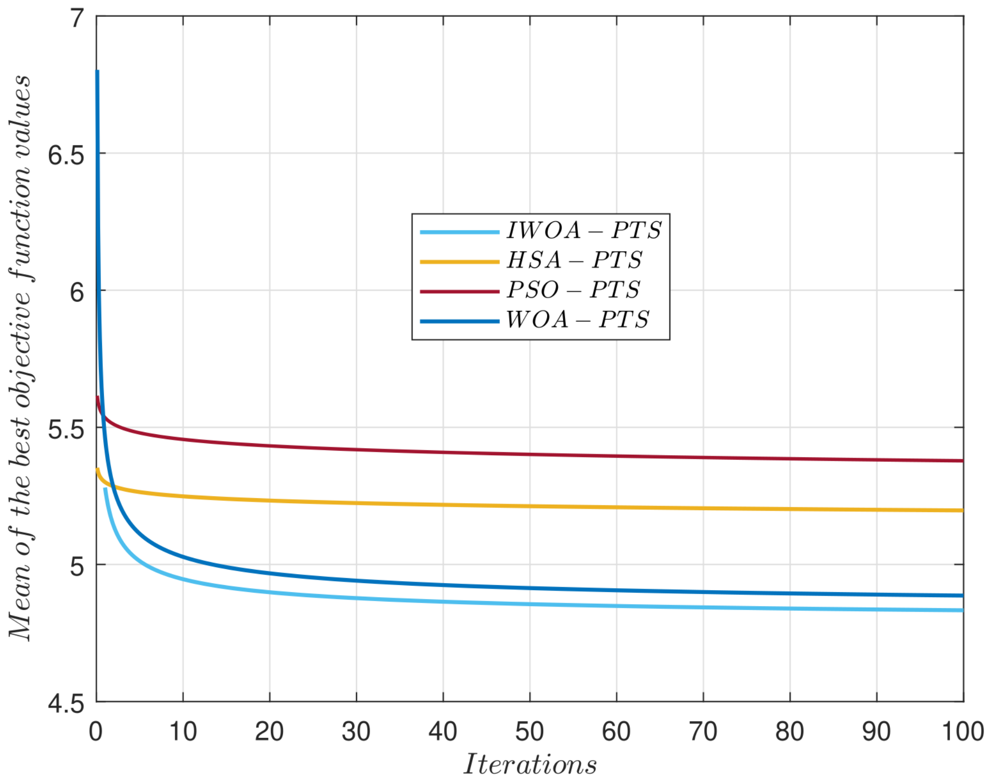

Figure 3.15: Convergence analysis of the IWOA-PTS versus other PTS techniques based on meta-heuristic algorithms.

the IWOA-PTS are adjusted in each comparison according to those of the compared method. It is clear from this comparison that the proposed method has proved its effectivenessin terms of both PAPR reduction and complexity.

In Figure 3.15, the PAPR convergence performance of the IWOA-PTS is illustrated and compared to other methods. Using V=16, 100 trials are executed for one OFDM symbol. As can be seen, the convergence performance is classified as follows:

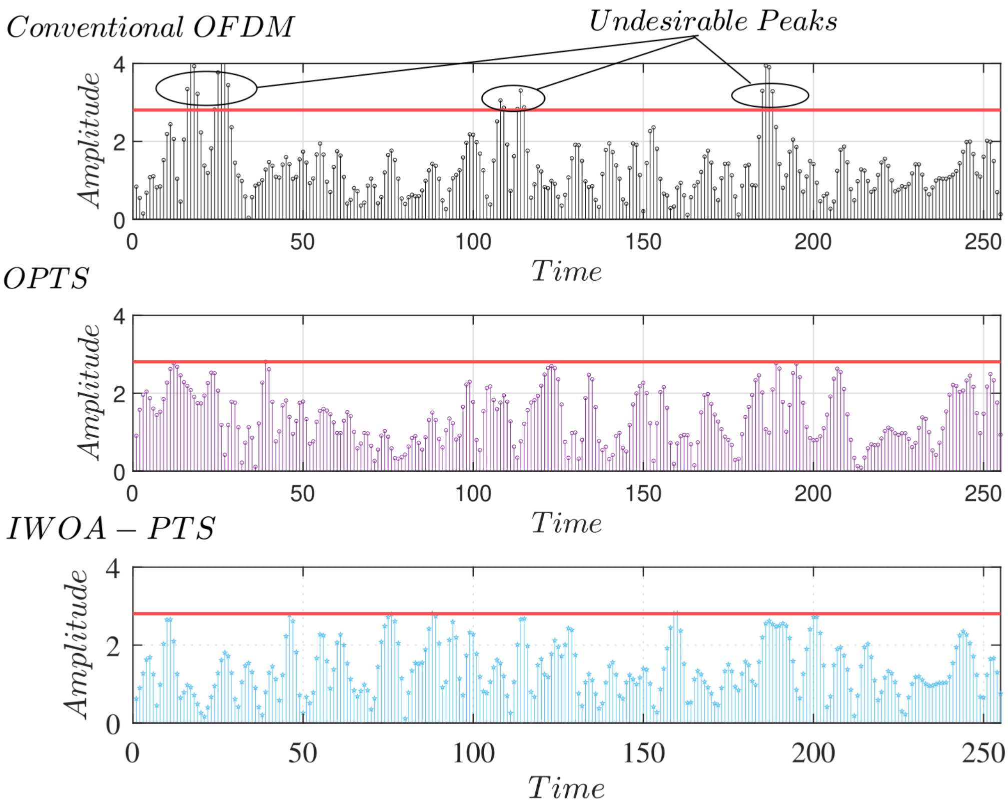

Figure 3.16: Time-domain peaks comparisons between the conventional OFDM, the OPTS, and the proposed IWOA-PTS.

IWOA-PTS > WOA-PTS > PSO-PTS > HSA-PTS. Thereby, the superiority of the IWOA-PTS in terms of convergence rate over its counterparts is justified.

Figure 3.16 shows the PAPR reduction performance of the IWOA-PTS for an OFDM symbol. After oversampling the transmitted symbol of N=64 with an oversampling factor of 4 and then performing an IFFT operation, a time domain signal of length 256 is obtained. The figure captures the amplitude of the OFDM symbol examined without PAPR reduction and compares it to that of OPTS and IWOA-PTS. As can be seen, IWOA-PTS robustly reduces undesirable peaks in the OFDM signal with a competitive performance with OPTS at only 6.1% of its complexity

3.5 Conclusion

This chapter presents two PTS methods with low complexity. The first method introduces a novel suboptimal low-complexity PTS scheme. In this approach, the exhaustive search is replaced by an enhanced PSO algorithm. Through simulations, the effectiveness of this scheme in minimizing PAPR is demonstrated. The enhanced PSO algorithm outperforms other compared swarm intelligence (SI) algorithms while maintaining the same level of search complexity. Additionally, a convergence analysis confirms the fast convergence of the improved PSO algorithm compared to the other algorithms considered. The search complexity of the PSO-PTS method is significantly reduced, accounting for only 0.92% compared to the original PTS method. This showcases a favorable trade-off between search complexity and PAPR reduction.

In the second contribution, a new PTS technique based on the IWOA algorithm is proposed to compensate for the exhaustive search in the OPTS technique, mainly due to its impracticality for large subblock partitions and phase factors sets. The simulated results show the superiority of the IWOA-PTS; it achieved approximately the same performance as that by the OPTS method (marginal gap of 0.07) while it counts only 6.1% of its complexity. Furthermore, the IWOA-PTS technique showcases its adaptability to different parameter sets, including V, N, I, and P. A comparative analysis between IWOA and WOA is conducted, considering various subblock partitions and an equal computational load, revealing the superiority of IWOA-PTS over WOA-PTS. Moreover, when compared to other techniques such as PSO-PTS, HGA-PTS, GWO-PTS, HSA-PTS, RS-PTS, as well as several efficient state-of-the-art techniques, the IWOA-PTS technique demonstrates the best PAPR reduction performance. Consequently, the proposed scheme can be deemed as a practical and effective technique for reducing PAPR in OFDM systems.

General Conclusion and Perspectives

The objective of this thesis was to develop advanced techniques that improve 5G systems. One significant challenge faced by 5G technology is the issue of PAPR, which is associated with the OFDM waveform utilized in 5G NR systems. Despite its advantages in terms of high spectral efficiency and the ability to achieve high data rates even in frequency-selective fading channels, the OFDM waveform presents challenges related to PAPR. Therefore, in this thesis two contributions have been presented in the aim of reducing the PAPR of the OFDM signals.

The initial chapter has provided a solid foundation for comprehending the fundamental aspects of 5G technology, which is crucial to grasp the subsequent chapters and to delve into the underlying causes of the PAPR problem. We have incorporated various details encompassing the architecture, features, use cases, requirements, and waveform of the 5G technology. Furthermore, we have delved into the architecture and numerology of 5G NR, emphasizing the adoption of OFDM as the preferred waveform. We have highlighted the characteristics that make OFDM well-suited for 5G, while also addressing its primary drawback, the PAPR, which necessitates mitigation before signal transmission.

In the second chapter, we presented a comprehensive and detailed overview of various techniques used for mitigating PAPR. Each approach was thoroughly explained, including its fundamental principles and modeling procedures. Additionally, we conducted an extensive literature review, encompassing earlier approaches as well as the latest state-of-the-art schemes, for each technique. Subsequently, a comparative analysis was conducted to evaluate the strengths and weaknesses of each method, ultimately leading to the selection of the most promising technique. After careful consideration, we identified the PTS scheme as the most compelling among the compared approaches.

In the final chapter, we introduced our contribution models. We addressed the issue associated with the high search complexity of the PTS technique and presented our models aimed at enhancing it while simultaneously reducing PAPR levels. Our goal was to achieve a beneficial compromise that effectively addresses the challenges posed by high search complexity and high PAPR levels. Both contributions in our research involved combining the PTS technique with an optimization algorithm. In the first contribution, we introduced the PSO-PTS technique, where the PSO algorithm was enhanced to prevent getting trapped in local optima. We presented a pseudo-algorithm detailing the improved PSO model, along with its mathematical formulas. The effectiveness of our proposed model was evaluated through a comparison with other efficient algorithms. We also conducted computational complexity and convergence analyses. In the second contribution, we proposed an improved whale optimization algorithm within the PTS technique to address the impracticality issue of the PTS scheme and effectively reduce PAPR levels. We provided a clear discussion of the formalism and mathematical modeling of the employed IWOA. Similar to the previous contribution, we conducted complexity and convergence analyses. Furthermore, we compared our approach to other algorithms and state-of-the-art techniques, demonstrating the robustness of our scheme.

Overall, both investigated models proved to be efficient in terms of reducing PAPR levels and managing complexity. They serve as viable alternatives for lowering PAPR levels in OFDM systems, thereby enhancing the performance of the 5G system.

At the end of the work carried out, encouraging perspectives can be envisioned for further exploration:

- Evaluate the efficacy of diverse PAPR lowering approaches in enhancing the performance of the system, encompassing key metrics like spectral efficiency, coverage, and bit error rate (BER).

- Assess the effectiveness of PAPR reduction methods and formulate solutions to address the PAPR phenomenon in alternative waveform candidates intended to meet the specifications of 5G technology, such as Filtered Multi-Carrier (UFMC), Filtered-OFDM (F-OFDM), and FBMC.

List of Publications

- **International publications**

  Taba, S., Redadaa, S., Benchana, M. A., & Ikni, S. A Low-Complexity PTS Technique based-Improved PSO Algorithm for PAPR Reduction in OFDM Systems. Telecommunications and Radio Engineering.10.1615/TelecomRadEng.2023047181

- **International communications**

  Taba, S., Redadaa, S., Benchana, M. A., & Ikni, S. A New Hybrid IFPSO Algorithm Based PTS Technique for PAPR Mitigation in OFDM Systems. ICAECE'2023, Tebessa, May 15-16, 2023.

Man's mind stretched to a new idea never goes back to its original dimensions ...

— Oliver Wendell Holmes

Bibliography

[1] Meraj, M., & Kumar, S. (2015). Evolution of mobile wireless technology from 0G to 5G. International Journal of Computer Science and Information Technologies, 6(3), 2545-2551.

[2] Nadeem, Lubna, Muhammad Awais Azam, Yasar Amin, Mohammed A. Al-Ghamdi, Kok Keong Chai, Muhammad Faisal Nadeem Khan, et Muhammad Adnan Khan. « Integration of D2D, Network Slicing, and MEC in 5G Cellular Networks: Survey and Challenges ». IEEE Access 9 (2021): 37590-612. https://doi.org/10.1109/ACCESS.2021.3063104.

[3] Hwang, Taewon, Chenyang Yang, Gang Wu, Shaoqian Li, et Geoffrey Ye Li. « OFDM and Its Wireless Applications: A Survey ». IEEE Transactions on Vehicular Technology 58, no 4 (mai 2009): 1673-94. https://doi.org/10.1109/TVT.2008.2004555.

[4] Chang, R., et R. Gibby. « A Theoretical Study of Performance of an Orthogonal Multiplexing Data Transmission Scheme ». IEEE Transactions on Communications 16, no 4 (août 1968): 529-40. https://doi.org/10.1109/TCOM.1968.1089889.

[5] Müller, Stefan H., Robert W. Bäuml, Robert F. H. Fischer, et Johannes B. Huber. « OFDM with reduced peak-to-average power ratio by multiple signal representation ». Annales Des Télécommunications 52, no 1-2 (janvier 1997): 58-67. https://doi.org/10.1007/BF03001051.

[6] Poli, Riccardo, James Kennedy, et Tim Blackwell. « Particle Swarm Optimization: An Overview ». Swarm Intelligence 1, no 1 (17 octobre 2007): 33-57. https://doi.org/10.1007/s11721-007-0002-0.

[7] Osseiran, Afif, Federico Boccardi, Volker Braun, Katsutoshi Kusume, Patrick Marsch, Michal Maternia, Olav Queseth, et al. « Scenarios for 5G mobile and wireless communications: the vision of the METIS project ». IEEE Communications Magazine 52, no 5 (mai 2014): 26-35. https://doi.org/10.1109 /MCOM.2014.6815890.

[8] Bhalla, Mudit Ratana, et Anand Vardhan Bhalla. « Generations of Mobile Wireless Technology: A Survey ». International Journal of Computer Applications 5, no 4 (10 août 2010): 26-32. https://doi.org/10.5120 /905-1282.

[9] Nitesh, Garsha Sai, et Ashna Kakkar. « Generations of Mobile Communication ». International Journal of Advanced Research in Computer Science and Software Engineering, 2016. 3. 32.

[10] Ramzan, M., et Javed Ahmed Shaheen. « Comparison: 3G Wireless Networks with 4G Wireless Networks Technology Wise ». International Journal of Advanced Science and Technology 108 (30 novembre 2017): 1-10. https://doi.org/10.14257/ijast.2017.108.01.

[11] Tsiropoulou, Eirini Eleni, Timotheos Kastrinogiannis, et Symeon Papavassiliou. « Uplink Power Control in QoS-aware Multi-Service CDMA Wireless Networks ». Journal of Communications 4, no 9 (1 octobre 2009): 654-68. https://doi.org/10.4304/jcm.4.9.654-668.

[12] Ezhilarasan, E., et M. Dinakaran. « A Review on Mobile Technologies: 3G, 4G and 5G ». In 2017 Second International Conference on Recent Trends and Challenges in Computational Models (ICRTCCM), 369-73. Tindivanam, Tamilnadu, India: IEEE, 2017. https://doi.org/10.1109/ICRTCCM.2017.90.

[13] Popovski, Petar, Kasper Floe Trillingsgaard, Osvaldo Simeone, et Giuseppe Durisi. « 5G Wireless Network Slicing for eMBB, URLLC, and mMTC: A Communication-Theoretic View ». IEEE Access 6 (2018): 55765-79. https://doi.org/10.1109/ACCESS.2018.2872781.

[14] Hill, Michael D, et David B Cruickshank. « Ceramic materials for 5G wireless communication systems ». American Ceramic Society Bulletin 98, no 6 (s. d.): 20-25.

[15] Marsch, Patrick, Ömer Bulakçı, Olav Queseth, et Mauro Boldi, éd. 5G System Design: Architectural and Functional Considerations and Long Term Research. 1re éd. Wiley, 2018. https://doi.org/10.1002 /9781119425144.

[16] Wang, Cheng-Xiang, Shangbin Wu, Lu Bai, Xiaohu You, Jing Wang, et Chih-Lin I. « Recent Advances and Future Challenges for Massive MIMO Channel Measurements and Models ». Science China Information Sciences 59, no 2 (février 2016): 1-16. https://doi.org/10.1007/s11432-015-5517-1.

[17] Islam, S. M. Riazul, Nurilla Avazov, Octavia A. Dobre, et Kyung-sup Kwak. « Power-Domain Non- Orthogonal Multiple Access (NOMA) in 5G Systems: Potentials and Challenges ». IEEE Communications Surveys & Tutorials 19, no 2 (2017): 721-42. https://doi.org/10.1109 /COMST.2016.2621116.

[18] Shental, Ori, Benjamin M. Zaidel, et Shlomo Shamai Shitz. « Low-density code-domain NOMA: Better be regular ». In 2017 IEEE International Symposium on Information Theory (ISIT), 2628-32. Aachen, Germany: IEEE, 2017. https://doi.org/10.1109/ISIT.2017.8007005.

[19] Wu, Zhanji, Kun Lu, Chengxin Jiang, et Xuanbo Shao. « Comprehensive Study and Comparison on 5G NOMA Schemes ». IEEE Access 6 (2018): 18511-19. https://doi.org/10.1109/ACCESS.2018.2817221.

[20] Hong, Tao, Shuli Zheng, Rongke Liu, et Weiting Zhao. « Design of MmWave Directional Antenna for Enhanced 5G Broadcasting Coverage ». Sensors 21, no 3 (22 janvier 2021): 746. https://doi.org/10.3390 /s21030746.

[21] Pi, Zhouyue, et Farooq Khan. « An introduction to millimeter-wave mobile broadband systems ». IEEE Communications Magazine 49, no 6 (juin 2011): 101-7. https://doi.org/10.1109/MCOM.2011.5783993.

[22] Busari, Sherif Adeshina, Shahid Mumtaz, Saba Al-Rubaye, et Jonathan Rodriguez. « 5G Millimeter-Wave Mobile Broadband: Performance and Challenges ». IEEE Communications Magazine 56, no 6 (juin 2018): 137-43. https://doi.org/10.1109/MCOM.2018.1700878.

[23] Rangan, Sundeep, Theodore S. Rappaport, et Elza Erkip. « Millimeter-Wave Cellular Wireless Networks: Potentials and Challenges ». Proceedings of the IEEE 102, no 3 (mars 2014): 366-85. https://doi.org /10.1109/JPROC.2014.2299397.

[24] Goudos, Sotirios K., Panagiotis I. Dallas, Stella Chatziefthymiou, et Sofoklis Kyriazakos. « A Survey of IoT Key Enabling and Future Technologies: 5G, Mobile IoT, Sematic Web and Applications ». Wireless Personal Communications 97, no 2 (novembre 2017): 1645-75. https://doi.org/10.1007 /s11277-017-4647-8.

[25] Kaur, Jasneet, M. Arif Khan, Mohsin Iftikhar, Muhammad Imran, et Qazi Emad Ul Haq. « Machine Learning Techniques for 5G and Beyond ». IEEE Access 9 (2021): 23472-88. https://doi.org/10.1109 /ACCESS.2021.3051557.

[26] Vouyioukas, Demosthenes. « A Survey on Beamforming Techniques for Wireless MIMO Relay Networks ». International Journal of Antennas and Propagation 2013 (2013): 1-21. https://doi.org/10.1155 /2013/745018.

[27] Vook, Frederick W., Amitava Ghosh, et Timothy A. Thomas. « MIMO and beamforming solutions for 5G technology ». In 2014 IEEE MTT-S International Microwave Symposium (IMS2014), 1-4. Tampa, FL, USA: IEEE, 2014. https://doi.org/10.1109/MWSYM.2014.6848613.

[28] Hoydis, Jakob, Mari Kobayashi, et Merouane Debbah. « Green Small-Cell Networks ». IEEE Vehicular Technology Magazine 6, no 1 (mars 2011): 37-43. https://doi.org/10.1109/MVT.2010.939904.

[29] Rajoria, Shweta, Aditya Trivedi, et W. Wilfred Godfrey. « A Comprehensive Survey: Small Cell Meets Massive MIMO ». Physical Communication 26 (février 2018): 40-49. https://doi.org/10.1016 /j.phycom.2017.11.004.

[30] Wang, Shuo, Xing Zhang, Yan Zhang, Lin Wang, Juwo Yang, et Wenbo Wang. « A Survey on Mobile Edge Networks: Convergence of Computing, Caching and Communications ». IEEE Access 5 (2017): 6757-79. https://doi.org/10.1109/ACCESS.2017.2685434.

[31] Beck, Michael Till, Martin Werner, Sebastian Feld, et Thomas Schimper. « Mobile edge computing: A taxonomy ». In Proceedings of the Sixth International Conference on Advances in Future Internet, 16 novembre 2014.

[32] Kholod, Ivan, Andrey Shorov, et Sergei Gorlatch. « Efficient Distribution and Processing of Data for Parallelizing Data Mining in Mobile Clouds ». Journal of Wireless Mobile Networks, Ubiquitous Computing, and Dependable Applications 11, no 1 (31 mars 2020): 2-17. https://doi.org/10.22667 /JOWUA.2020.03.31.002.

[33] Parkvall, Stefan, Erik Dahlman, Anders Furuskar, et Mattias Frenne. « NR: The New 5G Radio Access Technology ». IEEE Communications Standards Magazine 1, no 4 (décembre 2017): 24-30. https://doi.org/10.1109/MCOMSTD.2017.1700042.

[34] Lien, Shao-Yu, Shin-Lin Shieh, Yenming Huang, Borching Su, Yung-Lin Hsu, et Hung-Yu Wei. « 5G New Radio: Waveform, Frame Structure, Multiple Access, and Initial Access ». IEEE Communications Magazine 55, no 6 (2017): 64-71. https://doi.org/10.1109/MCOM.2017.1601107.

[35] 5G;NR; Physical Channels and Modulation—Release 15, document TS 38.211, V. 15.4.0, 3GPP, 2018.

[36] 5G Spectrum Public Policy Position, Huawei, Shenzen, China, 2017.

[37] Study on New Radio (NR) Access Technology, (Release 14), document TR 38.912 version 14.0.0, 3GPP, 2017.

[38] Litsyn, S. (2007) Peak Power Control in Multicarrier Communications, Cambridge University Press.

[39] Seung Hee Han et Jae Hong Lee. « Modulation, Coding and Signal Processing for Wireless Communications - An Overview of Peak-to-Average Power Ratio Reduction Techniques for Multicarrier Transmission ». IEEE Wireless Communications 12, no 2 (avril 2005): 56-65. https://doi.org/10.1109 /MWC.2005.1421929.

[40] Xu, Hong, Yuzhe Chen, Yuan Lu, Jianbo Liu, et Feng Hu. « Improved Elitist Genetic Algorithm Optimization based PTS to PAPR Reduction for Multi-Carrier Signals ». In 2022 IEEE 6th Information Technology and Mechatronics Engineering Conference (ITOEC), 1746-50. Chongqing, China: IEEE, 2022. https://doi.org/10.1109/ITOEC53115.2022.9734372.

[41] Anoh, Kelvin, Cagri Tanriover, et Bamidele Adebisi. « On the Optimization of Iterative Clipping and Filtering for PAPR Reduction in OFDM Systems ». IEEE Access 5 (2017): 12004-13. https://doi.org /10.1109/ACCESS.2017.2711533.

[42] F. Khan, LTE for 4G Mobile Broadband: Air Interface Technologies and Performance. Cambridge, U.K.: Cambridge Univ. Press, 2009, ch. 5, pp. 88–108.

[43] Rappaport, Theodore S., Shu Sun, Rimma Mayzus, Hang Zhao, Yaniv Azar, Kevin Wang, George N. Wong, Jocelyn K. Schulz, Mathew Samimi, et Felix Gutierrez. « Millimeter Wave Mobile Communications for 5G Cellular: It Will Work! » IEEE Access 1 (2013): 335-49. https://doi.org/10.1109 /ACCESS.2013.2260813.

[44] Huo, Yiming, Xiaodai Dong, et Wei Xu. « 5G Cellular User Equipment: From Theory to Practical Hardware Design ». IEEE Access 5 (2017): 13992-10. https://doi.org/10.1109/ACCESS.2017.2727550.

[45] Li, Wang, et Gu linfeng. « An Investigation of Peak-to-Average Power Reduction in MIMO-OFDM Systems ». Blekinge Inst, 2009.

[46] Rezaie, Sajad, Abbas Mohammadi, Navvab Afrashteh, et Vahideh Sanjaroonpouri. « Realization of Constant Envelope OFDM Using Quantization and CPM Technique ». AEU - International Journal of Electronics and Communications 80 (octobre 2017): 172-78. https://doi.org/10.1016/j.aeue.2017.06.035.

[47] Rahmatallah, Yasir, et Seshadri Mohan. « Peak-To-Average Power Ratio Reduction in OFDM Systems: A Survey And Taxonomy ». IEEE Communications Surveys & Tutorials 15, no 4 (2013): 1567-92. https://doi.org/10.1109/SURV.2013.021313.00164.

[48] Jones, Awinings E, Tim A Wilkinson, et S.K Barton. « Block coding scheme for reduction of peak to mean envelope power ratio of multicarrier transmission schemes ». Electronics letters, s. d. 25. 30.

[49] Chih-Peng Li, Sen-Hung Wang, et Chin-Liang Wang. « Novel Low-Complexity SLM Schemes for PAPR Reduction in OFDM Systems ». IEEE Transactions on Signal Processing 58, no 5 (mai 2010): 2916-21. https://doi.org/10.1109/TSP.2010.2043142.

[50] Jones, A.E, et T.A Wilkinson. « Combined coding for error control and increased robustness to system nonlinearities in OFDM ». In Proceedings of Vehicular Technology Conference-VTC, s. d. 904-908. 2.

[51] Davis, J.A, et J Jedwab. « Peak-to-mean power control and error correction for OFDM transmission using Golay sequences and Reed-Muller codes ». Electronics Letters, s. d. 4. 33.

[52] Davis, J.A, et J Jedwab. « Peak-to-Mean Power Control in OFDM, Golay Complementary Sequences, and Reed–Muller Codes ». IEEE Trans. Info. Theory, 1999. 7. 45.

[53] Paterson, K.G., et V. Tarokh. « On the existence and construction of good codes with low peak-to-average power ratios ». In 2000 IEEE International Symposium on Information Theory (Cat. No.00CH37060), 217. Sorrento, Italy: IEEE, 2000. https://doi.org/10.1109/ISIT.2000.866515.

[54] Chong, C.V., et V. Tarokh. « A simple encodable/decodable OFDM QPSK code with low peak-to-mean envelope power ratio ». IEEE Transactions on Information Theory 47, no 7 (novembre 2001): 3025-29. https://doi.org/10.1109/18.959282.

[55] O'Neill, R., et L.B. Lopes. « Envelope variations and spectral splatter in clipped multicarrier signals ». In Proceedings of 6th International Symposium on Personal, Indoor and Mobile Radio Communications, 1:71-75. Toronto, Ont., Canada: IEEE, 1995. https://doi.org/10.1109/PIMRC.1995.476406.

[56] Terry, John, et Juha Heiskala. OFDM wireless LANs: a theoretical and practical guide. Indianapolis, Ind: Sams, 2002.

[57] Armstrong, J. « Peak-to-Average Power Reduction for OFDM by Repeated Clipping and Frequency Domain Filtering ». Electronics Letters 38, no 5 (2002): 246. https://doi.org/10.1049/el:20020175.

[58] Wang, Y.-C., et Z.-Q. Luo. « Optimized Iterative Clipping and Filtering for PAPR Reduction of OFDM Signals ». IEEE Transactions on Communications 59, no 1 (janvier 2011): 33-37. https://doi.org/10.1109/TCOMM.2010.102910.090040.

[59] Lee, Byung Moo, et Youngok Kim. « An Adaptive Clipping and Filtering Technique for PAPR Reduction of OFDM Signals ». Circuits, Systems, and Signal Processing 32, no 3 (juin 2013): 1335-49. https://doi.org /10.1007/s00034-012-9512-0.

[60] Zhu, Xiaodong, Wensheng Pan, Hong Li, et Youxi Tang. « Simplified Approach to Optimized Iterative Clipping and Filtering for PAPR Reduction of OFDM Signals ». IEEE Transactions on Communications 61, no 5 (mai 2013): 1891-1901. https://doi.org/10.1109/TCOMM.2013.021913.110867.

[61] Sohn, Insoo, et Sung Chul Kim. « Neural Network Based Simplified Clipping and Filtering Technique for PAPR Reduction of OFDM Signals ». IEEE Communications Letters 19, no 8 (aout 2015): 1438-41. https://doi.org/10.1109/LCOMM.2015.2441065.

[62] Liu, Xiaoran, Xiaoying Zhang, Jun Xiong, Fanglin Gu, et Jibo Wei. « An Enhanced Iterative Clipping and Filtering Method Using Time-Domain Kernel Matrix for PAPR Reduction in OFDM Systems ». IEEE Access 7 (2019): 59466-76. https://doi.org/10.1109/ACCESS.2019.2915354.

[63] Bharati, Subrato, et Prajoy Podder. « Adaptive PAPR Reduction Scheme for OFDM Using SLM with the Fusion of Proposed Clipping and Filtering Technique in Order to Diminish PAPR and Signal Distortion ». Wireless Personal Communications 113, no 4 (août 2020): 2271-88. https://doi.org/10.1007/s11277-020-07323-0.

[64] Liu, Xiaoran, Xiaoying Zhang, Lei Zhang, Pei Xiao, Jibo Wei, Haijun Zhang, et Victor C. M. Leung. « PAPR Reduction Using Iterative Clipping/Filtering and ADMM Approaches for OFDM-Based Mixed- Numerology Systems ». IEEE Transactions on Wireless Communications 19, no 4 (avril 2020): 2586-2600. https://doi.org/10.1109/TWC.2020.2966600.

[65] Sun, Ying, et Hideki Ochiai. « Performance Analysis and Comparison of Clipped and Filtered OFDM Systems With Iterative Distortion Recovery Techniques ». IEEE Transactions on Wireless Communications 20, no 11 (novembre 2021): 7389-7403. https://doi.org/10.1109/TWC.2021.3083537.

[66] Acharya Nagarjuna University, Vijaya Padarti, Venkateswara Nandhanavanam, et Bapatla Engineering College. « An improved ASOICF algorithm for PAPR reduction in OFDM systems ». International Journal of Intelligent Engineering and Systems 14, no 2 (30 avril 2021): 353-60. https://doi.org/10.22266/ijies2021.0430.32.

[67] Nguyen, Quang, The Khai Nguyen, Ha H. Nguyen, et Brian Berscheid. « Novel PAPR Reduction Algorithms for OFDM Signals ». IEEE Access 10 (2022): 77452-61. https://doi.org/10.1109 /ACCESS.2022.3188675.

[68] Aimer, Younes, Boubakar Seddik Bouazza, Smail Bachir, et Claude Duvanaud. « Interleaving Technique Implementation to Reduce PAPR of OFDM Signal in Presence of Nonlinear Amplification with Memory Effects ». Journal of Telecommunications and Information Technology 3, no 2018 (octobre 2018): 14-22. https://doi.org/10.26636/jtit.2018.123517.

[69] Malathi, P., et P.T. Vanathi. « Improved Interleaving Technique for PAPR Reduction in OFDM-MIMO System ». In 2008 Second Asia International Conference on Modelling & Simulation (AMS), 253-58. IEEE, 2008. https://doi.org/10.1109/AMS.2008.52.

[70] Sakran, Hefdhallah Yahya, Mona Shokair, et Atef Abou Elazm. « COMBINED INTERLEAVING AND COMPANDING FOR PAPR REDUCTION IN OFDM SYSTEMS ». Progress In Electromagnetics Research C 6 (2009): 67-78. https://doi.org/10.2528/PIERC08122211.

[71] Jiang, T., Y. Yang, et Y.-H. Song. « Exponential Companding Technique for PAPR Reduction in OFDM Systems ». IEEE Transactions on Broadcasting 51, no 2 (juin 2005): 244-48. https://doi.org/10.1109 /TBC.2005.847626.

[72] Jeng, Shiann-Shiun, et Jia-Ming Chen. « Efficient PAPR Reduction in OFDM Systems Based on a Companding Technique With Trapezium Distribution ». IEEE Transactions on Broadcasting 57, no 2 (juin 2011): 291-98. https://doi.org/10.1109/TBC.2011.2112237.

[73] Anoh, Kelvin, Bamidele Adebisi, Khaled M. Rabie, et Cagri Tanriover. « Root-Based Nonlinear Companding Technique for Reducing PAPR of Precoded OFDM Signals ». IEEE Access 6 (2018): 4618-29. https://doi.org/10.1109/ACCESS.2017.2779448.

[74] Shaheen, Imad A., Abdelhalim Zekry, Fatma Newagy, et Reem Ibrahim. « PAPR Reduction of FBMC/OQAM Systems Based on Combination of DST Precoding and A-law Nonlinear Companding Technique ». In 2017 International Conference on Promising Electronic Technologies (ICPET), 38-42. Deir El-Balah: IEEE, 2017. https://doi.org/10.1109/ICPET.2017.13.

[75] Shaheen, Imad A., Abdelhalim Zekry, Fatma Newagy, et Reem Ibrahim. « Performance Evaluation of PAPR Reduction in FBMC System Using Nonlinear Companding Transform ». ICT Express 5, no 1 (mars 2019): 41-46. https://doi.org/10.1016/j.icte.2018.01.017.

[76] Ibraheem, Zeyid, Kawakib K, Yousef Fazea, Mohammed Madi, Fathey Mohammed, et Abdulrazzaq Qasem Ali. « Boosted PTS Method with Mu-Law Companding Techniques for PAPR Reduction in OFDM Systems ». Preprint. In Review, 1 juillet 2021. https://doi.org/10.21203/rs.3.rs-386678/v1.

[77] Xin, Duqiang, Qiang Xu, Shuang Qiao, et Tian Zhang. « Non-linear Companding Transform for DCOOFDM- based VLC Systems ». IET Communications 13, no 8 (mai 2019): 1110-14. https://doi.org /10.1049/iet-com.2018.5864.

[78] Jones, D.L. « Peak power reduction in OFDM and DMT via active channel modification ». In Conference Record of the Thirty-Third Asilomar Conference on Signals, Systems, and Computers (Cat. No.CH37020), 2:1076-79. Pacific Grove, CA, USA: IEEE, 1999. https://doi.org/10.1109 /ACSSC.1999.831875.

[79] Krongold, B.S., et D.L. Jones. « Par Reduction in Ofdm via Active Constellation Extension ». IEEE Transactions on Broadcasting 49, no 3 (septembre 2003): 258-68. https://doi.org/10.1109 /TBC.2003.817088.

[80] Bae, Kitaek, Jeffrey Andrews, et Edward Powers. « Adaptive active constellation extension algorithm for peak-to-average ratio reduction in OFDM ». IEEE Communications Letters 14, no 1 (janvier 2010): 39-41. https://doi.org/10.1109/LCOMM.2010.01.091168.

[81] Wang, Sen-Hung, Wei-Lun Lin, Bo-Rong Huang, et Chih-Peng Li. « PAPR Reduction in OFDM Systems Using Active Constellation Extension and Subcarrier Grouping Techniques ». IEEE Communications Letters 20, no 12 (décembre 2016): 2378-81. https://doi.org/10.1109/LCOMM.2016.2603529.

[82] Zhong, Ju, Xuelin Yang, et Weisheng Hu. « Performance-Improved Secure OFDM Transmission Using Chaotic Active Constellation Extension ». IEEE Photonics Technology Letters 29, no 12 (15 juin 2017): 991-94. https://doi.org/10.1109/LPT.2017.2700861.

[83] Lin, Wei-Lun, et Fan-Shuo Tseng. « Theory and Applications of Active Constellation Extension ». IEEE Access 9 (2021): 93111-18. https://doi.org/10.1109/ACCESS.2021.3093103.

[84] Mezghani, Amine, et Robert W. Heath. « Massive MIMO Precoding and Spectral Shaping with Low Resolution Phase-only DACs and Active Constellation Extension », 2020. https://doi.org/10.48550 /ARXIV.2012.00259.

[85] J. Tellado, Peak to Average Power Reduction for Multicarrier Modulation, Ph.D. dissertation, Stanford Univ., 2000.

[86] Al-Safadi, Eprahim B., et Tareq Y. Al-Naffouri. « On Reducing the Complexity of Tone-Reservation Based PAPR Reduction Schemes by Compressive Sensing ». In GLOBECOM 2009 - 2009 IEEE Global Telecommunications Conference, 1-6. Honolulu, Hawaii: IEEE, 2009. https://doi.org/10.1109 /GLOCOM.2009.5425904.

[87] Li, Haibo, Tao Jiang, et Yang Zhou. « An Improved Tone Reservation Scheme With Fast Convergence for PAPR Reduction in OFDM Systems ». IEEE Transactions on Broadcasting 57, no 4 (décembre 2011): 902-6. https://doi.org/10.1109/TBC.2011.2169622.

[88] Jung-Chieh Chen et Chih-Peng Li. « Tone Reservation Using Near-Optimal Peak Reduction Tone Set Selection Algorithm for PAPR Reduction in OFDM Systems ». IEEE Signal Processing Letters 17, no 11 (novembre 2010): 933-36. https://doi.org/10.1109/LSP.2010.2077278.

[89] Jiang, Tao, Chunxing Ni, Chang Xu, et Qi Qi. « Curve Fitting Based Tone Reservation Method with Low Complexity for PAPR Reduction in OFDM Systems ». IEEE Communications Letters 18, no 5 (mai 2014): 805-8. https://doi.org/10.1109/LCOMM.2014.032014.132174.

[90] Tosato, Filippo, Magnus Sandell, et Makoto Tanahashi. « Tone reservation for PAPR reduction: An optimal approach through sphere encoding ». In 2016 IEEE International Conference on Communications (ICC), 1-6. Kuala Lumpur, Malaysia: IEEE, 2016. https://doi.org/10.1109/ICC.2016.7511168.

[91] Li, Lanping, Chintha Tellambura, et Xiaohu Tang. « Improved Tone Reservation Method Based on Deep Learning for PAPR Reduction in OFDM System ». In 2019 11th International Conference on Wireless Communications and Signal Processing (WCSP), 1-6. Xi'an, China: IEEE, 2019. https://doi.org/10.1109 /WCSP.2019.8928103.

[92] El Hassan, Mariam, Matthieu Crussiere, Jean-Francois Helard, Youssef Nasser, et Oussama Bazzi. « EVM Closed-Form Expression for OFDM Signals With Tone Reservation-Based PAPR Reduction ». IEEE Transactions on Wireless Communications 19, no 4 (avril 2020): 2352-66. https://doi.org/10.1109 /TWC.2020.2964196.

[93] Tu, Yung-Ping, et Chiao-Che Chang. « A Novel Low Complexity Two-Stage Tone Reservation Scheme for PAPR Reduction in OFDM Systems ». Sensors 23, no 2 (13 janvier 2023): 950. https://doi.org/10.3390 /s23020950.

[94] Wattanasuwakull, T., et W. Benjapolakul. « PAPR Reduction for OFDM Transmission by using a method of Tone Reservation and Tone Injection ». In

2005 5th International Conference on Information Communications & Signal Processing, 273-77. Bangkok, Thailand: IEEE, 2005. https://doi.org/10.1109/ICICS.2005.1689049.

[95] Seung Hee Han, J.M. Cioffi, et Jae Hong Lee. « Tone Injection with Hexagonal Constellation for Peak-to- Average Power Ratio Reduction in OFDM ». IEEE Communications Letters 10, no 9 (septembre 2006): 646-48. https://doi.org/10.1109/LCOMM.2006.1714532.

[96] Chen, Jung-Chieh, et Chao-Kai Wen. « PAPR Reduction of OFDM Signals Using Cross-Entropy-Based Tone Injection Schemes ». IEEE Signal Processing Letters 17, no 8 (août 2010): 727-30. https://doi.org /10.1109/LSP.2010.2051617.

[97] Jacklin, Neil, et Zhi Ding. « A Linear Programming Based Tone Injection Algorithm for PAPR Reduction of OFDM and Linearly Precoded Systems ». IEEE Transactions on Circuits and Systems I: Regular Papers 60, no 7 (juillet 2013): 1937-45. https://doi.org/10.1109/TCSI.2012.2230505.

[98] Hou, Jun, Chintha Tellambura, et Jianhua Ge. « Clipping noise-based tone injection for PAPR reduction in OFDM systems ». In 2013 IEEE International Conference on Communications (ICC), 5759-63. Budapest, Hungary: IEEE, 2013. https://doi.org/10.1109/ICC.2013.6655514.

[99] Lee, Won Cheol, Joo Pyoung Choi, et Chuyen Khoa Huynh. « A Modified Tone Injection Scheme for PAPR Reduction Using Genetic Algorithm ». ICT Express 1, no 2 (septembre 2015): 76-81. https://doi.org /10.1016/j.icte.2015.09.007.ICT Express, 1(2), 76-81.

[100] Wang, Wei, Meixia Hu, Yongzhao Li, et Hailin Zhang. « A Low-Complexity Tone Injection Scheme Based on Distortion Signals for PAPR Reduction in OFDM Systems ». IEEE Transactions on Broadcasting 62, no 4 (décembre 2016): 948-56. https://doi.org/10.1109/TBC.2016.2570008.

[101] Hou, Jun, Xiangmo Zhao, Fengkui Gong, Fei Hui, et Jianhua Ge. « PAPR and PICR Reduction of OFDM Signals with Clipping Noise-based Tone Injection Scheme ». IEEE Transactions on Vehicular Technology, 2016, 1-1. https://doi.org/10.1109/TVT.2016.2547995.

[102] Chen, Houshou, Hsin-Ying Liang, Hung-Chi Chu, et Chuan-Bi Lin. « Improving the Peak-to-Average Power Ratio of the Single-Carrier Frequency-Division Multiple Access System through the Integration of Tone Injection and Tone Reservation Techniques: Improving the PAPR of the SC-FDMA System Through the TR-TI-Flipping ». International Journal of Communication Systems 31, no 1 (10 janvier 2018): e3408. https://doi.org/10.1002/dac.3408.

[103] Wang, Benwei, Qintuya Si, et Minglu Jin. « A Novel Tone Reservation Scheme Based on Deep Learning for PAPR Reduction in OFDM Systems ». IEEE Communications Letters 24, no 6 (juin 2020): 1271-74. https://doi.org/10.1109/LCOMM.2020.2980832.

[104] Han, S.H., et J.H. Lee. « Modified Selected Mapping Technique for PAPR Reduction of Coded OFDM Signal ». IEEE Transactions on Broadcasting 50, no 3 (septembre 2004): 335-41. https://doi.org/10.1109 /TBC.2004.834200.

[105] Le Goff, Stephane, Boon Khoo, Charalampos Tsimenidis, et Bayan Sharif. « A novel selected mapping technique for PAPR reduction in OFDM systems ». IEEE Transactions on Communications 56, no 11 (novembre 2008): 1775-79. https://doi.org/10.1109/TCOMM.2008.070021.

[106] Irukulapati, N.V., V.K. Chakka, et A. Jain. « SLM Based PAPR Reduction of OFDM Signal Using New Phase Sequence ». Electronics Letters 45, no 24 (2009): 1231. https://doi.org/10.1049/el.2009.1902.

[107] Malode, M. V., & Patil, D. B. (2010). PAPR reduction using modified selective mapping technique. Int. J. of Advanced Networking and Applications, 2(02), 626-630.

[108] Ferdosizadeh Naeiny, Mahmoud, et Farokh Marvasti. « Selected Mapping Algorithm for PAPR Reduction of Space-Frequency Coded OFDM Systems Without Side Information ». IEEE Transactions on Vehicular Technology 60, no 3 (mars 2011): 1211-16. https://doi.org/10.1109/TVT.2011.2109070.

[109] Badran, Ehab F., et Amr. M. El-Helw. « A Novel Semi-Blind Selected Mapping Technique for PAPR Reduction in OFDM ». IEEE Signal Processing Letters 18, no 9 (septembre 2011): 493-96. https://doi.org/10.1109/LSP.2011.2160720.

[110] Xiao, Yaoqiang, Ming Chen, Fan Li, Jin Tang, Yi Liu, et Lin Chen. « PAPR Reduction Based on Chaos Combined with SLM Technique in Optical OFDM IM/DD System ». Optical Fiber Technology 21 (janvier 2015): 81-86. https://doi.org/10.1016/j.yofte.2014.08.014.

[111] Namitha, A.S., et S.M. Sameer. « A Bandwidth Efficient Selective Mapping Technique for the PAPR Reduction in Spatial Multiplexing MIMO-OFDM Wireless Communication System ». Physical Communication 25 (décembre 2017): 128-38. https://doi.org/10.1016/j.phycom.2017.09.009.

[112] Mestdagh, D.J.G., J.L. Gulfo Monsalve, et J.-M. Brossier. « GreenOFDM: A New Selected Mapping Method for OFDM PAPR Reduction ». Electronics Letters 54, no 7 (avril 2018): 449-50. https://doi.org/10.1049 /el.2017.4743.

[113] Zhang, Si-yu, et Behnam Shahrrava. « A Selected Mapping Technique Using Interleavers for PAPR Reduction in OFDM Systems ». Wireless Personal Communications 99, no 1 (mars 2018): 329-38. https://doi.org/10.1007/s11277-017-5101-7.

[114] Fathy, Sameh A., Michael N. A. Ibrahim, Salah S. Elagooz, et Hadia M. El-Hennawy. « Efficient SLM Technique for PAPR Reduction in UFMC Systems ». In 2019 36th National Radio Science Conference (NRSC), 118-25. Port Said, Egypt: IEEE, 2019. https://doi.org/10.1109/NRSC.2019.8734569.

[115] Prasad, Sanjana, et Ramesh Jayabalan. « PAPR Reduction in OFDM Systems Using Modified SLM with Different Phase Sequences ». Wireless Personal Communications 110, no 2 (janvier 2020): 913-29. https://doi.org/10.1007/s11277-019-06763-7.

[116] Carcangiu, Sara, Alessandra Fanni, et Augusto Montisci. « A Closed Form Selected Mapping Algorithm for PAPR Reduction in OFDM Multicarrier Transmission ». Energies 15, no 5 (7 mars 2022): 1938. https://doi.org/10.3390/en15051938.

[117] Mounir, Mohamed, Mohamed Ibrahim Youssef, et Ashraf Mohamed Aboshosha. « Low-Complexity Selective Mapping Technique for PAPR Reduction in Downlink Power Domain OFDM-NOMA ». EURASIP Journal on Advances in Signal Processing 2023, no 1 (16 janvier 2023): 10. https://doi.org/10.1186/s13634-022-00968-y.

[118] Jayalath, A.D.S., C. Tellambura, et H. Wu. « Reduced complexity PTS and new phase sequences for SLM to reduce PAP of an OFDM signal ». In VTC2000-Spring. 2000 IEEE 51st Vehicular Technology Conference Proceedings (Cat. No.00CH37026), 3:1914-17. Tokyo, Japan: IEEE, 2000. https://doi.org/10.1109/VETECS.2000.851605.

[119] Cimini, L.J., et N.R. Sollenberger. « Peak-to-average power ratio reduction of an OFDM signal using partial transmit sequences ». IEEE Communications Letters 4, no 3 (mars 2000): 86-88. https://doi.org/10.1109 /4234.831033.

[120] Yang, L., R.S. Chen, Y.M. Siu, et K.K. Soo. « PAPR Reduction of an OFDM Signal by Use of PTS With Low Computational Complexity ». IEEE Transactions on Broadcasting 52, no 1 (mars 2006): 83-86. https://doi.org/10.1109/TBC.2005.856727.

[121] Xiao, Yue, Xia Lei, Qingsong Wen, et Shaoqian Li. « A Class of Low Complexity PTS Techniques for PAPR Reduction in OFDM Systems ». IEEE Signal Processing Letters 14, no 10 (octobre 2007): 680-83. https://doi.org/10.1109/LSP.2007.898351.

[122] Ghassemi, A., et T. A. Gulliver. « PTS-Based Radix FFT for PAPR Reduction in OFDM Systems ». In 2007 IEEE Wireless Communications and Networking Conference, 1323-28. Kowloon, China: IEEE, 2007. https://doi.org/10.1109/WCNC.2007.250.

[123] Chen, Jung-Chieh. « Partial transmit sequences for PAPR reduction of OFDM signals with stochastic optimization techniques ». IEEE Transactions on Consumer Electronics 56, no 3 (août 2010): 1229-34. https://doi.org/10.1109/TCE.2010.5606251.

[124] Vittal, M.V.R., et K. Rama Naidu. « A Novel Reduced Complexity Optimized PTS Technique for PAPR Reduction in Wireless OFDM Systems ». Egyptian Informatics Journal 18, no 2 (juillet 2017): 123-31. https://doi.org/10.1016/j.eij.2016.11.002.

[125] Joo, Hyun-Seung, Kee-Hoon Kim, Jong-Seon No, et Dong-Joon Shin. « New PTS Schemes for PAPR Reduction of OFDM Signals Without Side Information ». IEEE Transactions on Broadcasting 63, no 3 (septembre 2017): 562-70. https://doi.org/10.1109/TBC.2017.2711141.

[126] Singh, Mangal, et Sarat Kumar Patra. « Partial Transmit Sequence Optimization Using Improved Harmony Search Algorithm for PAPR Reduction in OFDM ». ETRI Journal 39, no 6 (décembre 2017): 782-93. https://doi.org/10.4218/etrij.17.0116.0919.

[127] Po-Yen Chen, Houshou Chen, et Jyun-Jie Wang. « A low complexity PTS technique for PAPR reduction in OFDM systems ». In 2008 International Symposium on Intelligent Signal Processing and Communications Systems, 1-4. Bangkok, Thailand: IEEE, 2009. https://doi.org/10.1109 /ISPACS.2009.4806734.

[128] Merah, Hocine, Mokhtaria Mesri, et Larbi Talbi. « Complexity Reduction of PTS Technique to Reduce PAPR of OFDM Signal Used in a Wireless Communication System ». IET Communications 13, no 7 (avril 2019): 939-46. https://doi.org/10.1049/iet-com.2018.5705.

[129] Al-Jawhar, Yasir Amer, Khairun Nidzam Ramli, Aida Mustapha, Salama A. Mostafa, Nor Shahida Mohd Shah, et Montadar Abas Taher. « Reducing PAPR With Low Complexity for 4G and 5G Waveform Designs ». IEEE Access 7 (2019): 97673-88. https://doi.org/10.1109/ACCESS.2019.2930121.

[130] Zhou, Zhuang, Lingyin Wang, et Chi Hu. « Low-Complexity PTS Scheme for Improving PAPR Performance of OFDM Systems ». IEEE Access 7 (2019): 131986-94. https://doi.org/10.1109 /ACCESS.2019.2941116.

[131] Sayyari, Reza, Jafar Pourrostam, et Hamed Ahmadi. « A Low Complexity PTS-Based PAPR Reduction Method for the Downlink of OFDM-NOMA Systems ». In 2022 IEEE Wireless Communications and Networking Conference (WCNC), 1719-24. Austin, TX, USA: IEEE, 2022. https://doi.org/10.1109 /WCNC51071.2022.9771812.

[132] Alameri, Thamer, Nabeel Salih Ali, Mothana L. Attiah, Mohammed Saad Talib, et Jawad Kadhim Mezaal. « Low Complexity Rotation Algorithm for PAPR Reducing Performance in Partial Transmits Sequence ». Wireless Personal Communications 124, no 2 (mai 2022): 1169-90. https://doi.org/10.1007 /s11277-021-09400-4.

[133] Naidu, Thalapaneni Penchala, M. Venkata Narayana, Govardhani Immadi, Sai Karthik Gamineedi, Arun Chowdary Nukavarapu, et P. Pavan Kumar. « LOW Complexity Segmentation With a Hybrid Subblock In MIMO OFDM Systems, The PTS Scheme For PAPR Reduction ». In 2022 First International Conference on Electrical, Electronics, Information and Communication Technologies (ICEEICT), 1-5. Trichy, India: IEEE, 2022. https://doi.org/10.1109/ICEEICT53079.2022.9768430.

[134] Yuan, Yazhou, Shiwei Wei, Xiaoyuan Luo, Zhezhuang Xu, et Xinping Guan. « Adaptive PTS Scheme Based on Fuzzy Neural Network for PAPR Reduction in OFDM System ». Digital Signal Processing 126 (juin 2022): 103492. https://doi.org/10.1016/j.dsp.2022.103492.

[135] Gupta, Prabal, H. Pal Thethi, et Ajay Tomer. « An Efficient and Improved PTS Algorithm for PAPR Reduction in OFDM System ». International Journal of Electronics 109, no 7 (3 juillet 2022): 1252-77. https://doi.org/10.1080/00207217.2021.1966671.

[136] Goel, Ashish, et Saruti Gupta. « Side Information Embedding Scheme for PTS Based PAPR Reduction in OFDM Systems ». Alexandria Engineering Journal 61, no 12 (décembre 2022): 11765-77. https://doi.org/10.1016/j.aej.2022.05.021.

[137] Hu, Feng, Hong Xu, Libiao Jin, JianBo Liu, Zhiping Xia, Guoting Zhang, et Jingting Xiao. « Continuous- Unconstrained and Global Optimization for PSO-PTS Based PAPR Reduction of OFDM Signals ». Physical Communication 55 (décembre 2022): 101825. https://doi.org/10.1016/j.phycom.2022.101825.

[138] Azeez, Abdul, et Suraiya Tarannum. « Multi-Objective Mayfly Optimization in Phase Optimization of OFDM ». IIUM Engineering Journal 24, no 1 (4 janvier 2023): 106-21. https://doi.org/10.31436 /iiumej.v24i1.2625.

[139] Naidu, Thalapaneni Penchala, M. Venkata Narayana, Govardhani Immadi, Sai Karthik Gamineedi, Arun Chowdary Nukavarapu, et P. Pavan Kumar. « LOW Complexity Segmentation With a Hybrid Subblock In MIMO OFDM Systems, The PTS Scheme For PAPR Reduction ». In 2022 First International Conference on Electrical, Electronics, Information and Communication Technologies (ICEEICT), 1-5. Trichy, India: IEEE, 2022. https://doi.org/10.1109/ICEEICT53079.2022.9768430.

[140] Nguyen, The Khai, Ha H. Nguyen, J. Eric Salt, et Colin Howlett. « Optimization of Partial Transmit Sequences for PAPR Reduction of OFDM Signals Without Side Information ». IEEE Transactions on Broadcasting 69, no 1 (mars 2023): 313-21. https://doi.org/10.1109/TBC.2022.3201639.

[141] Seung Hee Han et Jae Hong Lee. « Modulation, Coding and Signal Processing for Wireless Communications - An Overview of Peak-to-Average Power Ratio Reduction Techniques for Multicarrier Transmission ». IEEE Wireless Communications 12, no 2 (avril 2005): 56-65. https://doi.org/10.1109 /MWC.2005.1421929.

[142] Wang, Luqing, et Chmtha Tellambura. « An Overview of Peak-to-Average Power Ratio Reduction Techniques for OFDM Systems ». In 2006 IEEE International Symposium on Signal Processing and Information Technology, 840-45. Vancouver, BC, Canada: IEEE, 2006. https://doi.org/10.1109 /ISSPIT.2006.270915.

[143] Tao Jiang et Yiyan Wu. « An Overview: Peak-to-Average Power Ratio Reduction Techniques for OFDM Signals ». IEEE Transactions on Broadcasting 54, no 2 (juin 2008): 257-68. https://doi.org/10.1109 /TBC.2008.915770.

[144] Lim, Dae-Woon, Seok-Joong Heo, et Jong-Seon No. « An overview of peak-to-average power ratio reduction schemes for OFDM signals ». Journal of Communications and Networks 11, no 3 (juin 2009): 229-39. https://doi.org/10.1109/JCN.2009.6391327.

[145] Jawhar, Yasir Amer, Lukman Audah, Montadar Abas Taher, Khairun Nidzam Ramli, Nor Shahida Mohd Shah, Mustafa Musa, et Mustafa Sami Ahmed. « A Review of Partial Transmit Sequence for PAPR Reduction in the OFDM Systems ». IEEE Access 7 (2019): 18021-41. https://doi.org/10.1109 /ACCESS.2019.2894527.

[146] Mirjalili, Seyedali, et Andrew Lewis. « The Whale Optimization Algorithm ». Advances in Engineering Software 95 (mai 2016): 51-67. https://doi.org/10.1016/j.advengsoft.2016.01.008.

[147] Chakraborty, Sanjoy, Apu Kumar Saha, Sushmita Sharma, Seyedali Mirjalili, et Ratul Chakraborty. « A Novel Enhanced Whale Optimization Algorithm for Global Optimization ». Computers & Industrial Engineering 153 (mars 2021): 107086. https://doi.org/10.1016/j.cie.2020.107086.

[148] Wang, Yajun, Wen Chen, et Chintha Tellambura. « A PAPR Reduction Method Based on Artificial Bee Colony Algorithm for OFDM Signals ». IEEE Transactions on Wireless Communications 9, no 10 (octobre 2010): 2994-99. https://doi.org/10.1109/TWC.2010.081610.100047.

[149] Singh, Mangal, et Sarat Kumar Patra. « On the PTS Optimization Using the Firefly Algorithm for PAPR Reduction in OFDM Systems ». IETE Technical Review 35, no 5 (3 septembre 2018): 441-55. https://doi.org/10.1080/02564602.2018.1505563.

[150] Singh, Mangal, et Sarat Kumar Patra. « Partial Transmit Sequence Optimization Using Improved Harmony Search Algorithm for PAPR Reduction in OFDM ». ETRI Journal 39, no 6 (décembre 2017): 782-93. https://doi.org/10.4218/etrij.17.0116.0919.

[151] Suriavel Rao, R. S., et P. Malathi. « A Novel PTS: Grey Wolf Optimizer-Based PAPR Reduction Technique in OFDM Scheme for High-Speed Wireless Applications ». Soft Computing 23, no 8 (avril 2019): 2701-12. https://doi.org/10.1007/s00500-018-3665-0.

[152] Dorigo, Marco, et Christian Blum. « Ant Colony Optimization Theory: A Survey ». Theoretical Computer Science 344, no 2-3 (novembre 2005): 243-78. https://doi.org/10.1016/j.tcs.2005.05.020.

[153] Aghdam MH, Sharifi AA. A novel ant colony optimization algorithm for PAPR reduction of OFDM signals. Int J Commun Syst 2020; e4648.

[154] Wen, Jyh-Horng, Shu-Hong Lee, Yung-Fa Huang, et Ho-Lung Hung. « A Suboptimal PTS Algorithm Based on Particle Swarm Optimization Technique for PAPR Reduction in OFDM Systems ». EURASIP Journal on Wireless Communications and Networking 2008, no 1 (décembre 2008): 601346. https://doi.org/10.1155/2008/601346.

[155] Hosseinzadeh Aghdam, Mehdi, et Abbas Ali Sharifi. « PAPR Reduction in OFDM Systems: An Efficient PTS Approach Based on Particle Swarm Optimization ». ICT Express 5, no 3 (septembre 2019): 178-81. https://doi.org/10.1016/j.icte.2018.10.003.

[156] Prasad, Sanjana, et Ramesh Jayabalan. « PAPR Reduction in OFDM Using Scaled Particle Swarm Optimisation Based Partial Transmit Sequence Technique ». The Journal of Engineering 2019, no 5 (mai 2019): 3460-68. https://doi.org/10.1049/joe.2018.5340.

[157] Yuan, Yazhou, Shiwei Wei, Xiaoyuan Luo, Zhezhuang Xu, et Xinping Guan. « Adaptive PTS Scheme Based on Fuzzy Neural Network for PAPR Reduction in OFDM System ». Digital Signal Processing 126 (juin 2022): 103492. https://doi.org/10.1016/j.dsp.2022.103492.

[158] Gupta, Prabal, H. Pal Thethi, et Ajay Tomer. « An Efficient and Improved PTS Algorithm for PAPR Reduction in OFDM System ». International Journal of Electronics 109, no 7 (3 juillet 2022): 1252-77. https://doi.org/10.1080/00207217.2021.1966671.

[159] Goel, Ashish, et Saruti Gupta. « Side Information Embedding Scheme for PTS Based PAPR Reduction in OFDM Systems ». Alexandria Engineering Journal 61, no 12 (décembre 2022): 11765-77. https://doi.org/10.1016/j.aej.2022.05.021.

[160] Hu, Feng, Hong Xu, Libiao Jin, JianBo Liu, Zhiping Xia, Guoting Zhang, et Jingting Xiao. « Continuous- Unconstrained and Global Optimization for PSO-PTS Based PAPR Reduction of OFDM Signals ». Physical Communication 55 (décembre 2022): 101825. https://doi.org/10.1016/j.phycom.2022.101825.

[161] Azeez, Abdul, et Suraiya Tarannum. « Multi-Objective Mayfly Optimization in Phase Optimization of OFDM ». IIUM Engineering Journal 24, no 1 (4 janvier 2023): 106-21. https://doi.org/10.31436 /iiumej.v24i1.2625.

[162] Lu, Yuan, Feng Hu, LiBiao Jin, JianBo Liu, et Guoting Zhang. « Continuous Unconstrained PSO-PTS Strategy to Maximize HPA Energy Efficiency for FBMC-OQAM Systems ». IET Communications 17, no 5 (mars 2023): 614-31. https://doi.org/10.1049/cmu2.12567.

[163] Abed, Ahmed K., Riyadh Mansoor, et Ali K. Abed. « Particle Swarm Optimization-Based Dummy Sub- Carriers Insertion for Peak to Average Power Ratio Reduction in OFDM Systems ». ICT Express 8, no 1 (mars 2022): 135-41. https://doi.org/10.1016/j.icte.2021.07.005.

[164] Yadav K, Abhilasha RJ, Sethi D. «Analysis of PAPR Reduction in OFDM Using Hybrid ACO-PTS and Firefly-Based PTS Technique». Journal of Optoelectronics Laser 2022; 41(9), 148-161.

[165] Amhaimar, Lahcen, Ali Elyaakoubi, Mohamed Bayjja, Kamal Attari, et Saida Ahyoud. « A Comparison Study of PAPR Reduction in OFDM Systems Based on Swarm Intelligence Algorithms ». In Search Algorithm - Essence of Optimization, édité par Dinesh G. Harkut. IntechOpen, 2023. https://doi.org /10.5772/intechopen.99396.

[166] Naidu, Thalapaneni Penchala, M. Venkata Narayana, Govardhani Immadi, Sai Karthik Gamineedi, Arun Chowdary Nukavarapu, et P. Pavan Kumar. « LOW Complexity Segmentation With a Hybrid Subblock In MIMO OFDM Systems, The PTS Scheme For PAPR Reduction ». In 2022 First International Conference on Electrical, Electronics, Information and Communication Technologies (ICEEICT), 1-5. Trichy, India: IEEE, 2022. https://doi.org/10.1109/ICEEICT53079.2022.9768430.

[167] Nguyen, The Khai, Ha H. Nguyen, J. Eric Salt, et Colin Howlett. « Optimization of Partial Transmit Sequences for PAPR Reduction of OFDM Signals Without Side Information ». IEEE Transactions on Broadcasting 69, no 1 (mars 2023): 313-21. https://doi.org/10.1109/TBC.2022.3201639.

[168] Xu, Hong, Yuzhe Chen, Yuan Lu, Jianbo Liu, et Feng Hu. « Improved Elitist Genetic Algorithm Optimization based PTS to PAPR Reduction for Multi-Carrier Signals ». In 2022 IEEE 6th Information Technology and Mechatronics Engineering Conference (ITOEC), 1746-50. Chongqing, China: IEEE, 2022. https://doi.org/10.1109/ITOEC53115.2022.9734372.

[169] Kennedy, J., et R. Eberhart. « Particle swarm optimization ». In Proceedings of ICNN'95 - International Conference on Neural Networks, 4:1942-48. Perth, WA, Australia: IEEE, 1995. https://doi.org/10.1109 /ICNN.1995.488968.

[170] Zhang, Yudong, Shuihua Wang, et Genlin Ji. « A Comprehensive Survey on Particle Swarm Optimization Algorithm and Its Applications ». Mathematical Problems in Engineering 2015 (2015): 1-38. https://doi.org/10.1155/2015/931256.

[171] Hassan, Rania, Babak Cohanim, Olivier De Weck, et Gerhard Venter. « A Comparison of Particle Swarm Optimization and the Genetic Algorithm ». In 46th AIAA/ASME/ASCE/AHS/ASC Structures, Structural Dynamics and

Materials Conference. Austin, Texas: American Institute of Aeronautics and Astronautics, 2005. https://doi.org/10.2514/6.2005-1897.

[172] Millonas, Mark M. « Swarms, Phase Transitions, and Collective Intelligence », 1993. https://doi.org /10.48550/ARXIV.ADAP-ORG/9306002.

[173] Bonabeau E, Dorigo M, and Theraulaz G. Swarm Intelligence: From Natural to Artificial Systems. Oxford University Press, New York, NY, USA, 1999.

[174] Shi, Y., et R. Eberhart. « A modified particle swarm optimizer ». In 1998 IEEE International Conference on Evolutionary Computation Proceedings. IEEE World Congress on Computational Intelligence (Cat. No.98TH8360), 69-73. Anchorage, AK, USA: IEEE, 1998. https://doi.org/10.1109/ICEC.1998.699146.

[175] Shi, Y., & Eberhart, R. C. (2001, April). Particle swarm optimization with fuzzy adaptive inertia weight. In Proceedings of the workshop on particle swarm optimization (Vol. 2001). Indianapolis, IN: Purdue School of Engineering and Technology, IUPUI.

[176] Clerc, M., et J. Kennedy. « The particle swarm - explosion, stability, and convergence in a multidimensional complex space ». IEEE Transactions on Evolutionary Computation 6, no 1 (février 2002): 58-73. https://doi.org/10.1109/4235.985692.

[177] Parsopoulos, K.E., et M.N. Vrahatis. « UPSO: A Unified Particle Swarm Optimization Scheme ». In International Conference of Computational Methods in Sciences and Engineering 2004 (ICCMSE 2004), édité par Theodore Simos et George Maroulis, 1re éd., 868-73. CRC Press, 2019. https://doi.org /10.1201/9780429081385-222.

[178] Huang, V.L., P.N. Suganthan, et J.J. Liang. « Comprehensive Learning Particle Swarm Optimizer for Solving Multiobjective Optimization Problems ». International Journal of Intelligent Systems 21, no 2 (février 2006): 209-26. https://doi.org/10.1002/int.20128.

[179] Poli R, Kennedy J, Blackwell T. Particle swarm optimization. Swarm intelligence 2007; 1(1): 33–57.

[180] Goel, Ashish, et Saruti Gupta. « Side Information Embedding Scheme for PTS Based PAPR Reduction in OFDM Systems ». Alexandria Engineering Journal 61, no 12 (décembre 2022): 11765-77. https://doi.org/10.1016/j.aej.2022.05.021.

[181] Sharifi, Abbas Ali, University of Bonab, Hojjat Emami, et University of Bonab. « Increasing the Performance of OFDM Systems by PAPR Reduction in PTS Technique using Election Optimization Algorithm ». Signal and Data Processing 19, no 2 (1 septembre 2022): 13-26. https://doi.org/10.52547/jsdp.19.2.13.

[182] Sharifi, Abbas Ali, et Mehdi Hosseinzadeh Aghdam. « A Novel Hybrid Genetic Algorithm to Reduce the Peak-to-Average Power Ratio of OFDM Signals ». Computers & Electrical Engineering 80 (décembre 2019): 106498. https://doi.org/10.1016/j.compeleceng.2019.106498.

[183] Aghdam MH, Sharifi AA. A novel ant colony optimization algorithm for PAPR reduction of OFDM signals. Int J Commun Syst 2020; e4648.

[184] Suriavel Rao, R. S., et P. Malathi. « A Novel PTS: Grey Wolf Optimizer-Based PAPR Reduction Technique in OFDM Scheme for High-Speed Wireless Applications ». Soft Computing 23, no 8 (avril 2019): 2701-12. https://doi.org/10.1007/s00500-018-3665-0.

[185] Kermani, Emad Meimand, Hojjat Salehinejad, et Siamak Talebi. « PAPR reduction of OFDM signals using harmony search algorithm ». In 2011 18th International Conference on Telecommunications, 90-94. Ayia Napa, Cyprus: IEEE, 2011. https://doi.org/10.1109/CTS.2011.5898991.

[186] https://www.digi.com/blog/post/what-is-c-band-and-why-is-it-important-for-5g, 11/05/2023.

[187] Taba, S., Redadaa, S., Benchana, M. A., & Ikni, S. A Low-Complexity PTS Technique based-Improved PSO Algorithm for PAPR Reduction in OFDM Systems. Telecommunications and Radio Engineering.10.1615/TelecomRadEng.2023047181